2018-01-01

High Recovery Inland Desalination: A Technical And Economic Performance Evaluation Of Zero Discharge Desalination And Other Technologies

Malynda Aragon Cappelle
University of Texas at El Paso, malynda7@gmail.com

HIGH RECOVERY INLAND DESALINATION: A TECHNICAL AND ECONOMIC PERFORMANCE EVALUATION OF ZERO DISCHARGE DESALINATION AND OTHER TECHNOLOGIES

MALYNDA ARAGON CAPPELLE

Doctoral Program in Civil Engineering

APPROVED:

W. Shane Walker, Ph.D., Chair

Anthony Tarquin, Ph.D.

Pei Xu, Ph.D.

Mark Engle, Ph.D.

Charles Ambler, Ph.D.
Dean of the Graduate School

Dedication

This dissertation is dedicated to my loving parents who have always encouraged me to pursue my dreams, to my incredible husband who supports me in every way, and to all teachers for guiding me on my journey in life.

"A Dream You Dream Alone Is Only A Dream. A Dream You Dream Together Is Reality."
– John Lennon/Yoko Ono

HIGH RECOVERY INLAND DESALINATION: A TECHNICAL AND ECONOMIC PERFORMANCE EVALUATION OF ZERO DISCHARGE DESALINATION AND OTHER TECHNOLOGIES

by

MALYNDA CAPPELLE, B.S., M.S., MBA

DISSERTATION

Presented to the Faculty of the Graduate School of

The University of Texas at El Paso

in Partial Fulfillment

of the Requirements

for the Degree of

DOCTOR OF PHILOSOPHY

Department of Civil Engineering

THE UNIVERSITY OF TEXAS AT EL PASO

May 2018

Acknowledgements

My life has been made possible by parents and family support. My parents, Mary Beth and Don Tidwell, always encouraged me to learn new things, explore new places (even if it scared them!), and to meet new people. Don taught me the magic of algebraic proofs and introduced me to his Chemical Engineering friend that was helping to clean up environmental disasters in New Mexico. Learning that I could make the world a better place through engineering was key. My mom has shown me that with perseverance, hard work, and LOVE one can accomplish anything for which you set a goal in life. My sister, Andrea White, is a kind soul that sends me messages (and sometimes gifts) of love and encouragement when graduate work and life gets to be too much. My husband, Ian, has been an integral part of every one of my degrees and has been an unofficial team member on every single one of my research projects at UTEP. When I am down, he lifts me up. Thank you to my entire family and all of my friends for all that you have done to make me into the persion I am today.

I can't remember when I became interested in water. I think it is because water has always been part of my soul, nourishing and inspiring me. My career in water began in 1999 as a summer intern at Sandia National Laboratories working with an engineer responsible for water conservation and industrial water treatment. Anthony Baca hired me and supported me as a young engineer and I am thankful for the opportunities gained in the Facilities organization. My job offer allowed me to attend the University of California at Davis, where I received my MS, then return to Sandia to take over as the water treatment and water conservation engineer. My next opportunity brought me to arsenic removal and desalination research, working under Tom Hinkebein, who mentored me and helped me progress in a world that felt foreign to me. When funding became scarce, I moved to a group supporting the Department of Energy's non-proliferation program and had the great opportunity to work with and support Adriane Littlefield. While at Sandia, I met Dr. Tom Davis, then at the University of South Carolina. After he came the UTEP, he convinced me to make the journey down the Rio Grande. Tom and began work on a research project that

eventually became my dissertation. I have been a reluctant graduate student, but, with Shane Walker's belief in my abilities, I have been able to achieve far more than I ever thought possible. I am grateful to work in water, which makes life possible.

"Access to a secure, safe and sufficient source of fresh water is a fundamental requirement for the survival, well-being and socio-economic development of all humanity. Yet, we continue to act as if fresh water were a perpetually abundant resource. It is not."

-Kofi Annan, UN Secretary-General, as quoted in, Is the World Running Out of Water? Awake! magazine, (22 June 2001)

I am thankful for all of the teachers in my life. Thank you to the teachers at Kiddie College, Wherry Elementary, Van Buren Middle School, Highland High School, the University of New Mexico, the University of California at Davis, and The University of Texas at El Paso. I have learned so much about life, engineering, and research, and am grateful for all of the people and institutions that have helped me make it to this point in life.

This dissertation would not have been possible without my advisor, colleague, and friend, Dr. Shane Walker. He has a brilliant mind and a nurturing spirit that makes everything seem possible. Thank you for all of the learning experiences, even the ones that I didn't appreciate at the time, and for all of the guidance and support that you have provided me over the years. You are an inspiration to so many people and I am lucky to know you.

I would like to express my sincere gratitude to my committee members: Dr. Anthony Tarquin, who kindly provided me with data from his membrane technology (Concentrate Enhanced Recovery Reverse Osmosis); Dr. Pei Xu, who is an expert in desalination at New Mexico State University and stepped in at the last minute when I needed a committee member; and, Dr. Mark Engle, who is an expert in produced waters and brines at the USGS and is a professor in Geology at UTEP. This is a diverse committee and I am grateful for your time and guidance. Dr. Tom Davis served on my committee until he became ill recently. Thank you, Tom, for working with me this last decade on your Zero Discharge Desalination technology. Tom is the reason I moved to El Paso and the original inspiration for the research contained in this dissertation.

I am grateful for the financial support from the El Paso Water Utilities Desalination Concentrate Fellowship and the Texas Desalination Association's Ed Archuleta Desalter Scholarship. Additionally, the research that led to this dissertation was supported by the U.S. Bureau of Reclamation's Desalination and Water Purification Research Program (grant R10AP81212), Veolia Water Technologies, Desalitech, the Texas Emerging Technology Fund, NSF Nanosystems Engineering Research Center for Nanotechnology-Enabled Water Treatment (ERC-1449500), and Development Alternatives, Inc. (CDl-G-003, CDI-G-012) with funds from the US Agency for International Development.

Piloting and research take a lot of teamwork and support. I would like to thank all of the students, past and present, that have worked long hours with me in the field or in the laboratory. I especially want to thank Dr. Noe Ortega, Dr. Guillermo Delgado, Dr. Isaac Campos, Osvaldo Broesicke, Jesse Valles, Oluwaseye Owoseni, Shahrouz Jafarzade Ghadimi, Clara Borrego, Evelyn Rios, Denise Garcia, Melodie Armendariz, Ana Hernandez for supporting this researching by analyzing water samples, operating equipment, and performing experiments in support of this effort. Additionally, the El Paso Water has provided assistance with piloting at its Kay Bailey Hutchison Desalination Plant. Art Ruiz and his staff have supported my research since I arrived at UTEP. Finally, the Randy Shaw and staff at the Brackish Groundwater National Desalination Research Facility provided excellent support of piloting activities and their assistance was essential to the piloting success.

"I Can Do Things You Cannot, You Can Do Things I Cannot; Together We Can Do Great Things."

– Mother Teresa

General Abstract

Increasing population and diminishing freshwater resources are leading to increased competition between users of freshwater, both in terms of surface water and groundwater. Desalination can augment the water supply, but conventional approaches like reverse osmosis are usually limited to 70-80% recovery. Inland brine disposal options are often limited, presenting significant technical and economic obstacles to implementing desalination technology. In comparison to conventional desalination technologies, high recovery desalination methods such as Zero Discharge Desalination (ZDD) offer substantially higher potable water yield (*i.e.*, 95-98%) from brackish water. ZDD is a hybrid process that combines reverse osmosis (RO) or nanofiltration (NF) with electrodialysis metathesis (EDM). The goal of this research was to increase the sustainability of inland brackish desalination by improving the technical and economic feasibility of high recovery inland brackish desalination. The research objectives were to evaluate: 1) ZDD performance using different feed water chemistry to develop designs optimized for variations in water quality; 2) the performance tradeoffs in ZDD design on salinity removal, specific energy consumption, and hydraulic recovery; and, 3) the lifetime cost impacts of high recovery processes, as compared with conventional (low-recovery) treatment systems.

This research includes three distinct chapters, each of which is intended to be a standalone document that was, or will be, submitted for publication in a journal article. Chapter 1 presents the results of an article entitled, "Improving Desalination Recovery Using Zero Discharge Desalination (ZDD): A Process Model for Evaluating Technical Feasibility," which was published in Industrial & Engineering Chemistry Research [1]. A semi-quantitative model that incorporated pilot testing results, theoretical calculations, and membrane and antiscalant manufacturer models, was developed in order to evaluate the tradeoffs (*i.e.*, specific energy consumption vs. product water quality) involved in ZDD design. The model shows that 97% system recovery is theoretically possible for moderate feedwater salinity, relatively high multivalent ion concentrations, and less than 40 mg/L silica.

Chapter 2 evaluates the economic performance of ZDD and also updated the ZDD model to include potential for salt recovery, namely calcium sulfate, magnesium hydroxide, and sodium chloride. The chapter investigates the tradeoffs associated with capital and operating costs by way of a sensitivity analysis that compares the relative impacts of RO, EDM, and evaporation pond capital costs, and quantified the impact to ZDD costs from varied power costs. The updated model and associated economic analysis indicate that an optimized ZDD design involves choosing the maximum RO/NF recovery, minimum EDM ion removal, and balancing the salt rejection and silica passage of the RO or NF membrane in order to achieve the water quality desired while maximizing the ZDD system recovery. The incorporation of salt recovery processes led to a decreased unit cost, even when revenue from the sale of byproducts is excluded.

Chapter 3 compares ZDD performance with other commercially-available technologies that show potential for high recovery, namely UTEP's Concentrate Enhanced Recovery Reverse Osmosis (CERRO) and Desalitech's Closed Circuit Reverse Osmosis (CCRO). CERRO was developed at The University of Texas at El Paso by Dr. Anthony Tarquin and has been evaluated at the Kay Bailey Hutchison Desalination Plant (KBH) in El Paso, Texas, and other locations. CCRO is a technology that was pilot tested in 2013 at the KBH. Both CERRO and CCRO take advantage of the relatively slow scale formation of silica and other ions, but differ in their design. Pilot or full scale operational data from ZDD, CERRO, and CCRO were used for this research. While there are many caveats with the assumptions made, my results indicate that semi-batch processes like CERRO and CCRO may be better-designed for medium and high recovery desalination of brackish groundwaters with relatively low concentrations of divalent ions. While ZDD is able to achieve comparable recovery, the energy and cost requirements, and associated complexity, it may be less optimal relative to CERRO and CCRO. However, when the concentration of divalent ions is high (*e.g.*, greater than 60% of TDS), and there is a definite need for high recovery, it seems that ZDD is well-suited for desalination. Additional research is needed to fine tune the economic assessment of these technologies and models should be built to further evaluate the design choices.

Table of Contents

List of Tables

List of Figures

List of Abbreviations

BGNDRF	Brackish Groundwater National Desalination Research Facility
BWRO	brackish water reverse osmosis
CCRO	Closed Circuit Reverse Osmosis
CCD	Closed-Circuit Desalination (operational mode in CCRO)
CERRO	Concentrate Enhanced Recovery Reverse Osmsosis
DI	deionized (water)
ED	electrodialysis
EDM	electrodialysis metathesis
GFD	gallons per square foot per day
in	inch
KBH	Kay Bailey Hutchison (Desalination Plant)
LCD	limiting current density
LMH	liters per square meter per hour
Mixed Cl	Mixed chloride salt concentrate stream produced by EDM
Mixed Na	Mixed sodium salt concentrate stream produced by EDM
NF	nanofiltration
RO	reverse osmosis
PFD	Plug Flow Desalination (operational mode in CCRO)
SEC	specific energy consumption (subscripts may refer to ZDD, RO/NF, and EDM)
SWRO	sea water reverse osmosis
TDS	total dissolved solids
ZDD	Zero Discharge Desalination

List of Greek Symbols

β	EDM spacer shadow factor
Δ_{Ca}	molar concentration of calcium
Δ_{SO4}	molar concentration of sulfate
Δ_{CaSO4}	molar concentration of calcium sulfate
ΔC_{Mg}	molar concentration of magnesium hydroxide
ε	current efficiency used in model
ε_{feed}	current efficiency, based on ions removed from EDM feed
ε_{NaCl}	current efficiency, based on sodium chloride consumption
ε_{feed}	current efficiency, based on EDM feed composition
ρ_{CEM}	cation-exchange membrane resistance (Ω-cm^2)
ρ_{AEM}	anion-exchange membrane resistance (Ω-cm^2)
η	pump/motor efficiency

List of Mathematical Symbols

A_{stack}	exposed membrane area in EDM stack (cm^2)
A_{waste}	size of evaporation pond for silica purge and excess Mixed Cl or Mixed Na (acre)
A_{NaCl}	size of evaporation pond for sodium chloride concentration (acre)
Alk(CT,pH)	molar alkalinity concentration, function of CT and pH
$c_{b,i}$	concentration of ions (mg/L) in brackish water concentration (i=Ca, Mg, Na, Cl)
$c_{d,i}$	concentration of ions (mg/L) in EDM diluate concentration (i=Ca, Mg, Na, Cl)
$c_{E,i}$	concentration of ions (mg/L) in EDM feed concentration (i=Ca, Mg, Na, Cl)
$c_{mCl,i}$	concentration of ions (mg/L) in Mixed Cl solution (i=Ca, Mg, Na, Cl)
$c_{mNa,i}$	concentration of ions (mg/L)in Mixed Na stream (i=Na, Cl, HCO_3, SO_4)
$c_{mCl,AL}$	concentration of ions (mg/L)in Mixed Cl concentration after lime added and magnesium hydroxide precipitated (mg/L)
$c_{prod,i}$	concentration of ions (mg/L) in product concentration (i=Ca, Mg, Na, Cl)
$c_{ROc,i}$	concentration of ions (mg/L) in RO concentrate concentration (i=Ca, Mg, Na, Cl)
$c_{ROf,i}$	concentration of ions (mg/L) in RO feed concentration (i=Ca, Mg, Na, Cl)
$c_{ROp,i}$	concentration of ions in (mg/L) RO permeate concentration (i=Ca, Mg, Na, Cl)
CT	molar concentration of all carbonate system species (mol/L)
C_{CO32-}	molar concentration of carbonate (mol/L)
C_{HCO3-}	molar concentration of bicarbonate (mol/L)
C_{OH-}	molar concentration of hydroxide (mol/L)
C_{H+}	molar concentration of hydrogen ion (mol/L)
C_{Lime}	molar concentration of lime (mol/L)
$c_{sup,i}$	concentration of ions (mg/L) in supernatant before calcium sulfate precipitation (i=Ca, Mg, Na, Cl, HCO_3, SO_4)
E_{Ca}	percentage removal of calcium by EDM
E_{EDM}	Power needed for EDM (kW)
F	Faraday's constant (96,485 C/eq)
I	EDM stack current (A)
i_{edm}	EDM current density (A/cm^2)
m_{NaCl}	molar flow of sodium chloride into EDM stack (mol/day)
M_{CaSO4}	mass of calcium sulfate precipitated (lb/day)
M_{NaCl}	mass of sodium chloride consumed (lb/day)
N_E	normality of EDM feed stream (mEq/L)

N_d	normality of EDM diluate stream (mEq/L)
N_{quads}	number of quads in EDM stack (in design)
N_{stack}	number of EDM stacks (in design)
p_{silica}	silica purge fraction (of RO/NF concentrate)
P_{EDM}	power needed for EDM (kW)
P_{feed}	feed pressure for CCRO or CERRO (psi or Pa)
P_{RO}	power needed for RO/NF (kW)
P_t	power required for CCRO or CERRO at time step, t (kW)
Q_{avg}	average permeate flow (gpm)
Q_b	brackish water flow (gpm)
Q_d	EDM diluate flow (gpm)
Q_{d2E}	EDM diluate flow returned to EDM feed (gpm)
Q_{d2F}	EDM diluate flow returned to RO/NF feed (gpm)
Q_{DI}	DI water consumption (total) (gal/day)
Q_E	EDM feed flow (gpm)
Q_{mCl}	Mixed Cl Concentrate waste stream flow (gpm)
Q_{mNa}	Mixed Na Concentrate waste stream flow (gpm)
Q_{prod}	product flow (MGD)
Q_{ROc}	RO concentrate flow (gpm)
Q_{ROf}	RO feed flow (gpm)
Q_{ROp}	RO permeate flow (gpm)
Q_{Si}	silica purge flow (gpm)
Q_{waste}	ZDD waste flow (gpm)
r_{EDM}	EDM recovery, based on EDM feed and diluate
r_{evap}	evaporation rate (cm/month)
R_i	RO/NF salt rejection, by constituent i (i=Ca, Mg, Na, Cl, HCO_3, SO_4, SiO_2)
$R_{edm,i}$	EDM ion removal, by constituent i (i=Ca, Mg, Na, Cl, HCO_3, SO_4, SiO_2)
$R_{SO4/Ca}$	ratio of SO_4 (eq/L) in Mixed Na to Ca (eq/L) in Mixed Cl
RR_{EDM}	EDM recycle ratio
RRR_i	EDM ion removal relative to Ca removal, by constituent i (i=Mg, Na, Cl, HCO_3, SO_4, SiO_2)
r_{RO}	RO/NF recovery, based on RO feed and permeate
r_{ZDD}	ZDD recovery, based on brackish feed and product
t	time between data recordings
t_{spacer}	EDM spacer thickness (mm)
T_{ROf}	RO/NF feed temperature (^oC)

T	EDM feed temperature (^oC)
v_{stack}	velocity inside EDM stack (cm/s)
V	voltage required to achieve current density in EDM (V_{dc})
V_{mCl}	daily volume of Mixed Cl produced by EDM (gal/day)
$V_{mCl(toSRprocess)}$	daily volume of Mixed Cl sent to salt recovery process (gal/day)
V_{mNa}	daily volume of Mixed Na produced by EDM (gal/day)
$V_{mNa(toSRprocess)}$	daily volume of Mixed Na sent to salt recovery process (gal/day)
V_{perm}	volume of permeate produced (gal/day)
ΔV_{elec}	voltage needed for the electrodes (V_{dc})
ΔV_{dp}	electric potential loss associated with liquid junction potentials between cells (V/quad)
ΔV_{IR}	voltage loss associated with ohmic resistance through the membranes and solution (V/quad)
W_{stack}	EDM membrane width (cm)
z_{Ca}	charge of calcium ion

1. Improving Desalination Recovery Using Zero Discharge Desalination (ZDD): A Process Model for Evaluating Technical Feasibility[1]

ABSTRACT. Zero Discharge Desalination (ZDD) is a very high recovery hybrid desalination system, typically comprised of a primary desalter such as reverse osmosis (RO) or nanofiltration (NF), and electrodialysis metathesis (EDM). The EDM acts as a "kidney" by removing troublesome salts from the concentrate of the primary desalter, which allows for additional recovery of potable water. A mathematical model was developed to simulate ZDD system performance using mass balance, desalination design equations, and experimental data. Model results confirm that ZDD can achieve greater than 97% system recovery for brackish water with: (a) feed TDS less than 3 g/L; (b) relatively high fractions of multi-valent ions (e.g., calcium and sulfate mass concentrations greater than 60% of the TDS); and (c) silica less than 40 mg/L. Furthermore, model results indicate that the required ZDD specific energy consumption: (a) increases by 0.77 kWh per 1 g/L of feed TDS; (b) increases with lower permeate TDS, especially below 500 mg/L; and (c) generally decreases with higher recovery on the primary desalter (*e.g.*, RO or NF). ZDD system recovery generally decreases by approximately 1% per 1 g/L of feed TDS. Higher TDS feedwater (*e.g.*, 3.5 to 5 g/L) limits ZDD system recoveries to 94 to 90%, respectively.

1.1. Introduction

Inland brackish groundwater desalination can supplement or replace a portion of the water supply in many cities and regions, but conventional approaches like reverse osmosis (RO) and nanofiltration (NF) are typically limited to 75-85% hydraulic recovery in order to mitigate the precipitation of sparingly soluble salts (*e.g.*, calcium sulfate). Thus, 15-25% of brackish water supplies must be wasted or discarded as concentrate or brine. Typical brine disposal options

[1] This first chapter was published in Industrial & Engineering Chemistry Research (I&ECR) with co-authors W. Shane Walker, and Thomas A. Davis. Some slight edits were made to fix typographical errors and chemical symbols (*e.g.* $CaSO_4$) were replaced with words *(e.g.*, calcium sulfate).:
Ind. Eng. Chem. Res., 2017, 56 (37), pp 10448–10460, DOI: 10.1021/acs.iecr.7b02472

include: discharge to the sanitary sewer; deep well injection; treatment by an additional process; or evaporation ponds. These brine disposal options often generate permitting or financial obstacles to implementing desalination technology [7]. Additionally, gaining acceptance by the local or regional community can be challenging [7,8]. Effective concentrate management solutions are key to the design and operation of inland brackish desalination systems.

1.1.1. ZDD Technology Background

Zero Discharge Desalination (ZDD) is typically comprised of several main unit operations: pre-treatment, primary desalter (RO or NF), electrodialysis metathesis (EDM), and evaporation ponds (which can also include byproduct recovery). Figure 1.1 shows a simplified ZDD flow diagram for a greenfield (new) desalination site.

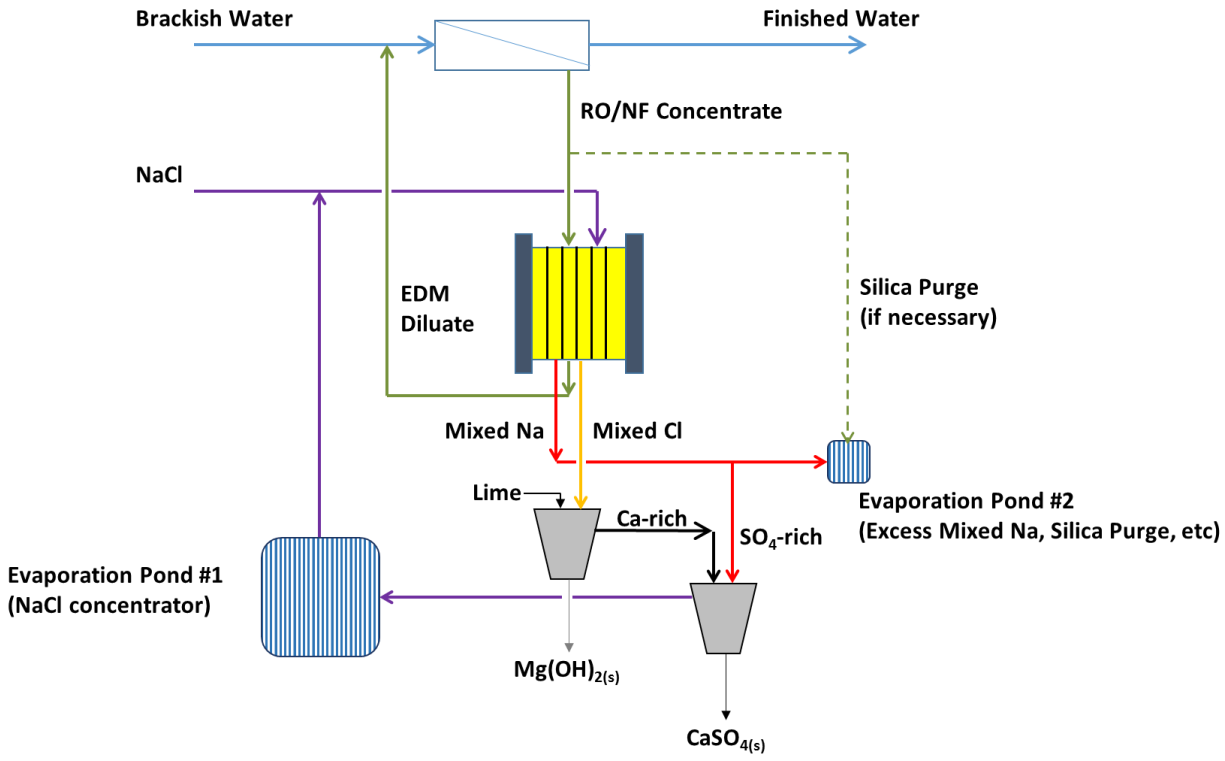

Figure 1.1. Simplified ZDD Diagram

Pre-treated brackish water is fed to an RO/NF system which is then operated at 50-80% recovery and its concentrate is fed to an EDM system. A second feed stream of sodium chloride

(NaCl) is also fed to the EDM. The EDM acts similar to a kidney, in that it removes most of the sparingly soluble salts from the concentrate (uncharged species such as silica are not removed by EDM). The EDM produces a desalinated stream, called diluate, which is returned to the RO/NF feed for recovery of more water. Two concentrated waste streams (Mixed Na and Mixed Cl) are produced by the EDM. The concentrate streams can be handled separately if there is a market for individual salts (*e.g.,* Na_2SO_4 or $CaCl_2$). Alternatively, the concentrate streams can be combined to precipitate calcium sulfate ($CaSO_4$), which allows production of a solid byproduct. The Mixed Cl stream can be treated with lime prior to being combined with the Mixed Na to precipitate magnesium hydroxide ($Mg(OH)_2$). The remaining fluid is then sent to evaporation pond(s). Since the supernatant from the combined concentrate streams contains mostly sodium and chloride ions, that sodium chloride rich solution can be used to dissolve sodium chloride pellets to reduce sodium chloride purchases.

ZDD has been piloted at several locations with a permeate production capacity of 7.6 to 151 L/min by The University of Texas at El Paso (UTEP) [9] and others [10–12]. This paper focuses on modeling based on piloting at the Brackish Groundwater National Desalination Research Facility (BGNDRF) in Alamogordo, New Mexico.

1.1.2. Research Goals & Objectives

A mathematical process model was developed to evaluate the tradeoffs associated with ZDD design decisions such as membrane choice, water recovery of the primary desalination process (RO/NF), EDM performance, and overall system recovery. While many authors have written about various design aspects and models of electrodialysis performance [13–19], no commercial design program is available to the public. There are many RO/NF design programs available for evaluating membrane choice, RO/NF design, and various operating programs. However, there are no models that integrate concentrate minimization or management options. This model is a first step in understanding design and operational decisions for ZDD. The main

goal of this research was to evaluate the feasibility of ZDD as a means of very high recovery brackish water desalination. The objectives of this study were to:

1. Analyze performance tradeoffs among ZDD design parameters
2. Evaluate ZDD performance sensitivity to water quality

1.2. Methods and Materials (ZDD Model Description)

An iterative mathematical model was developed to simulate steady-state ZDD system performance using equations based on the output from a membrane manufacturer's reverse osmosis system design program, mass balance, desalination design equations, and experimental data. Experimental data from ZDD pilot research at the BGNDRF were used to evaluate the impact of membrane choice in the RO/NF. A set of eight brackish waters was used to evaluate the ZDD performance sensitivity to water quality parameters. The ZDD model workflow, showing inputs and how the user interacts with both the model and external programs is shown in Figure 1.2. The ZDD model is described in greater detail in Appendix A, and a PDF of the Mathcad 14.0 model is provided in Appendix B.

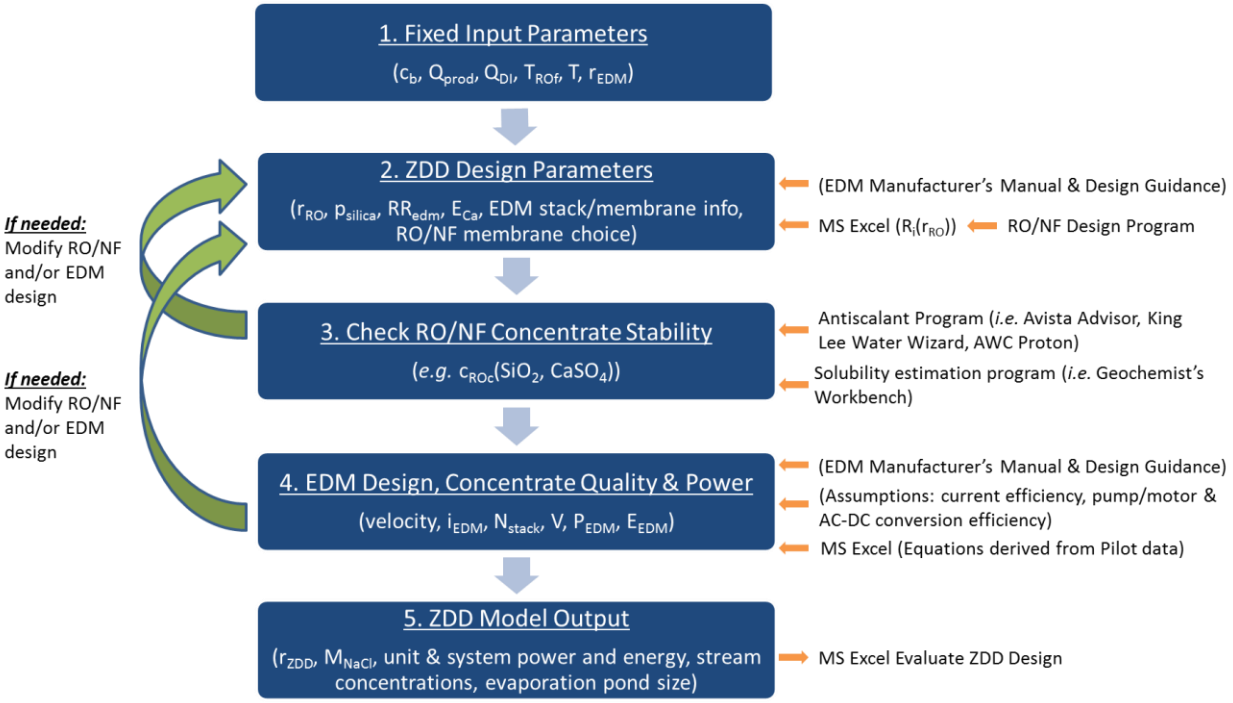

Figure 1.2. ZDD Model Inputs and Workflow

First, the user enters the desired product flow rate, estimated deionized (DI) water consumption, silica purge, RO/NF and EDM feed temperatures, and EDM recovery into the ZDD model. Second, the user enters desired parameters for the ZDD design. This involves selecting one of eight water chemistries, one of six RO/NF membrane choices, entering EDM stack and membrane specifications (*e.g.,* EDM stack membrane area, current efficiency, minimum and maximum velocities), and choosing a value for the desired reduction in calcium by the EDM system (the model calculates other ions' reduction as a function of the EDM calcium reduction). Based on the user's choice of RO/NF membrane, the ZDD model will automatically lead to model calculations for the RO/NF feed pressure and salt rejection, both of which were derived from DOW FILMTEC's design program, ROSA (Reverse Osmosis System Analysis) [20]. Other manufacturers have models as well; however, all UTEP piloting activities used DOW FILMTEC membranes, so it was reasonable to use ROSA to model the RO/NF performance. As described in a 2014 Texas Water Development Board report, computer models can be acceptable tools for

predicting membrane performance [21]. This report compared the accuracy and precision of RO/NF design programs to initial conditions at several desalination plants in the US and found that the models slightly over-predict RO feed pressure and salt rejection [16]. The ZDD model allows the user to manually enter feed pressure and salt rejection values, if desired.

EDM performance is based on ZDD pilot activities in 2013. The model then iterates to solve for steady state water quality solutions for all the streams except the EDM's concentrate streams. Third, the user can export the ZDD model water quality results to an antiscalant projection model (or other means) for determining whether the RO/NF concentrate is stable. If the RO/NF concentrate stream is determined to be too close to scaling or the user determines that another design choice is necessary, the user can adjust design parameters and re-run the ZDD model. Fourth, the ZDD model calculates the Mixed Na and Mixed Cl concentrations (based on mass balance from steady state values in the previous step) and the required membrane area necessary to achieve the EDM diluate concentration specified given the EDM specifications. The user can choose a design that fits into the EDM stack manufacturer guidelines (*e.g.* velocity) and operating parameters (*e.g.* safe current density). Several iterations may be required on the EDM and possibly RO/NF design to find a safe EDM velocity and current density. Fifth, the model calculates power, sodium chloride consumption, and evaporation area required for the design.

1.2.1. Brackish Feed Water Chemistry

In order to evaluate how the performance of ZDD is affected by feedwater quality (especially TDS, calcium, sulfate, and silica), and desired product water quality, several water chemistries were used in the model. Table 1.1 summarizes select water quality parameters for eight waters where ZDD has been tested in some configuration and scale (the values shown have been balanced for electroneutrality). This set of water quality spans a range of TDS and relative proportion of calcium and sulfate to other constituents, and all have moderate silica concentrations. The first three waters are wells from the BGNDRF in Alamogordo, NM, and the fourth water is a blend of BGNDRF Well 1 and Well 4 that was used in ZDD piloting research to simulate the

brackish groundwater available for the City of Alamogordo's planned desalination pilot (fifth column). The last three columns of the table show water quality data for municipalities where ZDD has been pilot tested, including two sites in Colorado and the Kay Bailey Hutchison desalination plant (KBH) in El Paso, Texas.

Two ratios are included in Table 1.1, namely Y-Index and divalents fraction, which are shown in Equations (1) and (2). The Y-Index is an attempt at describing the "Y" shape of a modified Stiff Diagram [17] in numerical form. In Stiff Diagrams, the concentrations are shown horizontally in meq/L for cations (left side) and anions (right side). The farther away from the center, the higher the concentration of the individual ion. For this paper, we have chosen a slightly different order of cations and anions, in that multivalent ions are shown first (authors that use Stiff Diagrams typically have monovalent ions followed by multivalent ions). In this form, our Stiff Diagrams allow for a graphical description of the applicability of ZDD for a given water chemistry; that is, the more the shape resembles a Y, the higher the Y-Index. A brackish water with a relatively high proportion of divalent ions could be desalinated using a nanofiltration membrane and achieve reasonable water quality, high recovery, and possibly lower energy usage. For example, the Stiff Diagram of the Alamogordo water has a distinct "Y" shape and a Y-Index of 0.59, but the Stiff Diagram of the KBH water is shaped like a chevron and has a Y-Index of 0.13. The divalents fraction and Y-Index are both figures of merit for the economic feasibility of ZDD (to be described in detail in a subsequent manuscript). Figure 1.3 shows the Stiff Diagrams for each of the waters summarized in Table 1.1.

$$Y\text{-}index = \frac{minimum\left\{c_{Ca}\left(\frac{meq}{L}\right),\ \ c_{SO4}\left(\frac{meq}{L}\right)\right\}}{Normality\left(\frac{meq}{L}\right)} \tag{1.1}$$

$$Divalents\ (mass) fraction\ (\%) = \frac{c_{Ca}\left(\frac{mg}{L}\right)+c_{Mg}\left(\frac{mg}{L}\right)+c_{SO4}\left(\frac{mg}{L}\right)}{TDS\left(\frac{mg}{L}\right)} \times 100 \tag{1.2}$$

Table 1.1. Selected Water Chemistry for Various ZDD Piloting Research Sites

Location	BGNDRF (Alamogordo, NM)				New Mexico	Colorado		Texas
Water Quality Constituent or Parameter	Well 1 (2016)	Well 2 (2016)	Well 3 (2016)	Well 1 & 4 blend (2013)	Alamogordo (2005-2006)	La Junta (2012)	Brighton (2013)	KBH El Paso (2016)
Ca^{2+} (mg/L)	134.9	495.6	398.3	286.5	417.4	167.4	107.4	163.9
Mg^{2+} (mg/L)	36.5	359.1	209.9	120.3	88.9	61	22.2	40.5
Na^{+} (mg/L)	470.5	720.2	388	377	165.7	111.3	118.2	801.5
Cl^{-} (mg/L)	34.5	518.3	611.7	343.8	131.6	45.4	134.1	1375
HCO_3^{-} (mg/L)	133.9	296.7	221.5	249.3	130.6	271.5	295.8	91.9
SO_4^{2-} (mg/L)	1297.9	3175.7	1592.3	1287.9	1418	599.8	177.8	291.5
SiO_2 (mg/L)	22	19.6	17.9	20	28	16	20.8	26
TDS (mg/L)	2130	5585	3439.5	2685	2391	1272	876	2790
Normality (N) (meq/L)	29.9	85.7	54.1	40.6	35.4	18.2	12.3	46.3
Y-Index	0.22	0.29	0.37	0.35	0.59	0.46	0.3	0.13
Divalents fraction	70%	72%	64%	63%	80%	65%	35%	18%

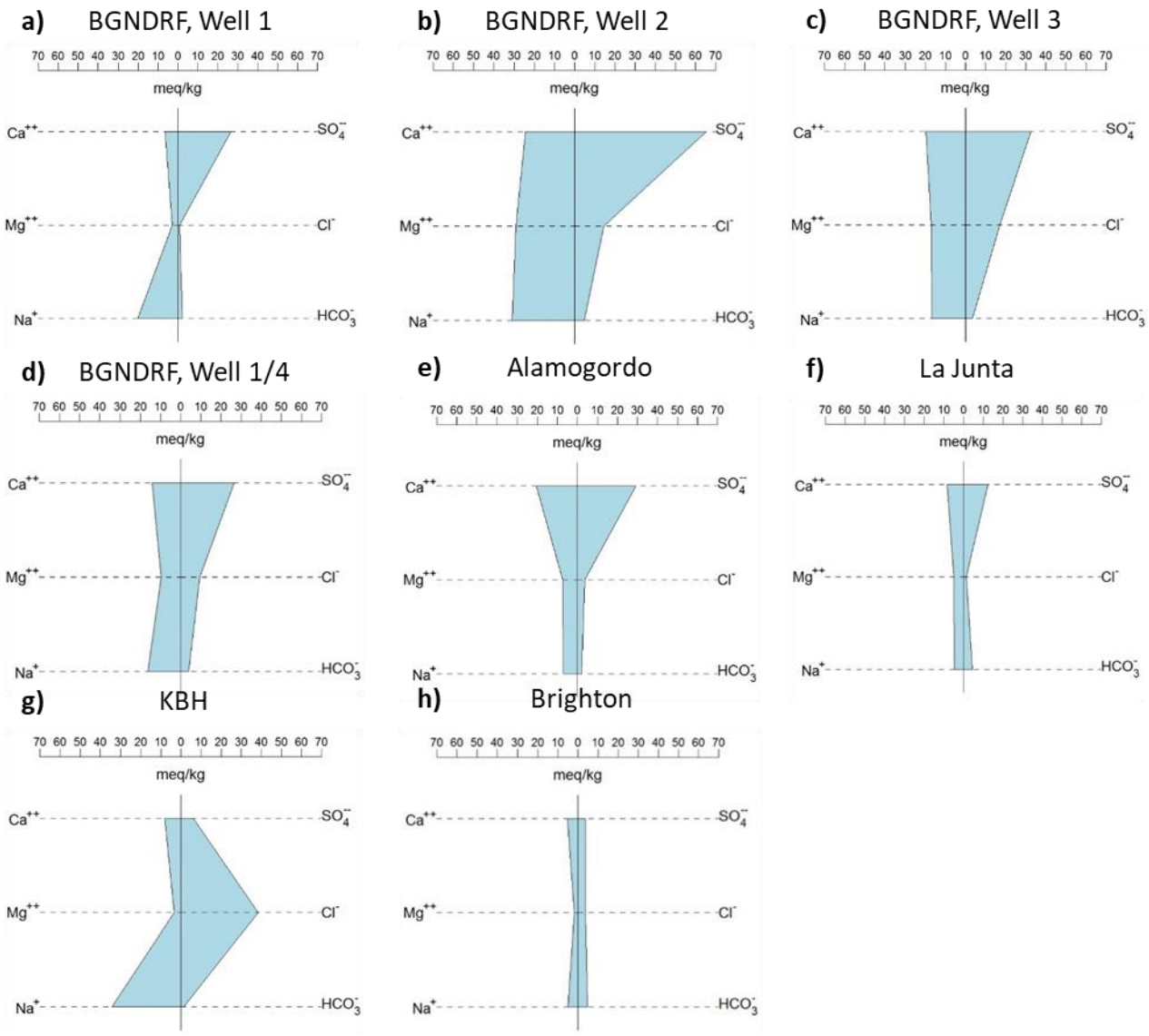

Figure 1.3. Stiff Diagrams of ZDD Piloting Site Waters listed in Table 1.1

1.2.2. Flow Balances

There are six separate streams that enter and leave the EDM stack (EDM feed-diluate, sodium chloride (NaCl), mixed sodium concentrate (Mixed Na), mixed chloride concentrate (Mixed Cl), anolyte/anode rinse, and catholyte/cathode rinse). For simplicity, the electrode rinse streams and most recirculating streams are not shown in Figure 1.4. As shown in Figure 1.4, Q represents volumetric flow rate, M represents mass rate, and C represents concentration. Dashed lines indicate the boundaries of control volumes for flow and mass balances.

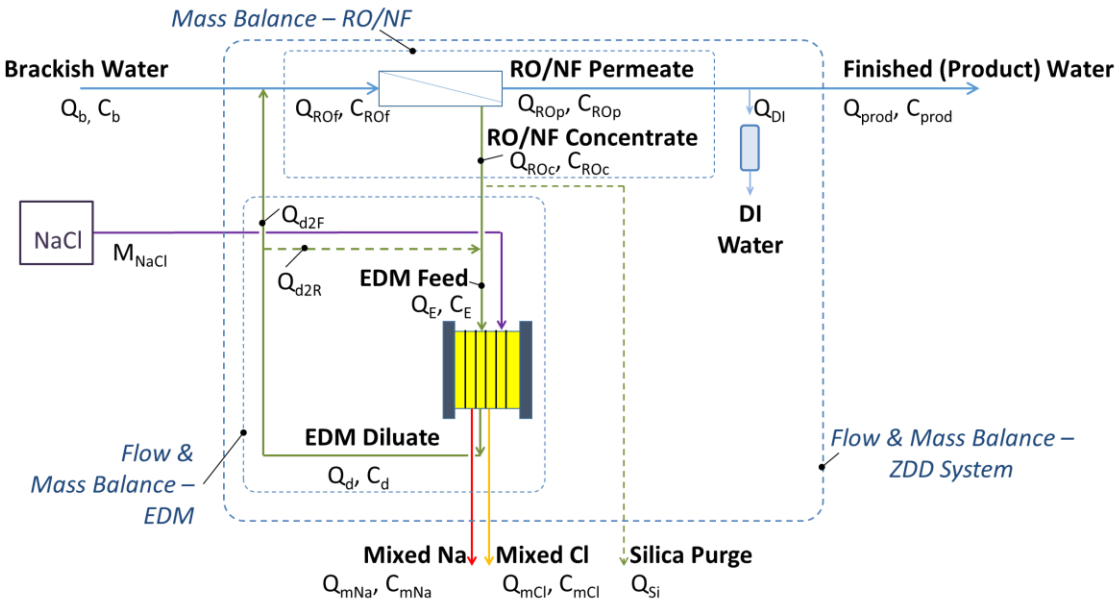

Figure 1.4. ZDD Flow Diagram used for Modeling[2]

The ZDD system design is controlled by the desired finished (product) flow rate, Q_p, product water quality requirements (e.g., TDS < 500 mg/L), and dissolved concentrations in the brackish feed, c_b. The finished (product) flow is less than the permeate flow, Q_{ROp}, since some of the RO/NF permeate might be used to produce DI water, Q_{DI}, for internal process use (e.g., dissolving sodium chloride pellets or diluting the Mixed Na stream). A small RO could be employed and the concentrate sent to the EDM, or a mixed bed ion exchange column could be used. The feed to the RO/NF, Q_{ROf}, is a mixture of the raw (untreated) brackish water, Q_b, and a portion of the EDM diluate sent to the RO/NF feed, Q_{d2R}. For a given RO/NF design, the flow rates of the RO/NF permeate, Q_{ROp}, and concentrate, Q_{ROc}, streams are related to the RO recovery ratio, r_{RO}. If needed, a small portion of the RO/NF concentrate (called the silica purge, Q_{Si}) can be purged to waste to prevent supersaturation of silica. The remaining portion of the RO/NF concentrate is then blended with the EDM diluate recycle, Q_{d2E}, to produce the EDM feed stream, Q_E. The EDM diluate flow, Q_d, is nearly equal to the EDM feed flow, as the only water losses are

[2] This figure was modified to correct the notation on the diluate returned to the EDM feed (Q_{d2R}) from what was in the manuscript (Q_{d2E}).

those associated with the water of hydration for the ions transferred to the EDM concentrate streams. Two concentrate waste streams leave the EDM (and ZDD) system, namely the Mixed Na, Q_{mNa}, and the Mixed Cl, Q_{mCl}. If any DI water is used for dilutions in the EDM streams, the contribution from Q_{DI} is accounted for in the waste flows. Similarly, all DI water used to prepare the sodium chloride, and transferred as part of the water of hydration for the Na and Cl ions transferred into the EDM concentrate streams, is accounted for in the waste flows. Empirical equations (based on DOW FILMTEC's ROSA model output) were incorporated in the ZDD model to simulate RO/NF feed pressure and salt rejection, as detailed in Appendix A. All of the governing mass and flow balance equations for RO/NF and EDM are detailed in Appendix A and B.

The equations summarizing the ZDD system recovery and the recovery of the individual RO/NF and EDM systems are shown here. The RO/NF recovery is the ratio of the RO/NF permeate to RO/NF feed flow (note: RO is used to simplify notation, but the membrane choice could include NF or a combination of RO and NF):

$$r_{RO} = \frac{Q_{ROp}}{Q_{ROf}} \quad (1.3)^3$$

Similarly, the EDM recovery is a ratio of the EDM diluate to EDM feed flow:

$$r_{EDM} = \frac{Q_d}{Q_E} \quad (1.4)$$

Finally, the ZDD system recovery can be expressed as the ratio of the product water to brackish water feed:

$$r_{ZDD} = \frac{Q_{prod}}{Q_b} \quad (1.5)$$

The ZDD system recovery can also be expressed using the RO/NF permeate and waste flows (used to compare to pilot results since limited or no flow data exists for raw and product flow in the pilot systems).

$$r_{ZDD} = \frac{Q_{ROp} - Q_{mNa} - Q_{mCl}}{Q_{ROp}} \quad (1.6)$$

The flow rates of the EDM concentrate streams include water that is transported along with the ions (called water of hydration) from the sodium chloride and EDM feed streams and DI water

[3] This equation was mofidifed to correct the notation for the RO feed (Q_{ROf}) from what was published in the manuscript (Q_f)

that is added to mitigate scale or back diffusion of ions. Researchers have modeled and estimated the water of hydration [8], however this model estimates transport of water of hydration by flow ratio using overflow rates from pilot activities when no dilutions were occurring. Mixed Na and Mixed Cl concentrate waste flow rates were carefully measured at BGNDRF under controlled conditions. This allows estimation of the relative amount of water transport with ion transport in each of the concentrate waste streams (see Section 1.3 in Appendices A and B).

Pilot data from BGNDRF were used to approximate the DI water used for solid sodium chloride pellet dissolution and dilution of the Mixed Na streams. The total amount of daily DI water consumption was approximately 1.0% of the daily NF permeate production. The Mixed Na stream contains several constituents that can become oversaturated, so DI water is used to prevent precipitation. Dilutions are not needed for the Mixed Cl stream (*i.e.*, Q_{DI_mCl}=0) because there are no issues with solubility of the chloride salts. The ZDD model assumes that half of the DI is used for Mixed Na dilutions (Q_{DI_mNa}) and the other half of the DI is used for sodium chloride dissolution (Q_{DI_NaCl}).

1.2.3. RO/NF Stream Concentration Calculations (by mass balance)

The RO/NF design was performed using DOW FILMTEC's ROSA software. ROSA models were created using four different membranes, ranging from loose NF to a tight BWRO (*i.e.*, NF270, NF90, XLE, BW30, respectively), for four recoveries (50%, 60%, 70%, 80%). The brackish feed quality includes the concentration of the major ions (Ca^{2+}, Mg^{2+}, Na^{+}, Cl^{-}, HCO_3^{-}, SO_4^{2-}) and silica (SiO_2).

For all models, the permeate flow was set at 11.4 megaliter per day (MLD), or 3 million gallons per day (MGD), and the average flux was set at 23.3 $L \cdot m^{-2} \cdot hr^{-1}$ (lmh), or 13.7 $gal \cdot ft^{-2} \cdot day^{-1}$ (gfd). The staging and permeate back pressure were modified to reach designs with no model errors for feed flow, permeate flux, or concentrate flow. For each membrane type, linear regression equations for species rejection as a function of recovery are shown in Appendix A. The RO/NF

rejection was calculated as the removal ratio, using the concentration of the dissolved species (*e.g.,* Ca^{2+}) in the brackish water feed ($c_{b,i}$) and RO/NF permeate ($c_{ROp,i}$):

$$R_i = \frac{(c_{b,i} - c_{ROp,i})}{c_{b,i}} \quad (1.7)$$

A blend of NF90 and NF270 membranes could offer the benefits of both membranes (*i.e.*, lower feed pressure than RO with the relatively high salt rejection of the NF90 and lower silica rejection of the NF270), so two more ROSA models were built to calculate ion removal and pressure values to compare full scale designs with better permeate water quality.

Using the input and design parameters, the concentration of each constituent in the permeate is calculated as the product of the feed concentration and the salt passage (1-R_i) of the constituent. The initial calculation assumes that the RO/NF feed concentration is equal to the brackish water feed quality. The ionic composition of the feed, RO product, and RO concentrate is adjusted to be electroneutral (the equations and functions are shown in Appendix A). The concentration of each constituent in the RO/NF concentrate is calculated based on the concentration factor and then balanced for electroneutrality (as shown in Appendix A).

1.2.4. EDM Stream Concentration and Sodium Chloride Consumption Calculations (by mass balance)

The EDM design in the ZDD model is based on the specifications of the MEGA ED-II/4x stacks used in UTEP research activities [18]. The EDM feed is a mixture of the RO/NF concentrate and a portion of the EDM diluate. The EDM recycle ratio, RR_{EDM}, is a ratio of the EDM diluate returned to the EDM feed (Q_{d2F}) relative to the RO concentrate that is sent to the EDM (Q_{ROc}-Q_{Si}).

$$RR_{EDM} = \frac{Q_{d2F}}{Q_{ROc} - Q_{Si}} \quad (1.8)$$

The sodium chloride and electrode rinse streams are assumed to have electrical conductivity of 50 mS/cm and 40 mS/cm, respectively. The Mixed Na and Mixed Cl stream compositions are based on the calculated mass transport from EDM feed and diluate streams. The ZDD model simulates realistic ion transport based on full-scale piloting research and thus, implicitly accounts for membrane non-ideality and back-diffusion. (It is assumed that there are no

hydraulic leaks within the EDM stack.) Thus, all of the cations that are removed from the EDM feed compartment are assumed to be transported to the Mixed Cl stream, and all of the anions that are removed from the EDM feed compartment are assumed to be transported to the Mixed Na stream. Sodium chloride is added at a rate equivalent to the ion removal from the EDM feed. The equivalent rate of chloride is equal to the sum of equivalent rates of cations transported to the Mixed Cl stream, and the equivalent rate of sodium is equal to the sum of equivalent rates of anions transported to the Mixed Na stream. Finally, the mass rate of sodium chloride consumption is calculated. Subsequent research will investigate the economic impacts of sodium chloride consumption and salt recovery.

1.2.5. Estimating EDM Voltage and Current

The driving force for ionic separation in electrodialysis is the applied voltage, and the ions being transported in the EDM stack are what constitute the electrical current. Others have described the chemical and electric potential gradients in EDM [5,19]. The current density, i_{edm}, required to accomplish a desired reduction in concentration from the EDM feed to diluate can be calculated using Faraday's Law [20]:

$$i_{edm} = \frac{Q_{EDMf} \cdot F \cdot (N_E - N_d)}{\varepsilon \cdot A} \tag{1.9}$$

where F is Faraday's constant (96,485 C/eq), N_E and N_d are the normality of the EDM feed and diluate, respectively, ε is current (Coulombic) efficiency, and A is the available membrane area for ion transport. The membrane area used in this model was based on MEGA stacks used in the BGNDRF piloting (100 quads per stack, 4200 cm^2 available membrane surface area, 5-11 cm/s velocity). Current efficiency was approximated as 75% based on piloting data.

The limiting current density (LCD) can be calculated by several methods [10,14,16,24–27]. While an electrodialysis system can be operated beyond the LCD, ED is less efficient (with respect to desalination) because additional voltage will not lead to a useful increase in ion removal. Additionally, equipment damage will occur if the EDM is operated at or above the LCD. Current density in general, and limiting current density in particular, is affected by operating conditions,

stream concentrations, and hydraulic conditions of the stack [5]. Increased concentration supports increased current density [22] and increased stream velocity also leads to increased current density [23]. As temperature decreases, the effective cell resistance increases, and the current density also decreases [24]. Piloting results from BGNDRF were used to develop an equation describing LCD as a function of velocity (v_{stack}) for use in the ZDD model (See Appendix A for additional details):

$$LCD = 74.98 \frac{A}{m^2} \cdot \left(\frac{v_{stack}}{\frac{cm}{s}} \right)^{0.2672} \tag{1.10}$$

The LCD test was performed at the BGNDRF, where the lowest salinity (EDM feed and diluate) was generally 3-5 g/L TDS. Additional tests would be required to verify the accuracy of this equation with other water chemistry, EDM membranes, or operating conditions. If the model's calculated current density exceeds the estimated limiting current density, then the ZDD model user can increase the size of the EDM in the model and re-run the model.

The required voltage drop per EDM quad can be estimated based on physical parameters (*e.g.* spacer thickness and stream conductivities) [5,19–21]. The total voltage (V) required to achieve a certain current density is the sum of the voltage needed for the electrodes (ΔV_{elec}), the voltage loss associated with liquid junction potentials between cells (ΔV_{dp}), and the voltage loss associated with ohmic resistance through the membranes and solutions (ΔV_{IR}).

$$V = \Delta V_{elec} + \Delta V_{dp} + \Delta V_{IR} \tag{1.11}$$

The voltage drop (or, energy loss) associated with electrical resistance (ΔV_{IR}) is typically greater than the voltage drop associated with concentration differences and electrode reactions [19], and ion exchange membranes with high resistance will exacerbate this effect. The highest resistance in the EDM is typically from the compartment with the lowest concentration, the EDM feed. In the ZDD model, the stream electrical conductivities are estimated based on experimental correlations with TDS (see Figure S.2 in Appendix A). One key factor is the shadow factor, which takes into account how much of the membrane's surface is blocked by the spacer material. The

shadow factor (β) is less than 1.0 [11,19]; the ZDD model uses a shadow factor of 0.65, which is based on the MEGA spacer characteristics. Additional details are provided in Appendix A.

The voltage drop required for the electrode rinse compartment decreases with increasing electrolyte concentration [6,25]. The ZDD model calculation for the required electrode voltage is based on Walker et al. [9], which includes the thermodynamic and kinetic aspects of the electrode reactions, as well as the electrical resistance of the electrolyte solution.

1.2.6. Specific Energy Consumption

The specific energy consumption (SEC) calculated by the ZDD Model is the total amount of power (P) required for desalination and internal pumping (for both the RO and EDM) divided by the total flowrate of product water from the ZDD system:

$$SEC_{ZDD} = \frac{P_{RO}+P_{EDM}}{Q_{prod}} \quad (1.12)$$

The power consumption of the RO/NF (P_{RO}) is based on the ZDD Model's predicted RO/NF feed pressure. The power consumption of the EDM (P_{EDM}) includes both desalination energy (based on calculated voltage, V, and current, i_{EDM}) and pumping energy for the five EDM streams. Additional details are provided in Appendix A, sections 4.3-4.5 and in the ZDD Model (Appendix B).

1.3. Results and Discussion

1.3.1. Analysis of Performance Tradeoffs among ZDD Design Parameters

In order to evaluate the impact of design choices for the RO/NF and EDM, five major combinations (cases) of design parameters were chosen for comparison of twelve unique scenarios (listed in Table 1.2) of desalinating the BGNDRF Well 1 & 4 blend (composition listed in Table 1.1). As described in Section 1.2.3, all models had the same design product flow (Q_{prod} = 11.4 MLD, or 3 MGD), and four different RO/NF membrane types were modeled (DOW FILMTEC NF270, NF90, XLE, and BW30). The average flux for all cases was 23.3 $L \cdot m^{-2} \cdot hr^{-1}$ (lmh) (13.7 $gal \cdot ft^{-2} \cdot day^{-1}$ (gfd)). For the two-stage cases, the first-stage flux was between 23.1 and 24.7 lmh

(14.2 and 15.2 gfd) and the second-stage flux was between 17.6 and 21.5 lmh (10.8and13.2 gfd). All models had the same RO/NF and EDM feed temperatures (T_{ROf} = 25 ºC, T_{EDMf} = 30 ºC). In each case, the silica purge flow was minimized in order to obtain a maximum ZDD recovery. Then the number of EDM stacks was chosen in order to ensure that the ZDD model's predicted EDM current density was below the LCD and that the EDM stack velocity was within the manufacturer's acceptable range.

Table 1.2. Summary of Primary Desalter Membranes Used and Independent Variables for ZDD Model Case Studies (QROp = 3.03 MGD and Qprod = 3.00 MGD)

Case	RO/NF Membranes	r_{RO}	RR_{EDM}	E_{Ca}
1	NF270, NF90, XLE, BW30	55%	0.25	30%
		55%	0.5	30%
		55%	1	30%
2	NF270, NF90, XLE, BW30	75%	3	30%
		75%	3.25	30%
		75%	3.5	30%
3	NF270, NF90, XLE, BW30	55%	1	30%
		55%	1	40%
		55%	1	50%
4	NF270, NF90, XLE, BW30	75%	3	30%
		75%	3	40%
		75%	3	50%
5	NF90-NF270 hybrid	55%	1	40%
		75%	3	40%

Cases 1 and 2 compare the impact of RO/NF recovery (r_{RO}) and EDM recycle ratio (RR_{EDM}) for constant RO flux and EDM removal. Case 1 (low RO recovery) varied the EDM recycle ratio from 0.25 to 1 with constant RO/NF recovery and EDM calcium removal (r_{RO} = 55%, E_{Ca} = 30%). A solution for Case 1a was not possible for the NF90, XLE, and BW30 membranes because the competing needs for LCD and EDM velocity could not be met. Similarly, Case 2 (high RO/NF recovery) varied the EDM recycle ratio from 3 to 3.5 for constant RO/NF recovery and EDM calcium removal (r_{RO} = 75%, E_{Ca} = 30%). Cases 3 and 4 compare the impact of shifting the

desalination load distribution between the RO/NF and EDM. Case 3 (low RO recovery) varied the EDM calcium removal from 30% to 50% with constant RO/NF recovery and EDM recycle ratio (r_{RO} = 55%, RR_{EDM} = 1). Case 4 (high RO recovery) varied the EDM calcium removal from 30% to 50% with constant RO/NF recovery and EDM recycle ratio (r = 75%, RR_{EDM} = 3). (Cases 3a and 4a are identical to Cases 1c and 2a, respectively.) Case 5 was the same design as Case 3b and Case 4b, except with the combination of NF90 and NF270 membranes for a higher (90-95% of the LCD) and lower (89-90% of the LCD) EDM current density. These cases are called a hybrid NF90-NF270 because a combination of membranes was used for the design. Appendix A includes a description of the membrane design and staging.

Higher salt rejection means that a better quality (lower TDS) permeate is produced, however, membranes with higher salt rejection generally require more pressure to produce the same flux of permeate. The ZDD model results for the four membranes and one membrane combination evaluated in this study indicates that membranes with higher salt rejection (*i.e.*, RO or tight NF) would be required to meet the secondary drinking water TDS standard (500 mg/L). This can lead to higher specific energy consumption for the ZDD (see Figure 1.5a) and lower ZDD recovery (see Figure 1.5b). Interestingly, even though the 75% RO/NF recovery designs (Cases 2 and 4) require higher feed pressure than the designs with 55% RO/NF recovery (Cases 1 and 3), the overall ZDD specific energy consumption was generally less than the designs with 55% NF/RO recovery for the NF90, XLE, and BW30 membranes (see Figure 1.5a). Designs with higher recovery require less RO/NF feed water flow which reduces the power lost to hydraulic pressure drop, and reduces the energy consumed by the RO/NF. Also, the lower concentrate flow (which is fed to the EDM) reduces the energy consumed by the EDM. Another reason for decreased energy consumption with 75% RO/NF recovery designs is that a larger silica bleed is required for the designs with NF90 and RO membranes; this greater silica bleed further reduces the RO/NF volume and salinity of the EDM feed.

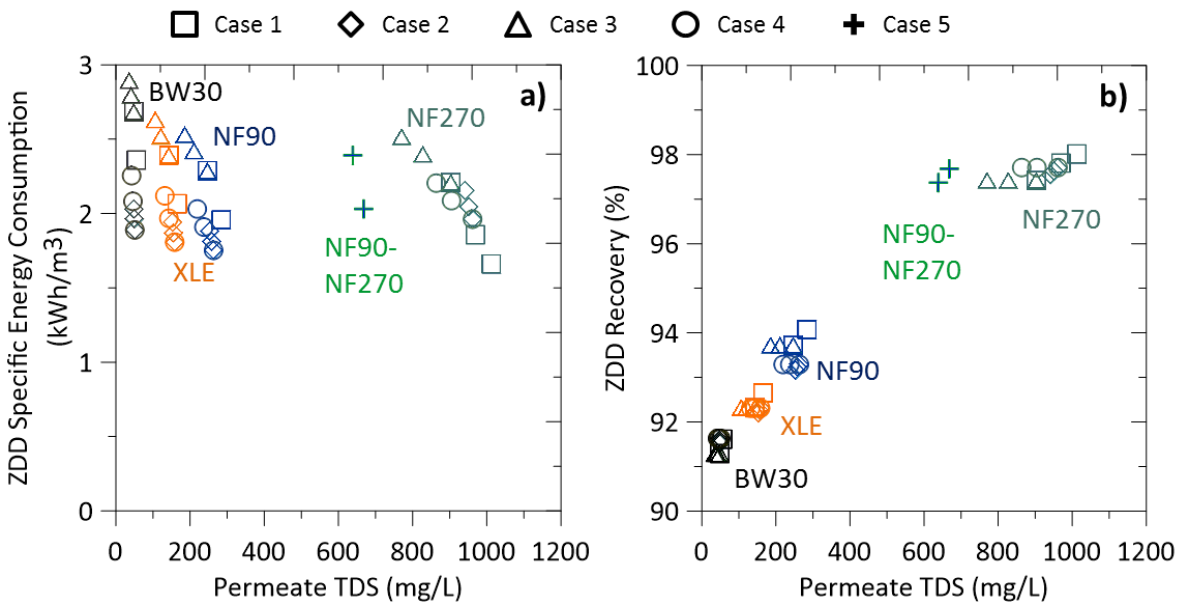

Figure 1.5. ZDD Specific Energy (a) and System Recovery (b) as a function of Permeate TDS for four RO/NF membranes treating the BGNDRF Wells 1&4 blend

The energy required for the EDM is the largest component of the total ZDD energy. The fraction of the ZDD specific energy that is required for the EDM (pumping and electrodes) ranges from approximately 63 to 72% for the BW30 designs to 79-89% for the NF 270 designs. The NF 270 designs have a lower energy demand for the RO/NF, and thus, the EDM fraction is higher.

The silica rejection of the NF90, XLE, and BW30 membranes is high enough that the silica accumulates to levels that would cause precipitation in the RO/NF unless some of the RO/NF concentrate is purged to waste, but higher purge flow rate reduces the system recovery. The NF270 membrane allows for the highest ZDD system recovery (see Figure 1.5**b**), but also produces a permeate with much higher TDS than the other membranes. A hybrid RO/NF membrane design (Case 5) could improve the product water quality at a reasonable ZDD system recovery and specific energy, as compared to designs with only a single membrane type. As shown in Figure 1.5, the Case 5 NF90-NF270 hybrid design allows for high recovery and reasonable quality NF permeate.

1.3.2. Evaluation of ZDD Performance Sensitivity to Water Quality

Obviously, feed water composition and product water quality requirements will affect the ZDD design. Higher silica in the brackish feedwater will require a greater silica purge, which will reduce the ZDD system recovery. The maximum silica concentration allowed in the NF/RO concentrate of the ZDD model is 260 mg/L because Avista Advisor, AWC PROTON (required acid addition), and King Lee Technologies Water Wizard were used to identify antiscalant products indicated to be able to control silica precipitation up to 260 mg/L for the chemistries input. As shown in Figure 1.6, the silica purge increases by a factor of 2-3 for the NF90 and XLE membranes. Even with a purge of 30% of the RO concentrate, the silica remains above the target value of 260 mg/L when BW30 membranes are employed.

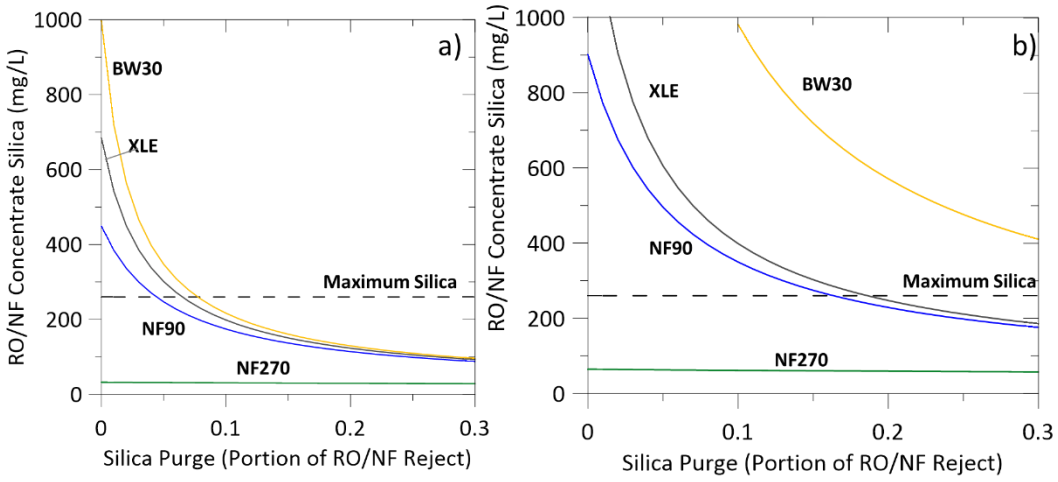

Figure 1.6. Impact of a) BGNDRF 1&4 Blend with 20 mg/L and b) BGNDRF 1&4 Blend with 40 mg/L Silica Concentration in Brackish Groundwater on Silica Purge Flow Rate

In order to evaluate ZDD performance on different water chemistries, seven brackish water qualities (see BGNDRF wells 1-3, Alamogordo, KBH, La Junta, and Brighton in Table 1.1) were input into the model and several designs were developed. This set of brackish water chemistries and associated ZDD designs does allow one to evaluate the impact of feedwater TDS, relative proportion of Ca^{2+} and SO_4^{2-} to other ions in the brackish feedwater (*Y-Index*), and design choices for the RO/NF and EDM. In each case, the goal was to maximize ZDD recovery, achieve RO/NF

permeate quality of 500 mg/L TDS, and ensure the ZDD model output satisfies solubility and LCD limits and manufacturer requirements. Table 1.3 summarizes the independent variables (r_{RO}, RR_{EDM}, E_{Ca}), RO/NF membrane and staging, and two important ZDD model output calculations for the sixteen cases. Since it is important to constrain the EDM stack current density to a value below the LCD, the ratio of the calculated current density to the LCD is shown in the sixth column. The final column includes the calculated ZDD recovery.

Most of the cases implemented the hybrid NF90-NF270 membrane choice. In a few, NF270 was used because the feedwater TDS was low enough to allow it, and the specific energy was also lower. The water quality at both the KBH and BGNDRF Well 3 sites necessitated higher salt rejection (to achieve good permeate water quality), so the NF90 membranes were used. Since the ZDD model suggests that operating the RO/NF at a higher recovery leads to lower ZDD system specific energy, most of the designs include relatively high RO/NF recovery ($r \geq 75\%$).

In the case of the Alamogordo and BNGNDRF water qualities, which have a relatively high fraction of calcium and sulfate present in the raw water (*e.g.*, approximately 60-70%), more ions must be removed by the EDM in order to achieve a sufficiently low concentration in the EDM diluate that is returned to the RO feed. Many of the Alamogordo cases required greater EDM extraction (E_{Ca}) to produce permeate with less than 500 mg/L TDS and ensure that the RO/NF concentrate water quality is stable in terms of precipitation of calcium sulfate compounds (*e.g.*, gypsum). It is possible that a design with lower energy requirements could be achieved with a higher permeate TDS.

The sixth column in Table 1.3 shows how close the EDM current density (i_{EDM}) is to the limiting current density (LCD) for each of the models. While all designs summarized are in the ohmic region of a LCD plot (see Figure S.1 in Appendix A), it is possible that a design with a lower current density (*e.g.* $i_{EDM}/LCD = 60\%$) would be more conservative and allow for more flexibility of water quality changes over time.

Table 1.3. Summary of ZDD Modeling for Water Quality Comparison.

Water (Table 1)	Membrane & Staging	r_{RO}	RR_{EDM}	E_{Ca}	i_{EDM}/ LCD	ZDD Recovery
BGNDRF, well 1	NF270 (78)	55%	0.5	30%	78%	98%
	NF270 (52x26)	75%	2	35%	90%	98%
BGNDRF, well 2	NF90 (78)	50%	2	30%	96%	94%
	NF90 (78)	50%	2	30%	92%	94%
BGNDRF, well 3	NF90-NF270 (78)	55%	2	40%	88%	97%
	NF90 (78)	55%	1.5	30%	90%	93%
Alamogordo	NF90-NF270 (52x26)	70%	2	40%	96%	98%
	NF90-NF270 (52x26)	70%	2	40%	89%	98%
	NF90-NF270 (52x26)	65%	2	30%	89%	97%
	NF90-NF270 (78)	55%	0.75	30%	90%	98%
La Junta	NF90-NF270 (52x26)	75%	1	30%	94%	98%
	NF90-NF270 (52x26)	75%	1	30%	90%	98%
KBH	NF90 (52x26)	70%	2	30%	95%	91%
	NF90 (52x26)	70%	2	30%	89%	91%
Brighton	NF90-NF270 (52x26)	80%	0.75	30%	70%	99%
	NF90-NF270 (52x26)	80%	0.75	30%	62%	99%

Generally, the required ZDD specific energy increases with decreasing permeate TDS (as shown in Figure 1.5a), but the relationship between increasing feedwater TDS and increasing ZDD specific energy is very clear (Figure 1.7a). In this case, feedwater TDS is used as a proxy for the sum of molar concentrations of the dissolved constituents. The ZDD model includes calculations for the rejection of major ions and silica, and TDS is calculated as a sum of all species in the ZDD Model. High TDS generally means that the feedwater will have a higher osmotic pressure, and more energy will be required to desalinate a given volume of water. The KBH data points deviate from the trend for the other sites because of the relatively large silica purge stream required, which restricts the overall system recovery and specific energy.

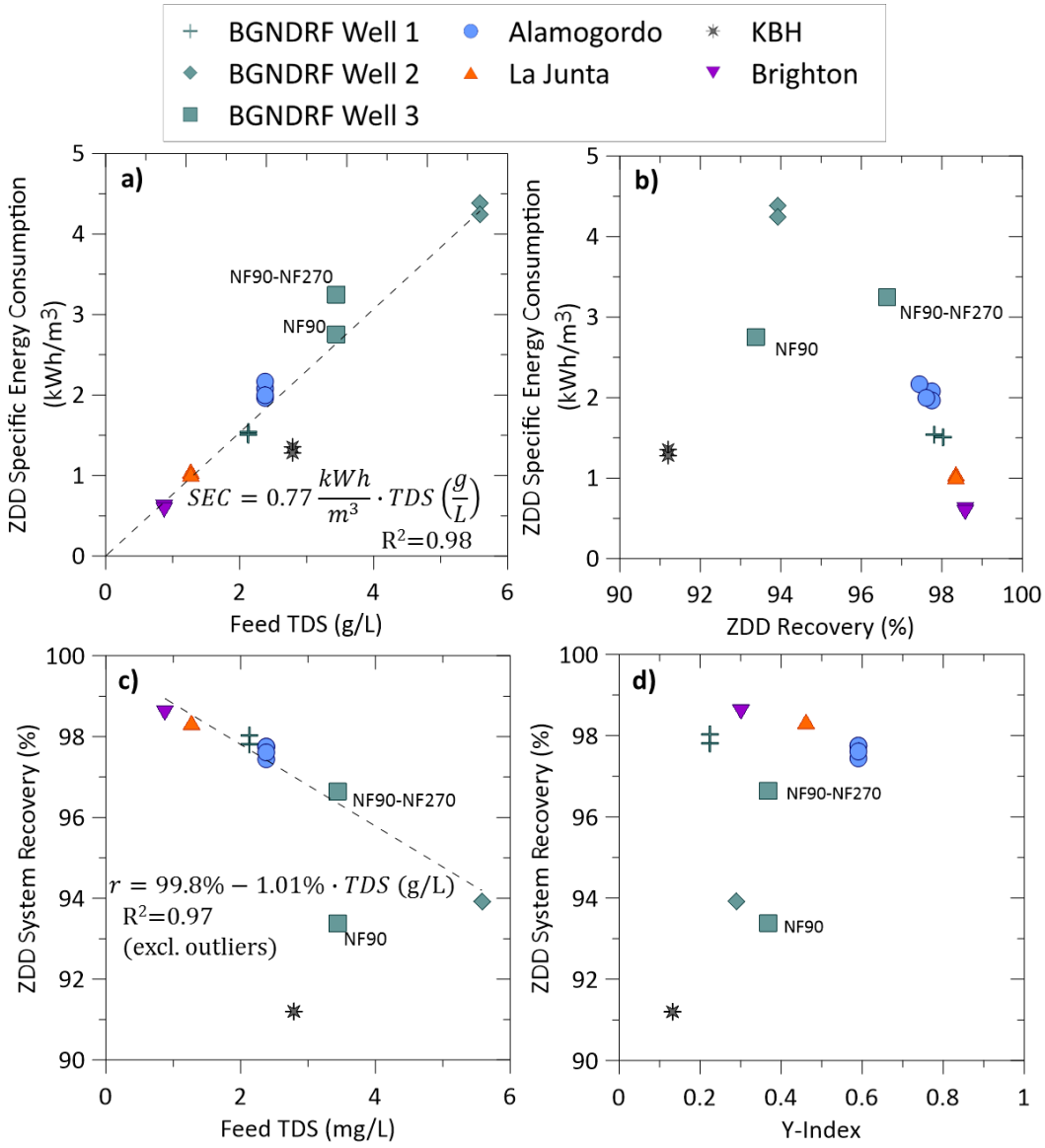

Figure 1.7. ZDD Performance Sensitivity to Water Quality

As shown in Figure 1.7b, the ZDD specific energy increases with increasing ZDD system recovery for a given feedwater composition (*e.g.*, BGNDRF Well 3). Because the ZDD recovery was intentionally maximized for the case studies, ZDD recovery is not an independent variable. The impact of Feed TDS is likely reflected in Figure 1.7b; that is, the higher recovery points correspond to lower Feed TDS. There are two noticeable outliers, namely the KBH and the NF90 Well 3 designs. Both designs involve NF90 membranes, which necessitates having a silica purge

(more so for the KBH) stream, so less energy is used by the EDM. As expected, the ZDD system recovery generally decreases with increasing Feed TDS (Figure 1.7c). The final comparison made was evaluation of the sensitivity of the system recovery to the proportion of calcium and sulfate (as measured by the *Y-Index*, Equation 1). In general, if the *Y-Index* is greater than 0.30, ZDD can achieve recovery of 95% or higher (Figure 1.7d). For the Well 3 chemistry, implementing the hybrid NF90-NF270 design allows for higher recovery than with NF90 and a silica bleed. For Well 1 and Brighton, high recovery is possible because the salinity is lower.

1.3.3. Comparison of ZDD Model Results and Pilot Data

A comparison was made of the ZDD model output to piloting results at the BGNDRF. Comparisons are not possible at the other pilot locations because the NF membrane design and ZDD configurations were different (*e.g.*, EDM before RO) from how the ZDD model was built. Since the feedwater quality was not constant (blend of two wells) and the operating conditions varied, the comparison was made to pilot data between June 24-28, 2017. In the pilot activities, the brackish water was acidified to mitigate sodium bicarbonate scale in the Mixed Na stream. Thus, the feedwater composition entered into the ZDD model included the reduced bicarbonate concentration (NF feed concentration) in order to compare the ZDD model's predicted permeate TDS. In comparison to the pilot tests, the ZDD model overpredicted the permeate TDS by 3% (see Table 4), underpredicted the electrical current by 6-10%, and underpredicted the voltage by 8-20%. However, during the ZDD pilot, some hydraulic leaks caused mineral scale formation in the Mixed Na compartments of the EDM stack, so it is likely that the higher voltage observed in pilot testing was due to the mineral scale.

Table 1.4. Comparison of ZDD Model and Pilot Data

Parameter	ZDD Model	Pilot Test
NF permeate	35 gpm	35 gpm
r_{RO}	55%	55%
RR_{EDM}	1	1
E_{Ca}	0.40	0.40
R_{ZDD}	97%	97%
Permeate TDS (sum of ions)	630 mg/L	650 mg/L
EDM Voltage/quad	1.1	1.2-1.4 (average)
EDM Current (amps)	40.5	43-45 (average)

1.4. Conclusions

A mathematical process model was created to evaluate the technical feasibility of implementing Zero Discharge Desalination (ZDD) for the desalination of brackish groundwater. This ZDD model uses a combination of proprietary software output (*e.g.,* Dow ROSA for RO/NF and Avista Advisor for antiscalant), pilot data, mass and energy balances, and theoretical calculations. The intent of this model was to evaluate "big picture" concepts in ZDD design, such as RO/NF recovery and EDM ion removal. For this reason, ROSA was used for the RO/NF portion for simplicity. A range of membranes (loose NF, tight NF, low-energy RO, standard RO) was chosen in order to evaluate a range of energy requirements and water quality performance. The ZDD model calculates the concentration of major ions and silica. Since there are many types of antiscalant available for different kinds of scale formation, the model assumes the user will consult antiscalant manufacturers or utilize other methods to evaluate solution stability. A variety of source water chemistries, NF-RO designs, and EDM designs were compared to develop a better understanding of the tradeoffs inherent in the ZDD design and operations. True feasibility, of course, depends on site-specific characteristics such as its available water supply options and the ability and cost of disposal of the desalination concentrate. However, some general observations can be made based on these modeling results:

- ZDD could produce permeate with 400-800 mg/L TDS from brackish water with up to 3,500 mg/L TDS while achieving ≥ 96% recovery and ≤ 2.7 kWh/m^3 (10 kWh/kgal) specific energy.
- Higher concentrations of silica in the feed will reduce the ability of ZDD to achieve a low TDS (<500 mg/L) product water and very high (>95%) recovery. Based on silica purge options, the ZDD system can tolerate up to approximately 40 mg/L as SiO_2 in the brackish feed.
- The specific energy of ZDD is lower with higher NF/RO recovery; however, care must be taken to mitigate scale formation and EDM operational costs.
- To reduce the specific energy consumption, design the EDM with a low current density and low recycle ratio (RR). Pilot results suggest that a minimum EDM velocity of 6-7 cm/s provided stable operation of the EDM stacks.
- ZDD is best-suited for brackish water with relatively high concentrations of calcium and sulfate. The model results suggest that ZDD is technically feasible over a wide range of Ca^{2+} and SO_4^{2-} concentrations. Based on this modeling, ZDD is expected to achieve high (>95%) recovery for feed waters with a *Y-Index* ≥ 0.30. Subsequent research will investigate the economic sensitivity to the Y-factor.) The higher the fraction of Ca^{2+} and SO_4^{2-} constituting the TDS, the more calcium sulfate can be recovered as a solid byproduct if salt recovery is implemented.
- Care must be taken in a ZDD design with nitrate, arsenic, boron, selenium, or other contaminants with low rejection by NF and RO membranes. These water quality parameters could constrain the design of a ZDD system but were not included in this model.

2. Zero Discharge Desalination with Salt Recovery: A Technical and Economic Evaluation

Globally, demand for water and energy are increasing with increasing population. High recovery desalination can mitigate environmental and economic concerns with brackish desalination by minimizing the amount of liquid waste. Zero Discharge Desalination (ZDD) has been demonstrated to achieve up to 98% recovery from brackish water while producing suitable water for drinking water, industrial, or agricultural purposes. ZDD combines a pressure-driven desalination process (reverse osmosis or nanofiltration) to produce high quality drinking and irrigation water and an electrically-driven process (electrodialysis metathesis) to reduce concentrate volume and improve system recovery. The ZDD model was expanded to include byproduct recovery, specifically sodium chloride (which is used for the EDM process in ZDD), as well as calcium sulfate and magnesium hydroxide. The updated ZDD model was used to evaluate the economic tradeoffs in ZDD design. The model results indicate that for a fixed water chemistry, the unit cost of water ($/m^3 product) 1) decreases with decreasing salt rejection of the primary desalting membrane (*e.g.*, designs utilizing NF membranes are less expensive than RO membranes), 2) decreases with increasing RO/NF recovery (*e.g.*, 75% versus 55%), and 3) decreases with decreasing EDM membrane resistance. A sensitivity analysis was performed for a ZDD design with NF operating at 75% recovery (hybrid NF90-NF270 staging), and the results of this analysis suggest that the unit cost 1) increases by 13-18% if more efficient, more expensive EDM membranes are employed, 2) is substantially affected by EDM equipment and power unit cost assumptions, and 3) is only slightly impacted by RO/NF equipment and evaporation pond cost assumptions; however the membrane choice and RO/NF recovery do have a noticeable impact on product water quality, ZDD specific energy consumption, and ZDD system recovery. Finally, model results with optimized ZDD designs (maximized RO/NF recovery, minimized EDM ion removal, NF membrane/staging chosen to achieve 500 mg/L or lower TDS product) indicate that the unit cost of water 1) generally decreases by $0.31/m^3 for every percent increase in ZDD

recovery (excludes KBH site), 2) increases by \$0.45/m^3 per kWh/m^3 increase in specific energy consumption (excludes KBH site), and 3) increases by \$0.37/m^3 per g/L increase in feed TDS. The incorporation of salt recovery decreased the cost of all ZDD designs by approximately 10-30%, even when revenue from salt sales was excluded.

2.1. Salt Recovery from Desalination Brine and Other Sources

Many useful salts, minerals, and metals can be extracted from both natural and desalination brines. The techniques for extraction include thermal processes like distillation, membrane separation such as electrodialysis or nanofiltration, and physical-chemical processes such as precipitation. Each process has its benefits and shortcomings, and surely, there is no one-size-fits-all approach. Each brine contains different dissolved constituents at unique concentrations, which means that the lowest cost recovery method will be unique for each location.

2.1.1. Solubility Limitations in Desalination Processes

Brackish water contains many dissolved salts that, when concentrated, may precipitate in desalination systems. This precipitation limits the recovery by processes such as reverse osmosis, nanofiltration, and electrodialysis alone. RO manufacturers have developed tools to predict membrane performance and solubility of RO concentrate streams, but as of yet, no commercial product is available for predicting ED membrane performance or high ionic strength solution solubility. Antiscalant manufacturers produce prediction software tools that are specific to their industry, and many allow non-vendors access. Geochemical software tools are available, but can be expensive.

Electrodialysis is able to concentrate solutions to a much higher degree than RO. However, there are limitations based on solubility and chemical potential. Electrodialysis Reversal (EDR) mitigates scaling by switching polarity, but this can reduce recovery. Electrodialysis Metathesis (EDM) offers a distinct advantage over RO and traditional ED in that it produces two product streams and two concentrate streams, each with highly soluble ionic composition [1,26]. All anions removed from the EDM feed are combined with Na^+ from the sodium chloride stream to produce

a concentrate stream with sodium salts (Mixed Na). All cations removed from the EDM feed are combined with Cl^- from the sodium chloride stream to produce a separate stream with chloride salts (Mixed Cl). Solubility data from Seidell for several pure salt solutions is shown in Figure 2.1 [27]. The chloride salts are all very soluble, and most have very little temperature dependence. Excluding sodium chloride (NaCl), the sodium salts have lower solubility as compared to the choride salts. Na_2SO_4 and Na_2CO_3 decline in solubility below 32 ºC.

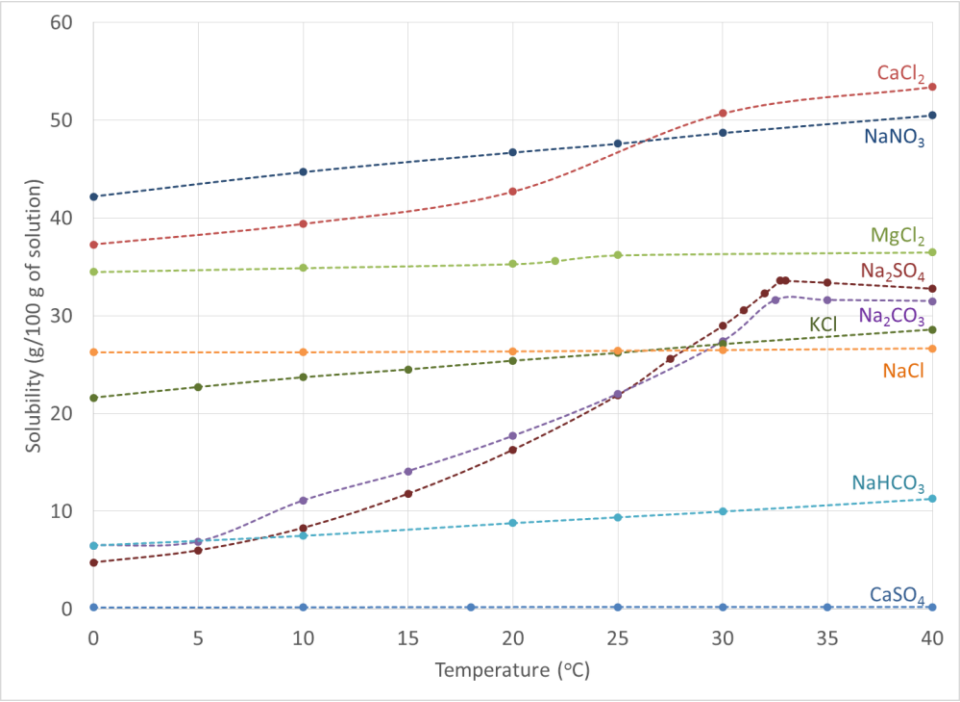

Figure 2.1. Solubility data for various salts as a function of temperature (Data from [27])

2.1.2. Mineral Recovery from Desalination Byproducts

An extensive report was produced for the WateReuse Research Foundation that describes the history of mining seawater for economically and socially useful products [28]. The authors also evaluated the potential for recovering useful products from desalination concentrate, as well. Recovery of salts and minerals from the sea has been in practice since 2200 BCE by the Chinese, and table salt recovery was implemented by the Maya in the Yucutan [28]. Seawater, and some desalination concentrate streams may contain enough metals (e.g. gold), salts (*e.g.* NaCl), or the

potential for mineral recovery (*e.g.* brucite ($Mg(OH)_2$)). However, the concentration, volume available, and capital and operating cost of recovery equipment will likely dictate the affordability of such recovery options. Several small scale pilot research projects have investigated the potential for byproduct recovery from brackish desalination concentrate [4,28–30]. Pilot and laboratory testing was performed at the East Cherry Creek Valley Water and Sanitation District in 2008 and in Sandoval County, New Mexico, in 2009 [30] that evaluated the potential for byproduct recovery. The authors looked at the potential for recovering $CaCO_3$, $CaSO_4$, Na_2SO_4, Na_2CO_3, NaCl, and $CaCl_2$ [30]. It was determined that the recovery of sodium chloride and deep well injection of sodium sulfate would be more "economical than the annual cost of RO concentrate disposal by deep well injection" for a brackish water with 12,000 mg/L TDS in New Mexico [30]. The Colorado study found that the "dried mixed salts had little commercial value" and that more advanced extraction techniques would likely be more expensive than the value of the products recovered [30]. In 2017, a company, EWM, opened a facility designed to recover calcium sulfate, magnesium hydroxide, hydrochloric acid, sodium hydroxide, and desalinated water from the Kay Bailey Hutchison (KBH) Desalination Plant concentrate [31]. EWM operated a pilot at the KBH plant prior to building their facility. A research group in Israel evaluated a ZLD process that employed a hybrid process using ED to treat RO concentrate and the combined concentrate was evaporated using a WAIV system [32]. WAIV is an enhanced evaporation system that shows promise to substantially reduce the size of evaporation ponds [33]. Katzir et al., concluded that salt recovery using the WAIV system as the means for salt precipitation and water evaporation was feasible. The ZDD process offers distinct advantages over the processes described above. The concentration of the target ions is higher than in seawater and typical desalination concentrate (which may help with revenue generation), the volume is lower (may help with capital cost expenditures), and distinct concentrate streams are produced (as opposed to multiple salts in a single stream).

2.2. Methods and Materials (Updated ZDD Model and Economic Considerations)

The ZDD model developed and described in a recent article [1] was expanded to include calculations for salt recovery using simple precipitation and evaporation equipment. The model data was output into Excel for spreadsheet evaluation of the potential for salt recovery and the impact on the unit cost of water (*i.e.*, cost per volume of water produced). The target byproducts for sale included calcium sulfate and magnesium hydroxide, along with sodium chloride, which would be used to offset the cost of salt purchased for desalination by ZDD. Visual MINTEQ (version 3.1) [34] was used with the Specific ion Interaction Theory (SIT) activity coefficient model (applicable for ionic strength less than 1M) to calculate the concentration of calcium sulfate and magnesium hydroxide that would precipitate.

2.2.1. EDM Design Considerations

Current efficiency can be calculated in several ways, but is essentially a ratio of the charge (calculated from concentration) that leaves or enters a stream in the EDM. Several were evaluated during ZDD pilot testing [26]. One method involves a ratio of the ions that are removed from the EDM feed to the current supplied:

$$\varepsilon_{feed} = \frac{F \cdot Q_E \cdot (C_E - C_d)}{I \cdot N_{quads}} \tag{2.13}$$

Where:

F = Faraday's Constant, 96,485 C/eq

I = Measured EDM Stack current, amps

N_{quads} = Number of quads in EDM stack

C_E = Equivalent concentration of the EDM feed

C_d = Equivalent concentration of the EDM diluate

The next method for estimating current efficiency is a ratio of the ions supplied by the sodium chloride stream to the current supplied:

$$\varepsilon_{NaCl} = \frac{F \cdot m_{NaCl}}{I \cdot N_{quads}} \tag{2.14}$$

Where m_{NaCl} (eq/sec) is the molar flow of sodium chloride into the EDM stack and is calculated from the daily sodium chloride consumption, M_{NaCl} (lb/day). Each of these current efficiency calculation methods is limited by the quality of the data gathered in the field. However, enough data was gathered to compare the various methods. The calculated current efficiency values for the Phase 2 operations in Alamogordo are summarized in Figure 2.2. Current efficiency values greater than 100 were assumed to be erroneous and excluded from the data set. Excluding the outliers, the calculated values for ε_{feed} were between 65-90% with an average of 72%. Similarly, the calculated values for ε_{NaCl} were between 76-95% with an average of 84%.

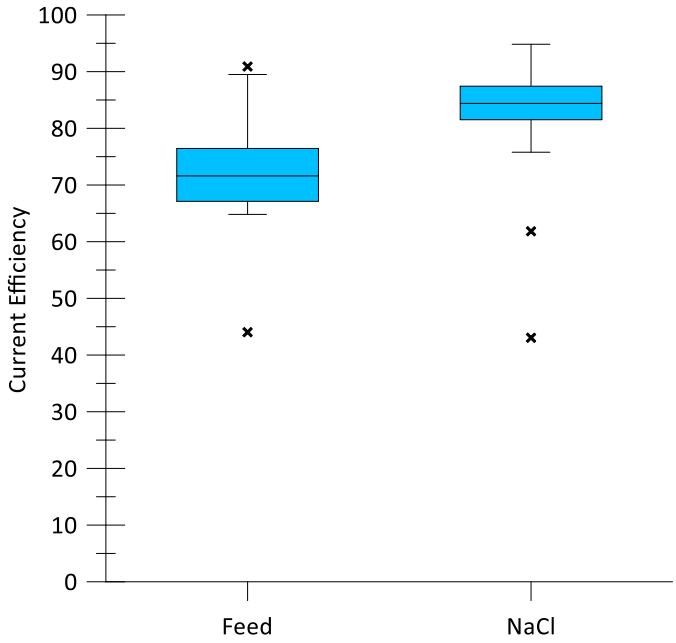

Figure 2.2. Current Efficiency Data from ZDD Pilot Activities Calculated from the Feed and Sodium Chloride (NaCl)

Three sets of EDM stack and membrane conditions were used to evaluate the capital and operating cost tradeoffs for several ZDD designs. As summarized in Table 2.1, two sets involved MEGA membranes and one involved NEOSEPTA membranes. The NEOSEPTA EDM design involves using normal anion- and cation-exchange membranes (AMX, CMX) for the EDM feed-diluate compartments and monovalent-selective anion- and cation-exchange membranes (ACS,

CMX-S). The membrane characteristics are mostly from the ASTOM website [35] and the EDM stack design was chosen to be identical to the MEGA stacks in order to facilitate a comparison of the membrane performance. It is acknowledged that this is not a realistic assumption since each ED/EDM stack is different. The current efficiency was chosen to be 93%, based on values reported in the literature ranging from 90-95% for NEOSEPTA and similarly performing membranes [14,36–38]. The MEGA stack and spacer information is taken from the user manual obtained during piloting. The shadow factor is defined herein as the portion of the EDM membranes available for desalination and the value used (0.64) is similar to what was reported by McGovern et al. (2014) and Lee et al. (2002) [11,39]. The difference between the two MEGA designs is the current efficiency (ε). The lower value (ε=75%) is the value used in Chapter 1 and was chosen based on a range of ε_{feed} values (see Figure 2.2). The higher value (ε=84%) is also based on ZDD pilot data, but is the average calculated value for ε_{NaCl} (see Figure 2.2). Jaroszek & Dydo (2018) studied EDM for the production of potassium nitrate and reported a current efficiency of 82-84% for RALEX & 94-95% for NEOSEPTA membranes [38].

Table 2.1. EDM Membrane and Stack Design Conditions & Assumptions used in Updated ZDD Model

	MEGA (low ε)	MEGA (high ε)	NEOSEPTA
ρ_{CEM}, Ω-cm^2 (cation-exchange membrane resistance)	10	10	CMX: 3, CMX-S[4]: 4.75
ρ_{AEM}, Ω-cm^2 (anion-exchange membrane resistance)	7.5	7.5	AMX: 2.4, ACS: 3.8
A_{stack}, cm^2 (exposed membrane area)	4,200		
W_{stack}, mm (membrane width)	320		
t_{spacer}, mm (spacer thickness)	0.8		
β, (shadow factor)	0.65		
ε	75%	84%	93%

[4] No published data is available for the CMX-S membrane, so a ratio of the ACS to AMX membranes was used as a multiplication factor with the CMX membrane to calculate the CMX-S resistance (3.8/2.4*3=4.75)

As described in Section 2.4 of Appendix A, the ion removal by the EDM is characterized using relative removal ratios for each ion (RRR_i). These are the relative removal of an ion as compared to calcium removal (E_{Ca}). Both MEGA cases (low ε and high ε) use the same values shown in Table S.7 of Appendix A. The NEOSEPTA case is based on unpublished experiments at the KBH Desalination Plant. The RRR_i values calculated from the EDM with NEOSEPTA membranes (CMX, AMX, CMX-S, ACS) are summarized in Table 2.2.

Table 2.2. EDM Performance and Relative Removal Ratios with NEOSEPTA membranes

	Average removal of ion (range of values)	Relative removal, (Ca as basis)	EDM Removal used in model (RRR_i)
$R_{EDM,Ca}$	24% (23-25%)0.	100%	E_{Ca}
$R_{EDM,Mg}$	31% (18-26%)	94%	$0.9*E_{Ca}$
$R_{EDM,Na}$	17% (15-18%)	71%	$0.7*E_{Ca}$
$R_{EDM,Cl}$	23% (21-25%)	96%	$1*E_{Ca}$
$R_{EDM,SO4}$	11% (10-13%)	48%	$0.5*E_{Ca}$
$R_{EDM,HCO3}$	9% (7-10%)	37%	$0.4*E_{Ca}$

2.2.2. Salt Recovery Methods Utilized

Three salt recovery techniques were evaluated in this research, ranging from low complexity (Salt Recovery 1, SR-1), to medium complexity (Salt Recovery 2, SR-2), to high complexity (Salt Recovery 3, SR-3). In Salt Recovery 1, the entire volume of Mixed Na and Mixed Cl concentrate streams from the ZDD are mixed and sent to a clarifier to precipitate calcium sulfate. If needed, a silica purge stream is sent to a separate evaporation pond. The supernatant from the calcium sulfate clarifier is then sent to an evaporation pond where the concentration is doubled after a 50% volume reduction. In Salt Recovery 2, the Mixed Na and Mixed Cl streams are mixed such that a stoichiometric ratio of 1:1 is achieved using Ca (in the Mixed Cl) and SO_4 (in the Mixed Na). If needed, excess Mixed Cl or Mixed Na is sent to a second evaporation pond (with the silica purge water). In Salt Recovery 3, the Mixed Cl stream is treated with lime in a clarifier to precipitate magnesium hydroxide and exchange Ca for Mg. The supernatant from this

clarifier is calcium-rich and is combined with the Mixed Na in a second clarifier to produce calcium sulfate using a stoichiometric ratio of 1:1 of $Ca:SO_4$. Each of the salt recovery methods are shown in Figure 2.3. The model allows for excess Mixed Na or Mixed Cl to be sent to an evaporation pond if necessary.

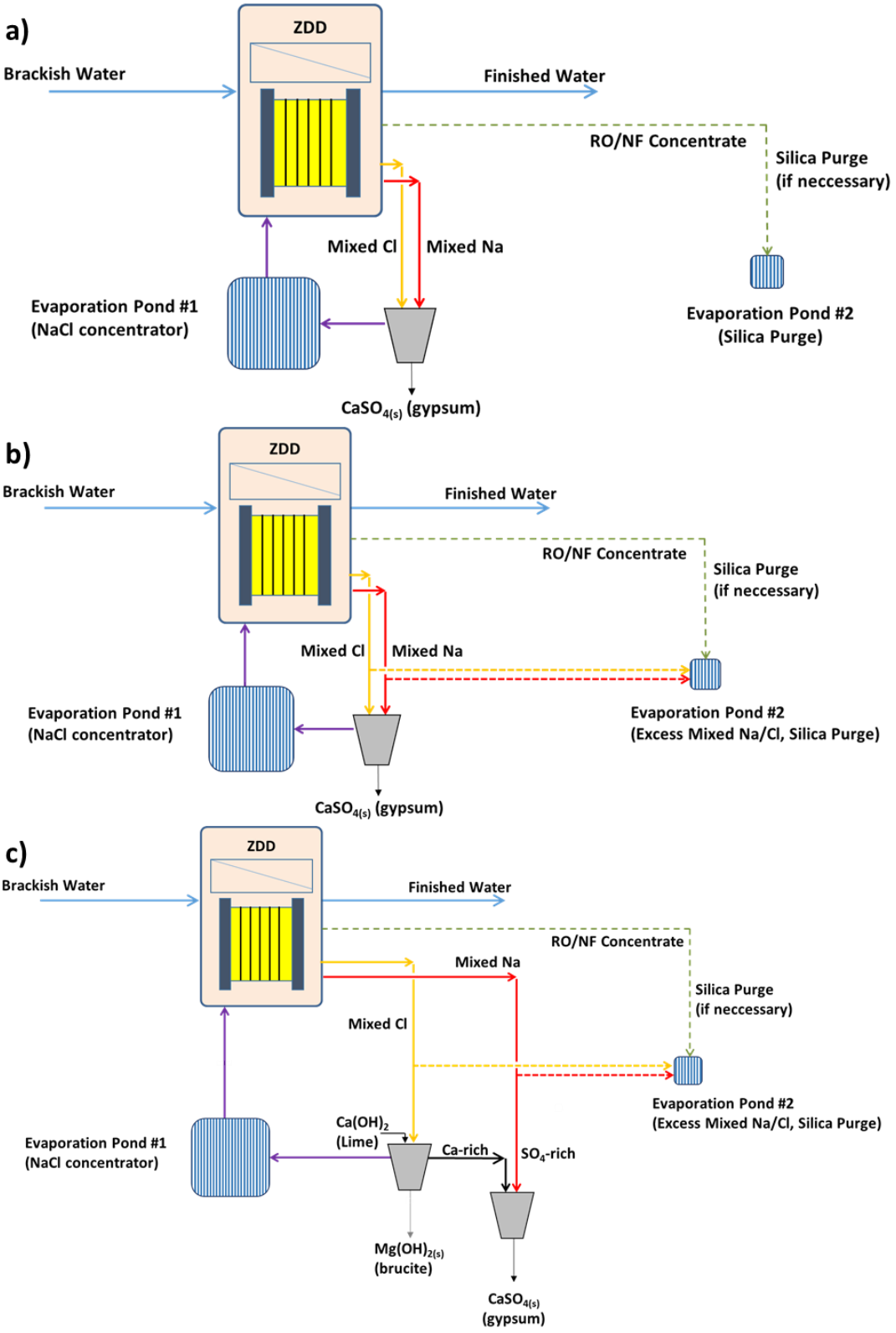

Figure 2.3. Simplified Diagrams of a) Salt Recovery 1, b) Salt Recovery 2, and c) Salt Recovery 3 Processes

The evaporation ponds required for ZDD with and without salt recovery are all calculated using the same general methodology and is described here briefly (see Appendix B, Section 6.1-6.3, for additional details). The acreage of the waste pond, A_{waste}, (Evaporation Pond #2 in Figure 2.3) is the flow of the silica purge, Q_{Si}, (and excess Mixed Na or Cl, if necessary) divided by the evaporation rate, r_{evap}.

$$A_{waste} = \frac{Q_{Si}+Q_{waste}}{r_{evap}} \tag{2.15}$$

In Salt Recovery 1, Q_{waste} is zero. For Salt Recovery 2 and 3, Q_{waste} is calculated based on daily volumes (V) using the excess Mixed Cl if the molar ratio of SO_4 to Ca ($R_{SO4/Ca}$) is less than 1 or using Mixed Na if the molar ratio of SO_4 to Ca is more than 1:

$$R_{SO4/Ca} = \frac{C_{SO4(Mixed\ Na)}}{C_{Ca(Mixed\ Cl)}} \tag{2.16}$$

$$Q_{waste} = \frac{V_{mCl}-V_{mCl(to\ SR\ process)}}{day} \tag{2.17}$$

$$Q_{waste} = \frac{V_{mNa}-V_{mNa(to\ SR\ process)}}{day} \tag{2.18}$$

If $R_{SO4/Ca}$ is less than 1, the daily volume of Mixed Na and Mixed Cl sent to the salt recovery process ($V_{mCl(to\ SR\ process)}$ and $V_{mNa(to\ SR\ process)}$) are calculated as:

$$V_{mNa(to\ SR\ process)} = V_{mNa} \tag{2.19}$$

$$V_{mCl(to\ SR\ process)} = V_{mCl} \cdot R_{SO4/Ca} \tag{2.20}$$

If $R_{SO4/Ca}$ is greater than 1, the daily volume (or flow per day) of Mixed Na and Mixed Cl sent to the salt recovery process ($V_{mCl(to\ SR\ process)}$ and $V_{mNa(to\ SR\ process)}$) are calculated as:

$$V_{mNa(to\ SR\ process)} = \frac{V_{mNa}}{R_{SO4/Ca}} \tag{2.21}$$

$$V_{mCl(to\ SR\ process)} = V_{mCl} \tag{2.22}$$

In order to concentrate the sodium chloride solution, half the volume of the supernatant from the calcium sulfate reactor is evaporated. The size of the evaporation pond for recovering sodium chloride is calculated as:

$$A_{NaCl} = 0.5 \cdot \frac{V_{mNa(to\ SR\ process)}+V_{mCl(to\ SR\ process)}}{r_{evap}} \tag{2.23}$$

The concentration of the ions in solution just before precipitation of calcium sulfate is calculated using volumetric blending. For example, the concentration of constituent *i* ($c_{sup,i}$) is:

$$c_{sup,i} = \frac{V_{mNa(to\ SR\ process)} \cdot c_{mNa,i} + V_{mCl(to\ SR\ process)} \cdot c_{mCl,i}}{V_{mNa(to\ SR\ process)} + V_{mCl(to\ SR\ process)}} \quad (2.24)$$

The calculated concentrations are then entered into Visual MINTEQ and with only allowing calcium sulfate to precipitate (sampling during piloting indicated that the solid was mostly calcium sulfate), the molar concentration of calcium sulfate (Δ_{CaSO4}) is extracted and used to calculate the daily mass of calcium sulfate produced from the ZDD concentrate:

$$M_{CaSO4} = (\Delta_{Ca} + \Delta_{SO4}) \cdot \left(V_{mNa(to\ SR\ process)} + V_{mCl(to\ SR\ process)}\right) \quad (2.25)$$

Where Δ_{Ca} and Δ_{SO4} are the concentration of calcium and sulfate (calculated from the Δ_{CaSO4} and the molar mass of calcium and sulfate)[5]. Finally, the concentration of the remaining supernatant is calculated and doubled since half the volume will be evaporated in the sodium chloride evaporation pond. Since only calcium sulfate was allowed to precipitate, the only concentrations that changed were the calcium and sulfate. The ZDD model calculates the mass of sodium chloride that is recovered by using the lesser of the two molar concentrations for Na and Cl in the supernatant.

In the Salt Recovery 3 process, the Mixed Cl stream is treated with lime to precipitate magnesium hydroxide. In some cases, this allows for more calcium sulfate to be recovered since there will be a closer stoichiometric ratio of calcium in the Mixed Cl and sulfate in the Mixed Na. Additionally, this will lead to a greater purity of recovered sodium chloride. The ZDD model's predicted chemistry for the Mixed Cl stream is entered into MINTEQ with an assumed solution pH of 11.1, which is ideal for maximum magnesium hydroxide precipitation [40]. The molar concentration of magnesium hydroxide (ΔC_{Mg}) is extracted and used to calculate the amount of

[5] In a few design cases, Visual MINTEQ indicated that the ionic strength was too high for the activity correction model chosen (SIT); however, it did converge on a solution and the values were used. Alternatively, another software such as PHREEQC could have been used with the Pitzer database to theoretically provide a more accurate estimation, but the difference in predicted precipitation of calcium sulfate between SIT and Pitzer models was assumed to be insignificant for the purposes of this manuscript.

lime necessary to accomplish the magnesium hydroxide precipitation. First, the amount of alkalinity (eq/L) in any solution is defined as:

$$Alk = 2\frac{eq}{mol} \cdot C_{CO_3^{2-}} + 1\frac{eq}{mol} C_{HCO_3^-} + 1\frac{eq}{mol} C_{OH^-} - 1\frac{eq}{mol} C_{H^+} \quad (2.26)$$

Where all concentrations are expressed in mol/L. Using known relationships for the speciation of bicarbonate and carbonate and the user input for the pH of the solution before and after lime addition (the ZDD model uses 7.0 and 11.1, respectively), the equation for total alkalinity is therefore:

$$Alk(CT, pH) = CT \cdot \left[\left(\frac{10^{-pH}}{10^{-6.3}} + 1 + \frac{10^{-10.3}}{10^{-pH}}\right)^{-1} + 2 \cdot \left(\frac{(10^{-pH})^2}{10^{-6.3} \cdot 10^{-10.3}} + 1 + \frac{10^{-pH}}{10^{-10.3}}\right)^{-1}\right] + \frac{10^{-14}}{10^{-pH}} - 10^{-pH} \quad (2.27)$$

Where CT is the total molar concentration of all carbonate system species. Activity coefficients were ignored in Equation 2.27 because CT was assumed to be zero for calculating the required lime dose (Equation 2.28), and pH is the negative logarithm of the activity of the hydrogen/hydronium ion. The concentration of lime necessary is then calculated as the difference between the alkalinity before and after lime addition, charge of calcium (z_{Ca}), and the MINTEQ-calculated molar concentration of precipitated magnesium hydroxide (ΔC_{Mg}):

$$C_{Lime}\left(\frac{mol}{L}\right) = \frac{\left(Alk(CT=0, pH_{AL}=11.1) - Alk(CT=0, pH_{BL}=7.0)\right)}{z_{Ca}} + \Delta C_{Mg}\left(\frac{mol}{L}\right) \quad (2.28)$$

The concentration of the Mixed Cl stream after lime treatment (C_{mCl_AL}) is then calculated by increasing the calcium concentration using C_{Lime} and decreasing the Mg concentration using ΔC_{Mg} (and converting both using the molar mass of lime or Mg, respectively). C_{mCl_AL} is then used, along with the daily volumes of Mixed Cl and Mixed Na sent to the salt recovery process to calculate the supernatant and recovered sodium chloride as described previously.

The final section of the expanded ZDD model outputs the calculated values for the area of the waste and sodium chloride recovery evaporation ponds, the daily production of calcium sulfate, sodium chloride, and magnesium hydroxide, the daily lime consumption, the modeled sodium chloride quality, the MINTEQ molar concentrate values used for the calcium sulfate and

magnesium hydroxide precipitation, and the calculated ratios of sulfate to calcium for SR-2 and SR-3.

A modified *Y-Index* (originally defined in Equation 1.1) was created to incorporate the possibility for magnesium hydroxide, which would also improve the calcium sulfate recovery in many cases since the calcium and sulfate concentrations would be more balanced:

$$Y\text{-}index_{w/Mg} = \frac{minimum\left\{\left[C_{Ca}\left(\frac{meq}{L}\right)+C_{Mg}\left(\frac{meq}{L}\right)\right],\ \ C_{SO4}\left(\frac{meq}{L}\right)\right\}}{Normality\left(\frac{meq}{L}\right)} \quad (2.13)$$

2.2.3. ZDD Cost Estimation Process

Since every desalination system will have a unique design that impacts both the capital cost (*i.e.,* building codes, land cost) and operating cost (*i.e.*, cost of electricity), the cost model used herein is expected to be in the correct order of magnitude. Thus, the cost comparisons provided here are expected to show the relative impact of design choices and whether salt recovery is beneficial from a cost perspective. The assumptions used are summarized in Table 2.3, and an example with equations is shown in Appendix C. CapEx and OpEx are shorthand for capital and operating cost, respectively.

Table 2.3. Capital and Operating Cost Assumptions

Capital or Operating Cost Item	Value used in Model	Details on Basis	Reference
CapEx Items			
EDM stack (MEGA)	\$1,300/m^2 (EDM active membrane area)	Estimated from ZDD final report	[26]
EDM stack (NEOSEPTA)	\$3,000/m^2 (EDM active membrane area)	Doubled the value from articles w/ similar membrane resistance per effective cell pair	[39], [41]
RO/NF	\$1.50/gal/day (RO/NF permeate)	Assumption; literature showed range of \$1.135-4.54/gpd (permeate)	[42], [43], [44], [45]

Capital or Operating Cost Item	Value used in Model	Details on Basis	Reference
Calcium Sulfate (gypsum) Recovery	$0.79 gal/day (feed)	Clarifier + Dewatering Equipment	Calculated from Appendix G-1 in [43]
Magnesium Hydroxide Recovery	$0.96 gal/day (feed)	Clarifier + Dewatering + Lime Dosing Equipment	Calculated from Appendix G-1 in [43]
OpEx Items			
Capacity Factor[6]	0.9	Assumption	
Installation Factor	1.5	Assumption	Similar to value calculated from Appendix G-1 in [43]
Borrowing Terms	6%, 20 years	Assumption	
Cost of Electricity	$0.10/kWh	Assumption	
Sodium Chloride	$0.058/lb	Bulk Solar Salt	Table 8 in [46]
Lime	$0.055/lb	Quick Lime	Table 5 in [47]
RO/NF Chemicals	$0.07/kgal (feed)		Calculated from Appendix G-1 in [43]
RO/NF Membrane Replacement	$0.16/kgal (feed)		Calculated from Appendix G-1 in [43]
EDM Membrane & Electrode Replacement	$0.32/kgal (product)	ZDD final report	[26]
Evaporation Pond Maintenance	0.5% of installed CapEx		[48]
Gypsum Sale Price	$0.0035/lb	Assume 25% of retail price to be conservative (gypsum market is saturated)	Table 1 in [49]

[6] Capacity Factor is the fraction of time that a plant is operational. A value of 0.9 assumes that the plant would be shut down for maintenance 10% of the year.

Capital or Operating Cost Item	Value used in Model	Details on Basis	Reference
Magnesium Hydroxide Price	$0.1072/lb	Assume 50% of retail price (market is stronger for Mg materials)	Table 3 in [50]

2.3. Results and Discussion

2.3.1. Impact of Primary Desalter (RO/NF) Membrane Choice

In order to evaluate the impact of RO/NF membrane choice and desalination load, the designs with the highest and lowest calculated ZDD specific energy (see Table 1.2 and Figure 1.5a) were analyzed for cost performance. The highest specific energy designs were Case 3c (see Table 2.4), which had low RO/NF recovery and high EDM calcium removal. The lowest specific energy designs were Case 2a (see Table 2.5), which had high RO/NF recovery and lower EDM calcium removal. For each of these designs, a second case with lower current density was created in order to assess the tradeoffs between capital and operating costs. The lower current density designs involve more EDM stacks and lower EDM energy consumption.

Table 2.4. Summary of ZDD Designs for Case 3c (r_{RO}=55%, RR_{EDM}=1, E_{Ca}=50%) treating the BGNDRF Wells 1&4 blend

Membrane		**NF270**		**NF90-NF270**		**NF90**		**XLE**		**BW30**	
i_{edm}		high	low	high	low	high	low	high	low	high	low
N_{stacks}		89	163	102	163	122	156	122	153	123	150
v_{stack}	cm/s	9.5	5.2	8.3	5.2	6.6	5.2	6.5	5.2	6.3	5.2
i_{edm}	A/m^2	131	71.7	126	79.0	117	91.8	117	93.6	117	95.6
LCD	A/m^2	137	116	132	116	124	116	123	116	123	116
i_{edm}/**LCD**		96%	62%	96%	68%	95%	79%	95%	81%	95%	82%

Table 2.5. Summary of ZDD Designs for Case 2a (r_{RO}=75%, RR_{EDM}=3, E_{Ca}=30%) treating the BGNDRF Wells 1&4 blend

Membrane		**NF270**		**NF90-NF270**		**NF90**		**XLE**		**BW30**	
$\mathbf{i_{edm}}$		high	low	high	low	high	low	high	low	high	low
$\mathbf{N_{stacks}}$		81	133	97	133	97	113	95	109	95	105
$\mathbf{v_{stack}}$	cm/s	8.5	5.2	7.1	5.2	6.1	5.2	5.9	5.2	5.7	5.2
$\mathbf{i_{edm}}$	A/m^2	126	76.9	120	87.8	115	99.1	115	100	114	103
LCD	A/m^2	133	116	127	116	121	116	121	116	120	116
$\mathbf{i_{edm}/LCD}$		95%	66%	95%	75%	95%	85%	95%	86%	95%	88%

In general, the unit cost ($/m^3 permeate produced from desalinating the Well 1-4 blend (Table 1.1)) increases as the RO/NF salt rejection increases (*i.e.,* designs with BW30 membranes were more expensive than designs with NF270 membranes), as shown in Figure 2.4. The higher current density (i_{edm}>90%) designs were slightly less expensive (1-6%) than the lower current density (i_{edm}<90%) designs. A more noticeable effect is visible between the Case 2a (r_{RO}=75%) and Case 3c (r_{RO}=55%), where the Case 2a designs were 13-21% less expensive than the Case 3a designs.

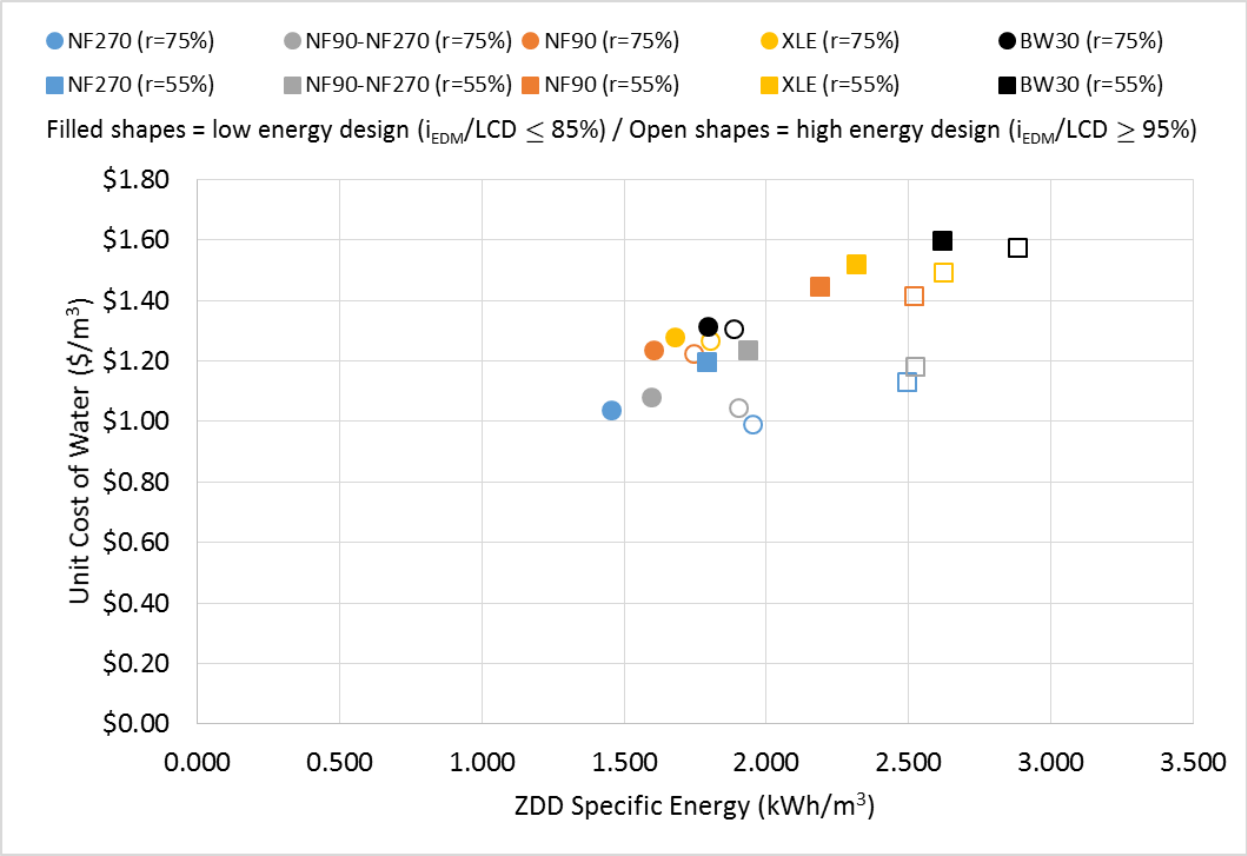

Figure 2.4. Impact of Primary Desalter Membrane Choice treating the BGNDRF Wells 1&4 blend: Unit Cost of Water vs ZDD Specific Energy

The relative proportions of energy used by the EDM and RO/NF systems for Case 2a and Case 3c are shown in Figure 2.5a and Figure 2.5b, respectively. As is visible, the EDM specific energy consumption dominates the ZDD specific energy consumption for both cases, but is around 30% higher for the Case 3c designs. The higher energy consumption leads to higher unit cost for the Case 3c designs (Figure 2.5c and d). Finally, even though the lower current density designs led to lower operating costs of water, the increased capital cost expenditure leads to an overall increase in the unit cost of water.

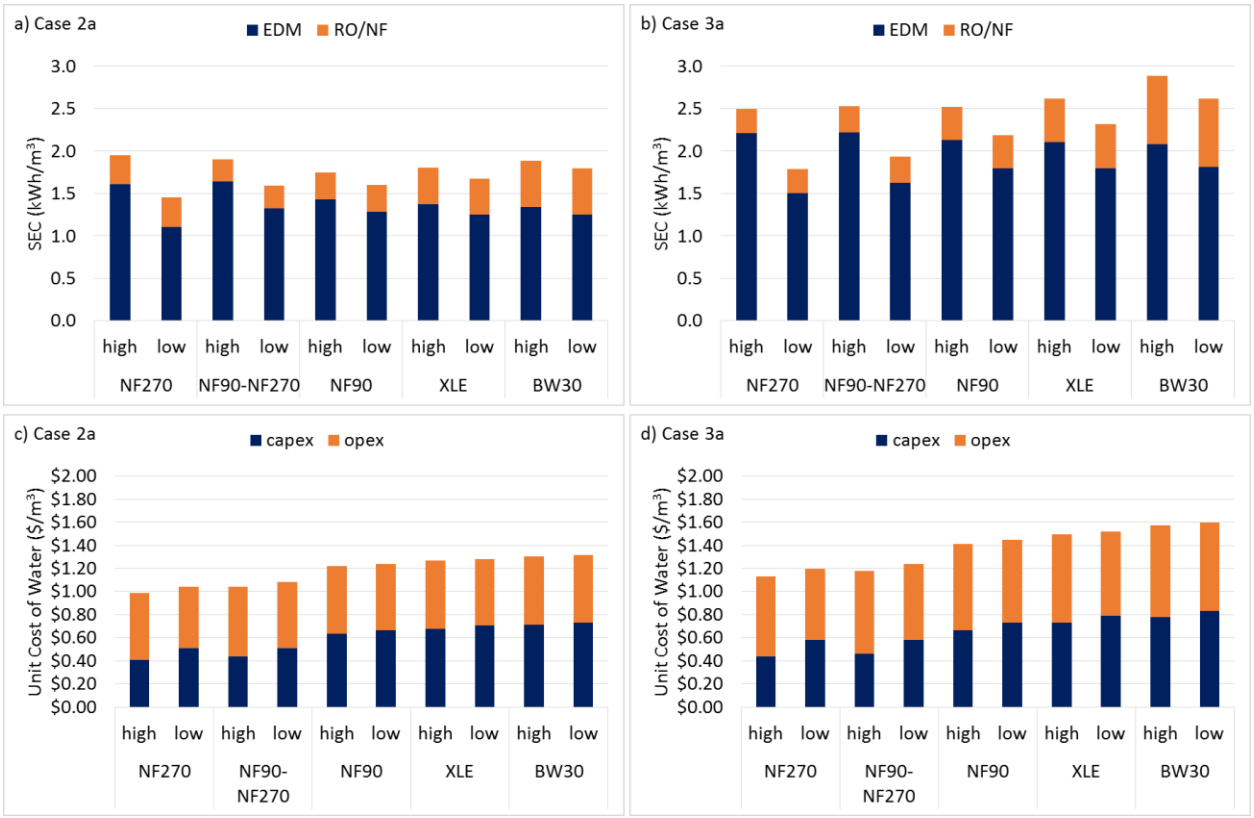

Figure 2.5. Breakdown of EDM and RO/NF Impact on Specific Energy Consumption and Unit Cost of Water for treating the BGNDRF Wells 1&4 blend using Case 2a (r_{RO} = 75%/E_{Ca} = 0.3, parts a and c) and Case 3a (r_{RO} = 55%/ E_{Ca} = 0.5, parts b and d)

If a desalination plant wants to install higher salt rejection membranes to achieve lower permeate TDS, it comes with a greater cost. The BW30 membrane designs are 25-29% more expensive than the NF270 membrane designs. Operating at higher RO/NF recovery (75% versus 55%) reduces the ZDD unit cost by 12-18% versus and allows for somewhat (<1%) higher ZDD recovery (Figure 2.6 and Figure 2.7). Designs with higher salt rejection will have lower recovery and higher cost. For example, the NF designs allow for 6% higher recovery and around 30% less expensive than the BW30 Case 2a (75% recovery) designs.

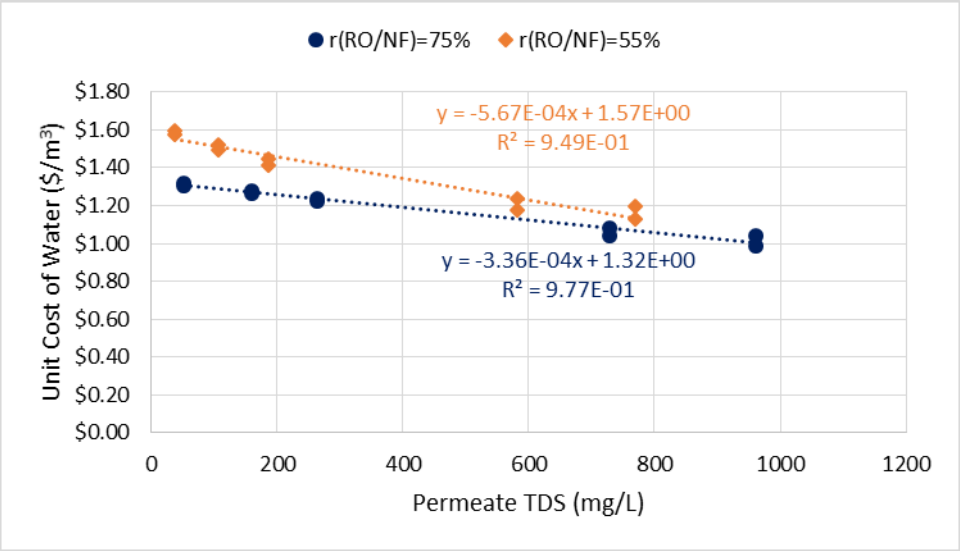

Figure 2.6. Relationship between Unit Cost of Water and Permeate TDS for treating the BGNDRF Wells 1&4 blend

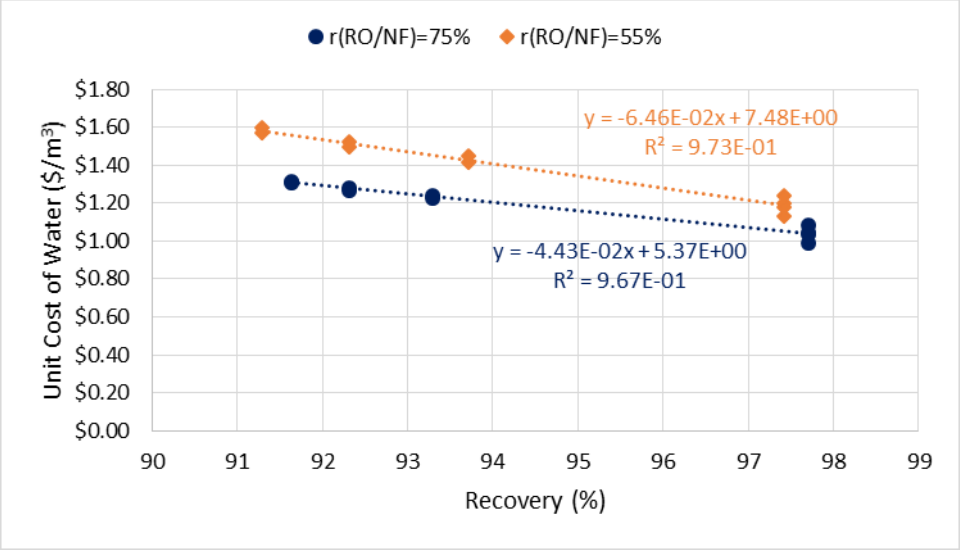

Figure 2.7. Relationship between Unit Cost of Water and ZDD Recovery for desalinating the BGNDRF Wells 1&4 blend

2.3.2. Cost Sensitivity Analysis and Capital versus Operating Tradeoffs

In order to further evaluate how capital and operating cost factors impact the cost of ZDD desalination of the Well 1&4 blend water, several cases were chosen. The cost basis is the Case 2a design with MEGA membranes as described earlier. Two other EDM membrane choices are also evaluated, namely MEGA with higher current efficiency (84% versus 75%) and NEOSEPTA

membranes (See Table 2.1 and Table 2.2 for EDM membrane characteristics). High and low cost versions of EDM, RO/NF, evaporation ponds, and cost of electricity were used to evaluate the sensitivity of ZDD cost.

Table 2.6. Sensitivity Analysis Assumptions for Evaluation of ZDD System Cost Estimates

	MEGA EDM CapEx	**NEOSEPTA EDM CapEx**	**RO/NF CapEx**	**Cost of Electricity**	**Evaporation Pond CapEx**
cost basis	$1300/m^2	$3000/m^2	$1.50/gpd ROp	$0.10/kWh	$200K/acre
high cost EDM	$2600/m^2	$4500/m^2	$1.50/gpd ROp	$0.10/kWh	$200K/acre
low cost EDM	$800/m^2	$1500/m^2	$1.50/gpd ROp	$0.10/kWh	$200K/acre
high cost evap	$1300/m^2	$3000/m^2	$1.50/gpd ROp	$0.10/kWh	$300K/acre
low cost evap	$1300/m^2	$3000/m^2	$1.50/gpd ROp	$0.10/kWh	$100K/acre
high cost RO	$1300/m^2	$3000/m^2	$2/gpd RO	$0.10/kWh	$200K/acre
low cost RO	$1300/m^2	$3000/m^2	$1/gpd RO	$0.10/kWh	$200K/acre
high cost kWh	$1300/m^2	$3000/m^2	$1.50/gpd ROp	$0.15/kWh	$200K/acre
low cost kWh	$1300/m^2	$3000/m^2	$1.50/gpd ROp	$0.05/kWh	$200K/acre

The largest changes to the ZDD cost of desalinating the BGNDRF Wells 1&4 blend involved the EDM capital cost and the cost of electricity, as shown in Figure 2.8. Doubling the unit cost ($/m2) for the EDM caused the unit cost of ZDD to increase by 16-18% for the three EDM designs. A 50% increase or decrease in the cost of electricity caused the unit cost of ZDD to increase or decrease by nearly 10%. The other options tested yielded small changes (5% or lower difference from the cost basis). In most cases the incorporation of salt recovery reduces the unit cost of ZDD by 20-30%. The high cost EDM case is the only exception, with a 5% or lower decrease in cost. While the design and capital cost may be different for a NEOSEPTA membrane design, it is interesting to note that even though the ZDD specific energy consumption is lower by about 22% for the NEOSEPTA designs, the impact is negated by the higher capital cost in all cases. Additional calculations were made with higher current density to reduce the number of EDM

stacks by 10-11%, but even then the unit cost decreased only slightly (≤5%). Similarly, additional calculations were made with the MEGA stacks to produce designs with lower current density (6% lower i_{EDM}, 11% higher EDM CapEx), but the impact on unit cost was even less visible (≤3%).

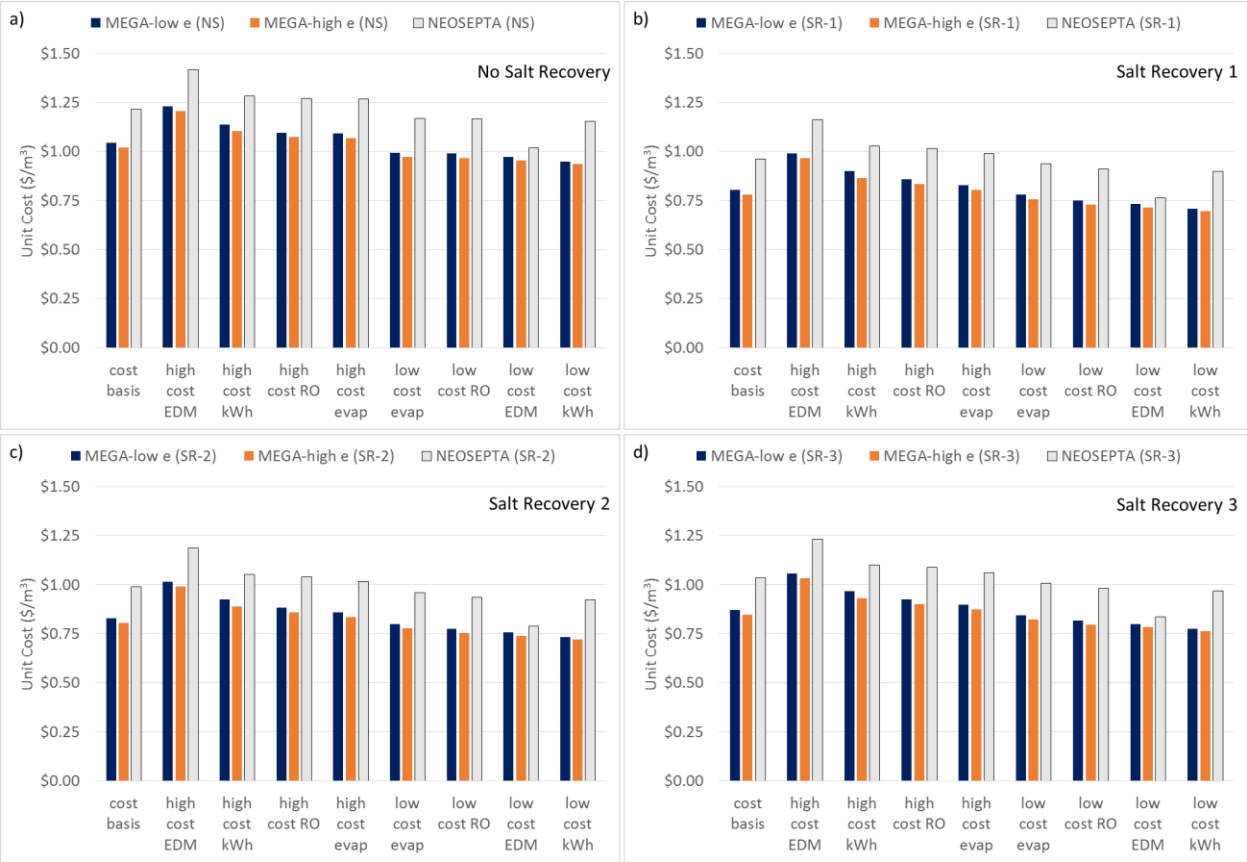

Figure 2.8. Impact of EDM Membrane Choice on Unit Cost for treating the BGNDRF Wells 1&4 blend with a) No Salt Recovery (NS), and Salt Recovery b) Option 1 (SR-1), c) Option 2 (SR-2), and d) Option 3 (SR-3) (Note: no revenue is included in b-d)

The inclusion of salt recovery processes such as clarifiers to precipitate calcium sulfate and magnesium hydroxide and evaporation ponds for the waste streams and sodium chloride recovery decreases the cost of ZDD treatment in all three cases. As shown in Figure 2.9, the ZDD unit cost decreases by as much as 25% when salt recovery is included in the design. Salt (NaCl) purchases account for approximately 20-25% of the unit cost of ZDD treatment for both MEGA and the

NEOSEPTA designs. By recovering sodium chloride from the ZDD concentrate streams, salt purchases decrease to 2-7% of the unit cost of ZDD treatment.

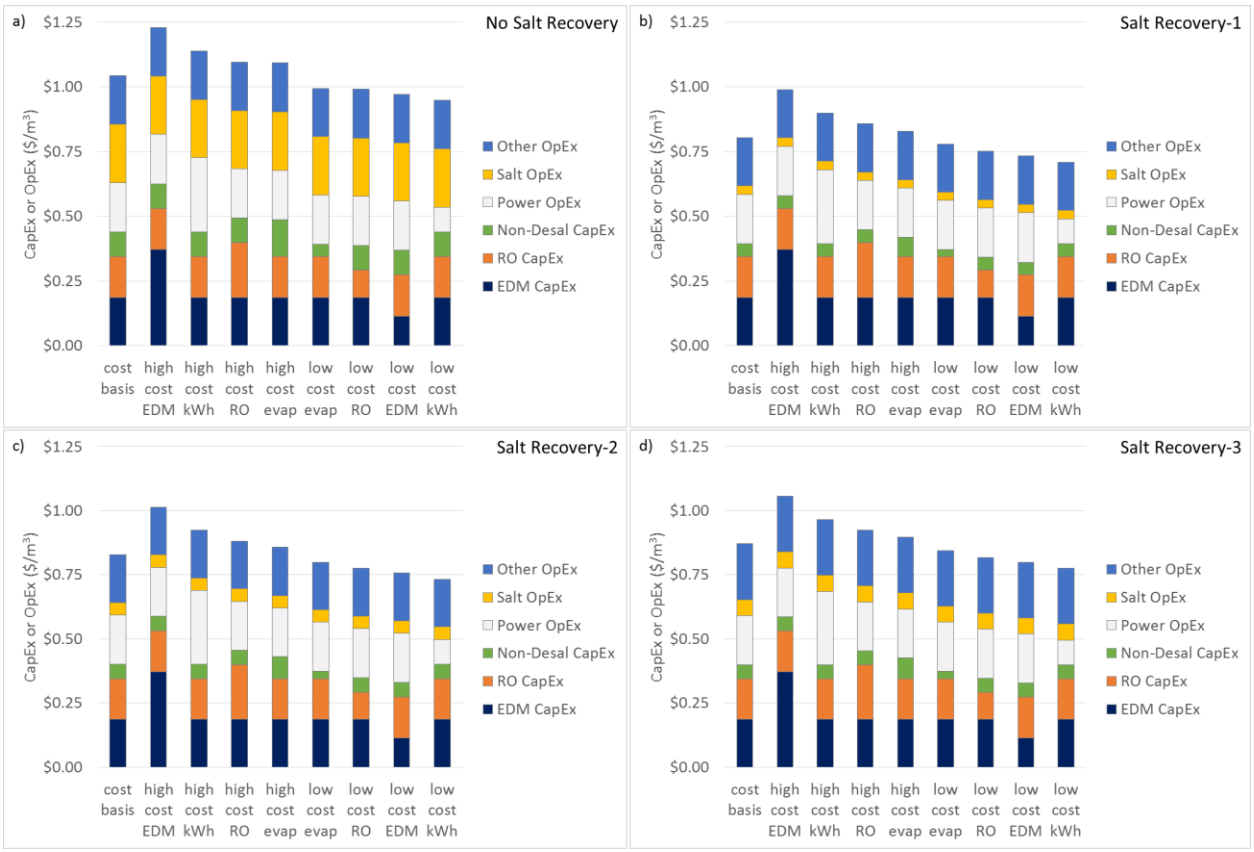

Figure 2.9. Sensitivity Analysis Using MEGA Membranes and ZDD Pilot Observations for a) No Salt Recovery, and Salt Recovery b) Option 1, c) Option 2, and d) Option 3 (Note: no revenue is included in b-d)

Table 2.7 includes comparisons between the Cost Basis Design with and without salt recovery (which may not be obvious from Figure 2.8 and Figure 2.9). Even though the salt recovery cases involve purchasing additional equipment, the CapEx decreases by 42-48% for the salt recovery designs because the size of the evaporation ponds decreases substantially. The salt purchases decrease substantially (72-85%) with the incorporation of salt recovery. The SR-1 design offers the greatest reduction in sodium chloride purchases (85%), but SR-3 offers the most revenue potential and least net operating expenses (21% decrease in OpEx costs).

Table 2.7. Summary of Capital and Operating Cost Differences with Salt Recovery

CapEx Cost		
Non-Desal Equipment - Salt Recovery 1	comparison to no salt recovery	48% lower
Non-Desal Equipment - Salt Recovery 2		40% lower
Non-Desal Equipment - Salt Recovery 3		42% lower
OpEx Costs w/o Revenue		
Salt Purchase - salt recovery 1	comparison to no salt recovery	85% lower
Salt Purchase - salt recovery 2		78% lower
Salt Purchase - salt recovery 3		72% lower
Net OpEx Costs (OpEx minus Revenue)		
Remaining (Other) OpEx - salt recovery 1	comparison to no revenue	3% lower
Remaining (Other) - salt recovery 2		3% lower
Remaining (Other) OpEx - salt recovery 3		21% lower

2.3.3. Evaluation of ZDD Economic Performance Sensitivity to Water Quality

Since the technical performance and sensitivity analysis seemed to point towards an optimum ZDD design including the highest possible RO/NF recovery, lowest possible EDM current density and silica purge, seven cases were evaluated using various water qualities (see Table 1.1). In comparison to the previous study [1], the ratio of the operating current density to the limiting current density (LCD) was lower for each design (*e.g.*, 83% versus 89-96% for the Alamogordo case with r_{RO}=70%). The designs summarized in Table 2.8 were chosen such that the recovery was maximized and the product TDS would be less than 500 mg/L.

Table 2.8. Primary Desalter Membranes Used and Independent Variables for ZDD Performance Sensitivity to Water Quality (Q_{ROp} = 3.03 MGD and Q_{prod} = 3.00 MGD)

Location	Feed TDS (mg/L)	Membrane	r_{RO}	RR_{EDM}	E_{Ca}	Q_{si} (gpm)	i_{EDM}/ LCD	r_{ZDD}
BGNDRF, well 1	2,130	NF270	75%	2.5	30%	0	79%	98%
BGNDRF, well 2	5,585	NF90	50%	2.0	25%	53	92%	94%
BGNDRF, well 3	3,440	NF90	55%	3.0	25%	34	81%	94%
Alamogordo	2,390	NF90-NF270	70%	2.5	25%	0	83%	98%
La Junta	1,272	NF90-NF270	75%	1.0	25%	0	81%	98%
Brighton	876	NF90-NF270	80%	0.75	25%	0	64%	99%
KBH	2,790	NF90	70%	2.0	30%	158	91%	91%

Even though the designs summarized in Table 2.8 are slightly different from those summarized in Table 1.3, the predicted unit cost of water follows a similar pattern with respect to recovery, specific energy consumption, and feed TDS. If the results for the KBH case are ignored (because of the high silica purge and resulting lower flow to the EDM), the unit cost of ZDD decreases with increasing recovery (Figure 2.10a). As expected, the unit cost of water increases with increasing specific energy, which related to feed TDS (Figure 2.10b-c). Since the designs were chosen to produce a product water with 500 mg/L or lower TDS, no observable trend is visible for the unit cost of water (Figure 2.10d). In all cases, the inclusion of salt recovery reduces the overall cost. The salt recovery data shown in Figure 2.10 does not include any revenue that could be generated from the sale of calcium sulfate or magnesium hydroxide. As shown in Figure 2.11, when revenue is included, the overall cost is decreased by 2-10% for the High Recovery design.

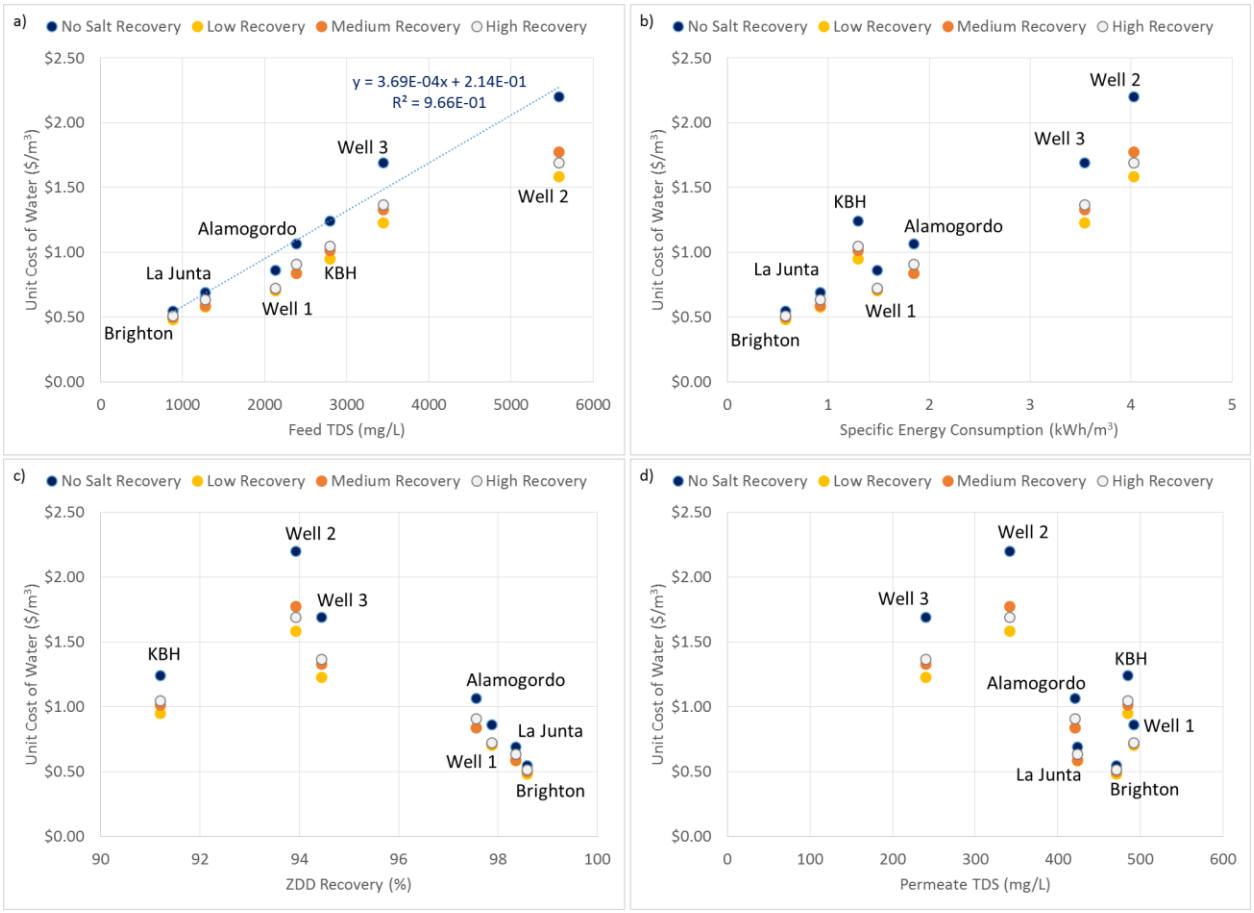

Figure 2.10. Unit Cost for No Salt Recovery and Salt Recovery Designs as a Function of a) Feed TDS, b) Specific Energy Consumption, c) ZDD Recovery, and d) Permeate TDS (Q_{ROp} = 3.03 MGD and Q_{prod} = 3.00 MGD)

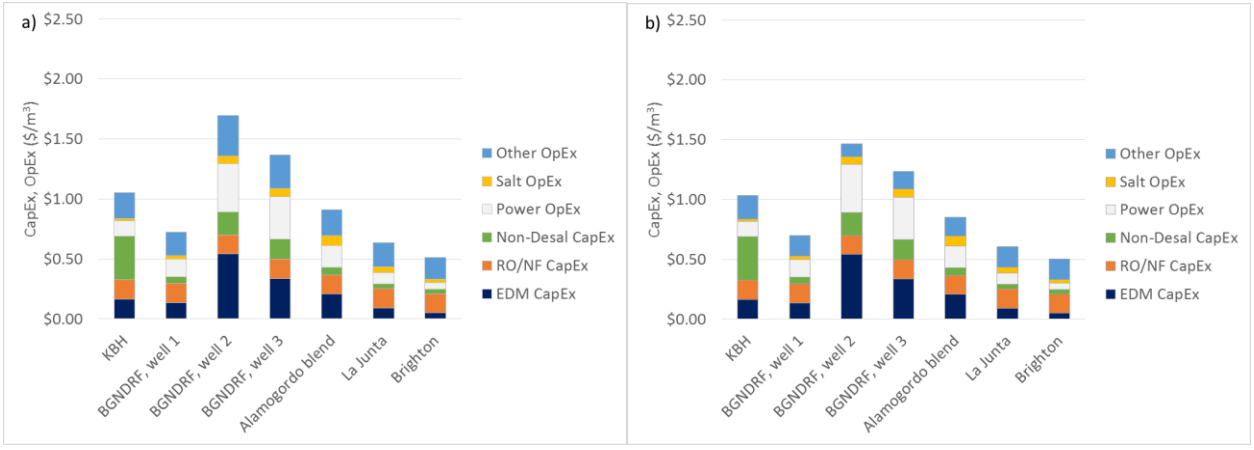

Figure 2.11. Breakdown of Capital and Operating Costs for ZDD System with High Recovery With a) No Revenue and b) Revenue Included

In order to evaluate the sensitivity to cost for varying water qualities, the calculated ZDD unit costs were graphed as a function of the lesser of the calcium and sulfate concentrations (eq/L) in the brackish water feed (as defined in the numerator of the *Y-Index* (originally defined in Equation 1.1)) and as a function of the sulfate concentration (eq/L). As shown in Figure 2.12a, in general, as the concentration of calcium or sulfate increases, so does the unit cost of ZDD. If the KBH site is ignored, a stronger correlation (R^2 = 0.77 vs 0.65) is observed (Figure 2.12b). This suggests that calcium and sulfate still play a role in the cost, because the KBH site has a relatively low proportion of calcium and sulfate relative to the TDS. All of the sites in Figure 2.12b have a *Y-Index* greater than 0.2, which may be the minimum for ZDD applicability. When the ZDD unit cost is graphed using the sulfate concentration (see Figure 2.12c), the relative position of the Alamogordo unit costs is shifted slightly. As shown in Figure 2.12d, when the KBH site is ignored, the correlation improves (R^2 = 0.88 vs 0.71), which may suggest that a $Y\text{-}Index_{w/Mg}$ of 0.3 is the minimum for ZDD applicability (all sites in Figure 2.12d have a $Y\text{-}index_{w/Mg}$value of 0.3 or greater).

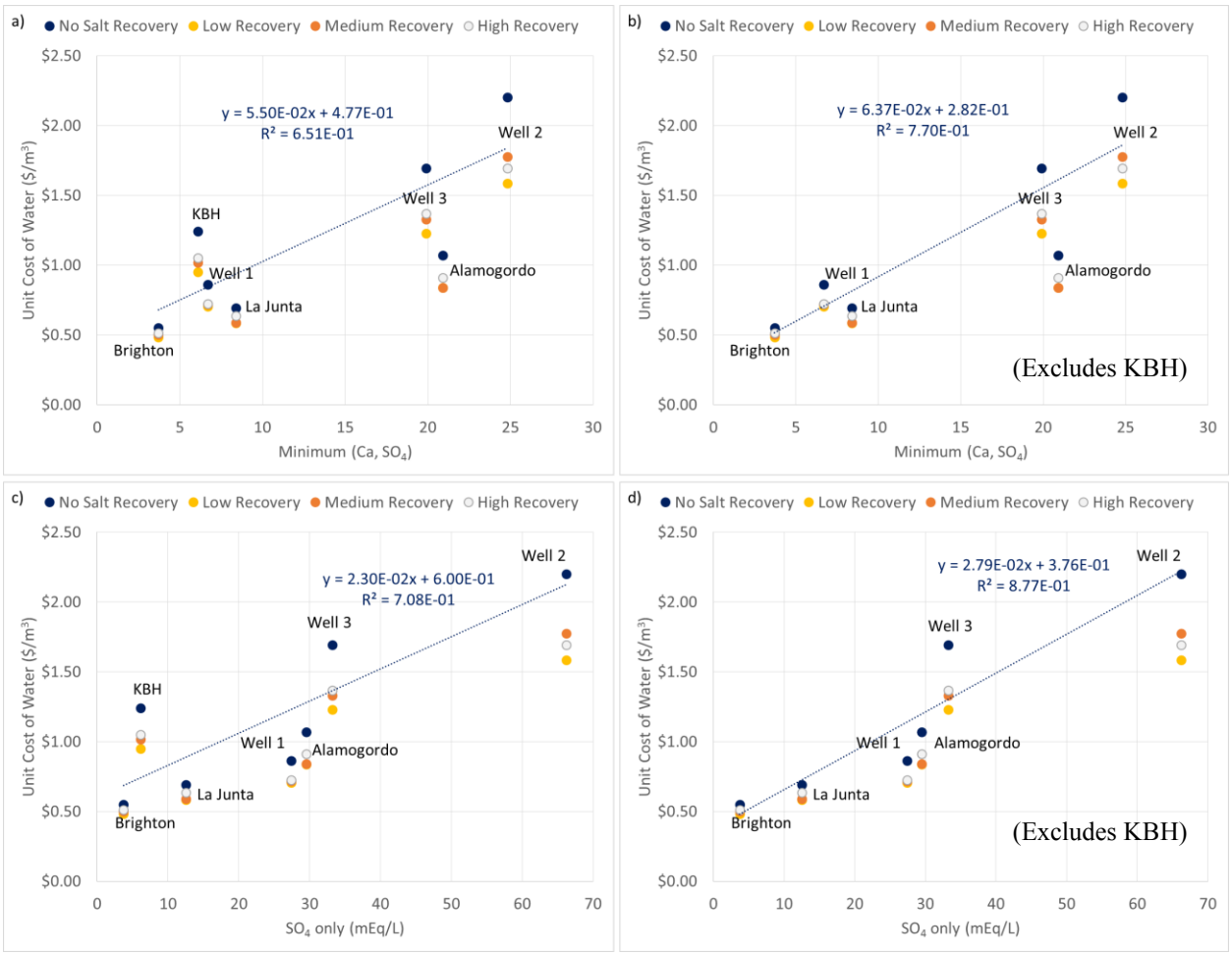

Figure 2.12. Unit Cost for No Salt Recovery and Salt Recovery Designs as a Function of a-b) the Minimum of the Feed Ca and SO_4 Equivalent Concentrations, and c-d) Equivalent SO_4 Feed Concentration (Q_{ROp} = 3.03 MGD and Q_{prod} = 3.00 MGD)

2.3.4. Evaluation of Sodium Chloride Quality for use in ZDD

The ZDD model predicts the concentration of the recovered sodium chloride solution. In general, there was an improvement in purity (as measured by the sum of Na^+ plus Cl^- ions divided by TDS) with the salt recovery methods 2 and 3 versus salt recovery method 1. The solutions have a predicted purity of 80-90% for the Alamogordo and KBH locations and 60-70% for the Colorado locations. In order to utilize the recovered sodium chloride solution in the EDM process, the purity must be sufficient to not cause scale formation. This is especially true if monovalent-selective anion- and cation-exchange membranes are not used. One way of measuring the quality of the salt solution is to calculate the equivalent ratio of Na^+ to Ca^{2+} or Cl^- to SO_4^{2-}. The higher the ratios, the

lower the impact of impurities. Laboratory tests performed during ZDD piloting indicated that a salt solutions with a Na^+/Ca^{2+} and Cl^-/SO_4^{2-} ratio of at least 20 could be used without scale forming in the EDM stack. The results from the ZDD model were used to calculate the Na/Ca and Cl/SO_4 ratios. The Na^+/Ca^{2+} and Cl^-/SO_4^{2-} ratios were also calculated for the various sites used in the water quality study. Similar to the results for the BGNDRF Well 1&4 blend design (not shown), most of the resulting salt solutions have sufficient Na^+/Ca^{2+} ratios but low Cl^-/SO_4^{2-} ratios. Since the KBH water has a much higher concentration of Na^+ and Cl^- relative to the other ions, a higher purity recovered salt solution is obtained.

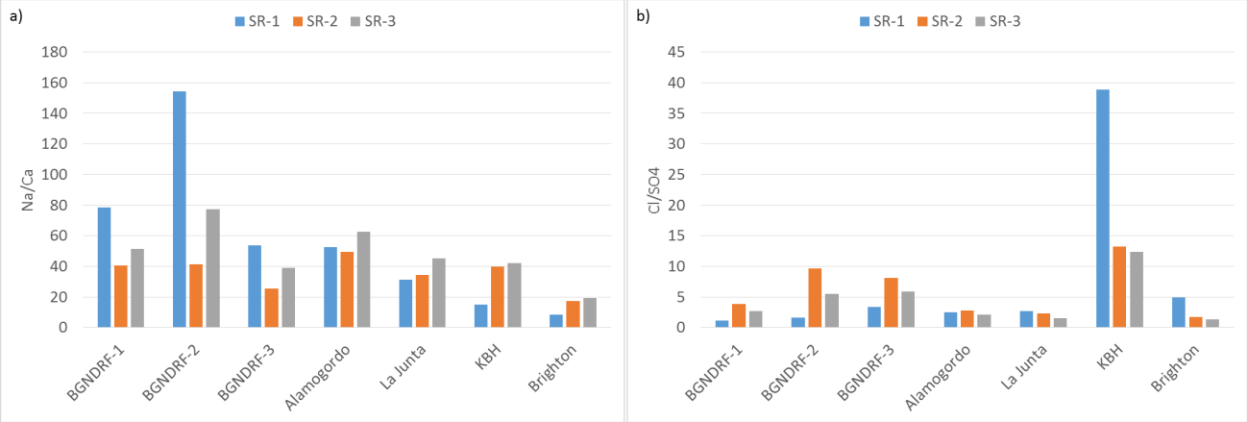

Figure 2.13. Modeled Sodium Chloride Quality for Various Water Quality Designs using a) Na/Cl Ratio and b) Cl/SO4 ratios

2.4. Conclusions

The ZDD mathematical model was updated to incorporate salt recovery and the results were used to evaluate the cost performance of ZDD with different designs and for sites with different water quality. The new sections of the model utilize the output from previous modeling [1], along with Visual MINTEQ to calculate the daily production of useful byproducts from ZDD desalination. The byproducts recovered include calcium sulfate, magnesium hydroxide, and sodium chloride. The recovered sodium chloride solution is assumed to be concentrated by a factor of two using an evaporation pond. A spreadsheet analysis was used to evaluate the impact of the various ZDD designs on the unit cost ($/m^3$). While site-specific factors and additional

piloting would improve the accuracy of the cost estimates, it is possible to make general observations:

- The optimum design for a ZDD system includes an optimization of the desalination load. The lowest overall ZDD specific energy consumption, and, therefore lowest ZDD unit cost for a given water quality, is found when maximizing the RO/NF recovery (r_{RO}), minimizing the EDM calcium removal (E_{Ca}), and minimizing the EDM recycle ratio (RRR_{EDM}).
- The choice of membrane for the primary desalter impacts the product water quality (higher salt rejection NF/RO membranes yield lower TDS product water and lower ZDD system recovery). The membranes studied herein suggest that increasing the salt rejection (*e.g.*, BW30 versus NF270 membranes) decreases the unit cost of the ZDD system.
- The incorporation of salt recovery could reduce the ZDD unit cost by 15-25%, without any revenue included. If revenue is included, the cost can be decreased by an additional 2-10%. This reduction is because the sodium chloride purchase cost is such a large proportion of the unit cost of water. Salt purchases increase with increasing feed TDS since sodium chloride is added to match the amount of ions removed from the RO/NF concentrate.
- The normalized Y-indices (with and without magnesium) allow for one to compare the type of water chemistry, but the correlation to ZDD performance was not strong. However, the feedwater sulfate equivalent concentration does predict ZDD cost performance for brackish waters with a $Y\text{-}Index$ greater than 0.2 or a $Y\text{-}index_{w/Mg}$ greater than 0.3. As the sulfate concentration increases, the unit cost of ZDD increases. TDS seems to be a better predictor for recovery, energy, and cost, so more water qualities should be evaluated.

- The ZDD model results indicate that the sodium chloride solution purity may not be good enough to use directly in the EDM, however previous pilot tests suggest otherwise. It is expected that the recovered sodium chloride solution could be used to dissolve purchased sodium chloride pellets. More research is needed to improve the accuracy of the model prediction of chemical compositions of the concentrates.

3. A Comparison of Medium and High Recovery Brackish Water Desalination Processes

Freshwater supplies are becoming more stressed in more areas because of population increases, decreases in the amount and quality of water supplies, climate change, and increased competition between user groups is becoming more common. Desalination, will play a role in increasing and diversifying city and regional water supplies. Conventional desalination processes like reverse osmosis and electrodialysis have been around for decades and the cost has decreased substantially. Typical RO plants are limited (at least on a practical level) to 75-80% recovery without increasing the complexity of the plant design. Additionally, acceptable brine disposal options are often limited in these areas, presenting a major obstacle to implementing membrane-based desalination technology. This chapter evaluates the technical and economic performance of three technologies capable of achieving higher than usual recovery for challenging water chemistries: (1) Zero Discharge Desalination (ZDD), (2) UTEP's Concentrate Enhanced Recovery Reverse Osmosis (CERRO), and (3) Desalitech's Closed Circuit Reverse Osmosis (CCRO). Cost-effective high-recovery desalination processes could allow inland communities to implement desalination to supplement their dwindling water supplies. Four sites are included that have a range of salinity, a range of proportions of divalent ions, and enough silica to possibly limit recovery. Based on research presented in this chapter, the water chemistry does have an impact on medium and high recovery desalination, but more research is needed to identify the causal relationships. A numerical matrix ranking approach was developed to compare the relative performance of the three technologies with respect to system recovery (30%), technology readiness (25%), system complexity (15%), specific energy consumption (15%), and cost (15%). Using this method, the relative performance for desalinating brackish water with relatively low divalent ion concentrations is: CCRO > CERRO > ZDD. Using the same method to evaluate CERRO and ZDD, the relative performance for the desalination of brackish water with relatively high concentrations of divalent ions is: CERRO = CCRO > ZDD (even though CCRO was not piloted at Well 2, it is

assumed to be the same as CERRO), although this is subject to the assumptions made in the chapter. Site-specific details such as the feasibility of deep-well injection or evaporation ponds will change the order of technology preference.

3.1. Defining Medium and High Recovery For Brackish Water Desalination

Typical brackish water reverse osmosis (BWRO) desalination plants operate with two or three stages in order to maximize recovery. In general, BWRO plants can achieve 50-60% recovery with one stage, 75-80% recovery with two stages, and 85-90% recovery with three stages (ignoring solubility limitations). As the number of stages increases, so does the required pumping energy. Also, the concentration of sparingly soluble salts (*e.g.*, silica) increases. In order to mitigate the scaling potential, some plants have installed (or have considered installing) some method of pre-treatment (*e.g.*, acid addition to raw feed and/or third stage feed) [2,3] or treatment to remove possible scale-forming constituents [4–6]. For the purpose of this paper, "conventional recovery" will be defined as 75-80%. Processes that can achieve 90-95% will be defined as "medium recovery"; Desai et al. (2016) used a similar metric, but called it medium liquid discharge [7]. Finally, "high recovery" is defined as 95% or higher recovery. Zero liquid discharge (ZLD) systems may or may not be high recovery.

Many techniques have been developed to achieve medium and high recovery with desalination processes using pre-treatment or interstage treatment to prevent scale formation in the RO membranes (see [8,9] for summaries). Many of the high recovery and ZLD processes involve physical water treatment processes that produce voluminous solids that must be disposed of properly. Some, such as Zero Discharge Desalination (ZDD), GeoProcessors, and EWM, have devised a mechanism for recovering useful byproducts from the desalination brine [8–11]. ZLD approaches typically employ thermal processes such as brine concentrators and crystallizers that have a high cost. Some researchers have evaluated conventional and high recovery desalination coupled with thermal ZLD approaches [12].

The University of Texas at El Paso's Concentrate Enhanced Recovery Reverse Osmosis (CERRO) and Desalitech's Closed Circuit Reverse Osmosis (CCRO) processes were designed in order to improve desalination recovery while maintaining simplicity. Both of these technologies take advantage the relatively slow formation of silica and other constituents in membrane systems [13–15]. While the methodology is different between each of these technologies, the general principles are similar. Both are considered semi-batch processes [16–18]. The term semi-batch means that there is some sort of interruption or flush step during which permeate production is slowed or stopped. The timing of the interruption is chosen to ensure that the concentration of sparingly soluble constituents is raised for a time period less than the induction time of precipitation. Both CCRO and CERRO employ minimal pre-treatment (acid, antiscalant, cartridge or media filtration) and have been shown to achieve system recoveries of at least 90% for brackish water [13,19,20]. Several researchers have analyzed the benefits of continuous, batch, and semi-batch RO processes. For example, Warsinger et al. (2016) and Werber et al. (2017) provide useful descriptions and modeling techniques [17,18]. Warsinger et al. (2016) found that CCRO can be up to 37% more efficient than staged BWRO without energy recovery [18]. Werber et al. (2017) developed a theoretical model that compared the specific energy consumption of RO systems with energy recovery devices with one to three stages against semi-batch RO with and without energy recovery. Similar to Warsinger, Werber found that semi-batch systems are more energy efficient than staged RO without energy recovery devices or interstage booster pumps [17]. Werber et al. (2017) used a sodium chloride solution with 5840 mg/L TDS for their brackish water desalination modeling and did not evaluate the economic or other reasons for why a semi-batch process might be preferred [17].

ZDD and other hybrid desalination systems are able to achieve very high recovery, as well as produce saleable byproducts that can lower the cost of desalination. However, the cost is generally higher because of increased power consumption, capital equipment costs, and other factors. The ability to achieve medium recovery might make thermal ZLD approaches feasible, as

the volume would be minimized enough to minimize capital and operating costs of a crystallizer. This chapter will compare the relative performance of ZDD, CERRO, and CCD as a function of water chemistry, system recovery, and specific energy consumption.

3.1.1. Concentrate Enhanced Recovery Reverse Osmosis (CERRO) Process Background

The CERRO process was invented at UTEP by Dr. Anthony Tarquin. Several designs were piloted at the KBH plant in El Paso, Texas, and BGNDRF in Alamogordo, New Mexico. The first research projects focused on demonstrating CERRO using a batch processing method, and is summarized in Figure 3.1. Brackish water or reverse osmosis concentrate is added to a feed tank, then is sent through a system with seawater reverse osmosis (SWRO) membranes. The SWRO concentrate is returned to the feed tank and the process continues until the feed tank is empty or a conductivity set point is reached. At this time, a valve opens to drain the rest of the tank. The SWRO is then flushed with permeate or brackish feed water (not shown in Figure 3.1), the feed tank refilled, and the process restarts. The batch CERRO and its associated chemical feeds have been studied and much of the work is summarized by Delgado [21] and Tarquin [13,19,22]. Three of the most important design features of CERRO design were identified by Delgado [21]. Induction time was found to be of more importance than crossflow velocity in terms of scale formation. Each CERRO design will have a specific processing time that will maximize recovery while minimizing scale formation potential. Acid dosage might be required, but moderate dosages (*e.g.*, pH 6.0) are typically all that is required for prevention of calcium carbonate scale. Antiscalant choice and dosage were identified as a very important consideration, especially as it relates to calcium sulfate. Proper flushing of the CERRO system after each batch is necessary to mitigate scale formation as well. Flushes generally require a small volume, and can be done with permeate or a water with lower salinity than what is being desalinated. Finally, water quality plays a role in the maximum recovery attainable by CERRO. Brackish water with very high concentrations of calcium and sulfate can limit the recovery, as it did in Alamogordo piloting. Other factors (temperature,

constant flow versus constant pressure) were evaluated, but found to be less important in comparison.

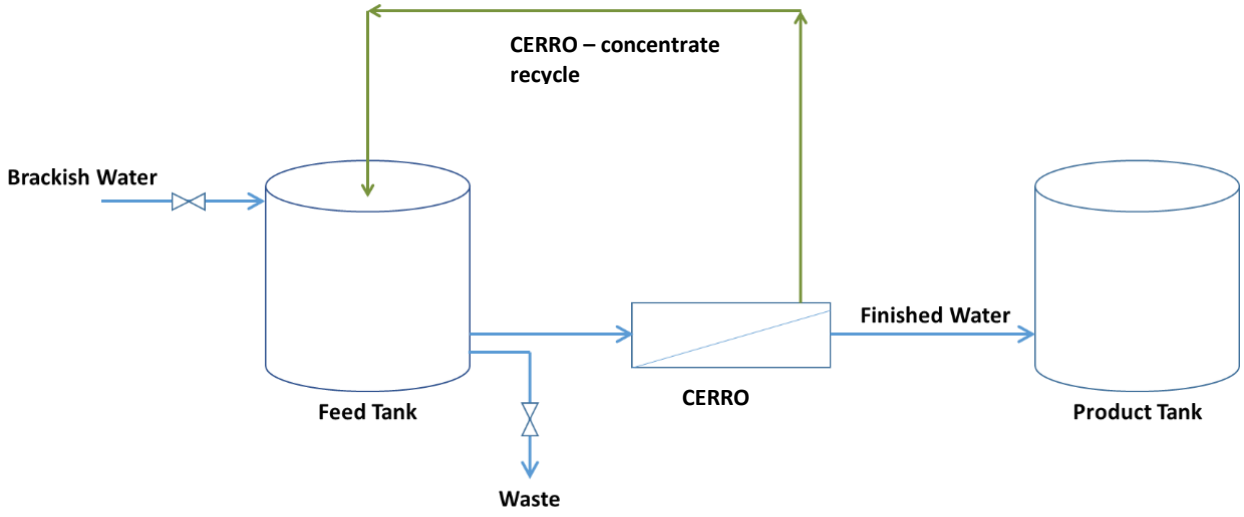

Figure 3.1. Simplified Batch CERRO Flow Diagram (as tested at the KBH and BGNDRF)

An early attempt at making a continuous flow CERRO still contained the recycling step and was intended to simplify the design, however it was found to be infeasible [22]. The current semi-batch CERRO system was designed to maximize cross-flow velocity in the SWRO system and can involve 3:2:1 membrane staging as described in the CERRO patent application [23] and shown schematically in Figure 3.2. This design removes the recirculation step and has been demonstrated at a wellhead desalter in El Paso, Texas. This chapter performs an initial assessment of the CERRO system using pilot and full scale data at the El Paso Water Well 412B location, as well as reviewing data in previous piloting reports. Pilot testing and commissioning of a full scale CERRO system at the Well 412B site occurred during 2015 and the work was sponsored by the U.S. Bureau of Reclamation's WaterSMART program [24]. The CERRO system was initially started with a conservative set point of 70% recovery for desalination of the Well 412 concentrate (the primary BWRO operates at 75%). When the flush volume is accounted for, the CERRO system recovery is 60%, and the BWRO + CERRO system recovery is therefore 90%. Some

operational problems have occurred, but most have been related to chemical supplies and conductivity probe problems.

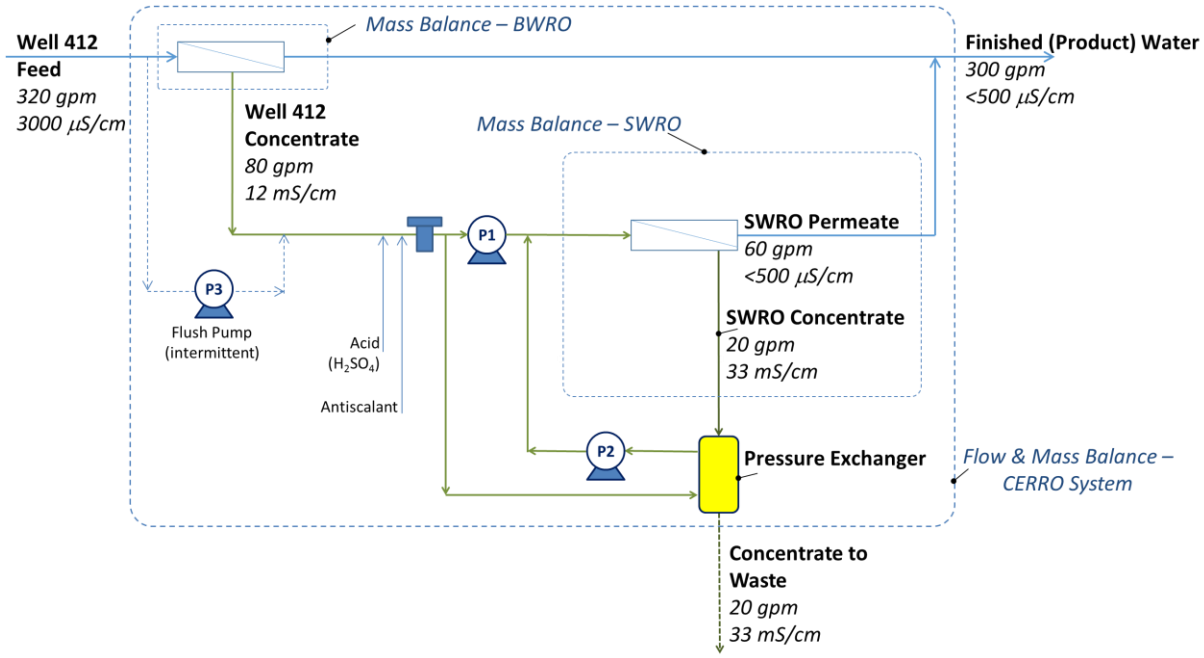

Figure 3.2. Simplified CERRO Flow Diagram (as installed at the El Paso Water Well 412)

The batch CERRO system was shown to achieve at least 80% recovery when desalinating the KBH concentrate, which would increase the overall recovery at the desalination plant to 97% from 82.5% [13]. When the batch CERRO was tested at the BGNDRF, lower system recoveries were achieved (around 30-40%) unless sodium chloride and/or high doses of antiscalant were added to the Well 3 feed or RO concentrate; the combination of RO + batch CERRO with 20 ppm antiscalant was able to achieve 76% recovery [19]. A preliminary version of a continuous flow CERRO were not able to achieve the same high recovery as the batch CERRO [22] because of calcium sulfate precipitation in the membranes. The semi-batch CERRO has achieved pass recoveries (CERRO permeate/CERRO feed) of at least 70% have been achieved when desalinating the concentrate from the Well 412 BWRO; the system recovery of the BWRO + CERRO (combined permeate/Well 412 feed) is 90%.

3.1.2. Closed Circuit Reverse Osmosis (CCRO) Process Background

Closed Circuit Desalination is a technology patented by Desalitech. In comparison to CERRO, CCRO is operated at constant permeate flow (flux) with increasing pressure during a batch. As shown in Figure 3.3, and described in articles elsewhere (for example: [14] and [25]), water is fed to a set of pressure vessels fitted with BWRO or SWRO membranes. Instead of being sent to drain, the brine pressure is boosted and then mixed with feedwater and sent through the membranes again. This circulation (called closed-circuit desalination, or CCD) occurs until a set point (*e.g.*, volumetric recovery, pressure, internal or concentrate conductivity or a custom set-point) is reached. At this point, a valve allows the concentrate to be sent to drain and the system is flushed with feedwater (called plug-flow desalination, or PFD), while maintaining permeate production at a reduced capacity. The feedwater flow during CCD is equal to the permeate being produced. The flush is performed at a lower pressure and generally constitutes a small portion of the total water fed to the CCRO. The system piloted at the KBH plant involved three pumps: P1 was a feed pump used to transport water from a feed tank to the CCD pilot system; P2 was the high pressure pump used to desalinate the brackish groundwater; and, P3 was the circulation pump which boosted the concentrate pressure to match the outlet of P2. Pre-treatment included sulfuric acid (H_2SO_4) and antiscalant addition followed by cartridge filtration (5-micron cartridge filters were used in the pilot).

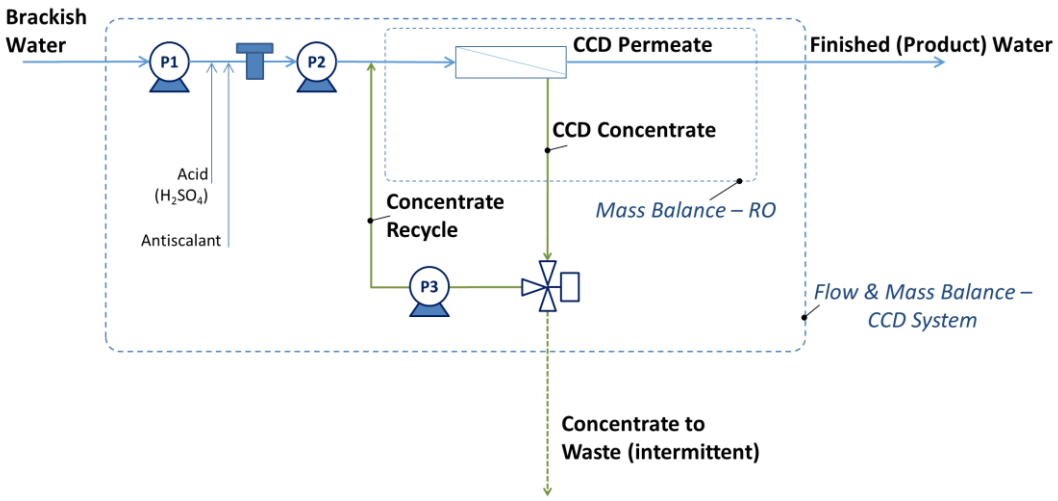

Figure 3.3. Simplified CCRO™ Flow Diagram (as piloted at the KBH desalination plant)

The pilot involved three phases that tested two types of BWRO membranes and evaluated system recoveries ranging from 80 to 95%. The primary focus of this pilot was to prove that high silica concentrations could be achieved without causing scale. During the first phase, the CCD system employed Hydranautics ESPA2-MAX membranes and the target operations were 22 LMH (13.7 GFD) flux and a 40% module recovery (permeate/feed). The membranes were fouled due to algae and/or bacterial growth in the feed tank so they were replaced. During the second phase, ESPA2 MAX membranes were used again, but the flux and module recovery were reduced to 20-21 LMH (12-12.5 GFD) flux and 30% module recovery, which was more reasonable for the 3-membrane design installed in the pilot system. During Phase 2 operations, it was determined that the HPP was undersized and not capable of producing permeate at the end of the sequence. Biofouling occurred again due to the suspected source of contamination (feed tank) and was removed from the system for the third phase. ESPA4-MAX membranes were installed to cater to the smaller high pressure pump in the CCRO pilot. While the ESPA4-MAX membranes are not able to produce high quality permeate, the silica rejection was thought to be high enough to test the feasibility of high recovery desalination of BWRO with CCRO.

3.1.3. Zero Discharge Desalination (ZDD) with Salt Recovery Background

ZDD is a hybrid desalination process that combines reverse osmosis or nanofiltration (RO/NF) and electrodialysis metathesis (EDM). As described in Cappelle, et al. (2017), salt recovery can be added in order to achieve zero liquid discharge, reduce sodium chloride purchases, and potentially provide a revenue stream by selling recovered minerals from the concentrate [1]. This chapter compares the performance of ZDD with Salt Recovery Method 1 (see Figure 2.3a) against CERRO and CCRO. This form of ZDD was shown to usually have the lowest unit cost, even without revenue being included, and involves a brackish water being fed to a primary desalination system, in this case nanofiltration. The NF concentrate is then fed to the EDM which is operated so that its desalinated product (diluate) can be returned to the NF feed for additional water recovery. The two EDM concentrates (Mixed Na and Mixed Cl) are mixed to produce a solid calcium sulfate byproduct and a liquid stream that is mostly sodium chloride. An evaporation pond is used to increase the sodium chloride concentration prior to being used in the EDM. The ZDD designs considered in this chapter have Dow NF90 membranes or a combination of NF90 and NF270 membranes as described in Chapters 1 and 2.

3.2. Methodology

Pilot data, the updated ZDD model (Chapter 2), and manufacturer information and design programs were utilized to compare the technical and economic performance of three technologies capable of achieving higher recovery than conventional desalination systems alone. CERRO and CCRO can be operated in a manner that achieves medium or high recovery, depending on site requirements and customer preferences. ZDD is a high recovery process that, with incorporation of salt recovery, can achieve high recovery and zero liquid discharge without the need for thermal processes for concentrate disposal. Technical performance metrics used to compare the technologies include the system recovery, product water quality (TDS), specific energy consumption, and system complexity. The unit cost of water, expressed as $\$/m^3$, is the sole economic performance metric, which includes the capital and operating costs.

3.2.1. Comparison of Water Quality at Desalination Sites

In order to assess whether brackish water quality has an impact on the cost of desalination by ZDD, CCRO, and CERRO, several feed water chemistries were chosen for evaluation. As summarized in Table 3.1, two sites are in El Paso, Texas, and two sites are in Alamogordo, New Mexico. The sites were chosen because of piloting and/or full scale system operation. CERRO has been demonstrated at the KBH desalination plant, BGNDRF (Well 2), and El Paso Well 412 sites. CCRO has been demonstrated at the KBH plant. Finally, ZDD has been piloted at KBH and BGNDRF (Well 1/4 blend) and modeled for desalination at the BGNDRF Well 2 location. As can be seen in Table 3.1, a wide range of brackish water salinity is covered (approximately 1,900 to 5,600 mg/L TDS) with the choice of brackish waters. Also, there is a distinct difference in the type of water chemistry, as evidenced by the Y-indices and divalent fractions. The Alamogordo waters are predominately calcium sulfate type waters (high *Y-Index*, divalent fraction) and the El Paso waters are predominately sodium chloride/sodium bicarbonate type waters (low *Y-Index*, divalent fraction). All of the waters have enough silica present to be problematic for recoveries above 80% using reverse osmosis or nanofiltration alone.

Table 3.1. Comparison of Brackish Water Chemistry

Water Quality Constituent or Parameter	Well 1 & 4 blend Alamogordo, NM (2013)	Well 2 Alamogordo, NM (2016)	KBH El Paso, TX (2016)	Well 412 El Paso, TX (2016)
Ca^{2+} (mg/L)	287	496	164	92.7
Mg^{2+} (mg/L)	120	359	40.5	22.9
Na^{+} (mg/L)	377	720	802	534
Cl^{-} (mg/L)	344	518	1380	856
HCO_3^{-} (mg/L)	249	297	91.9	107
SO_4^{2-} (mg/L)	1290	3180	292	258
SiO_2 (mg/L)	20	19.6	26	32
TDS (mg/L)	2690	5590	2790	1850
Normality (N) (meq/L)	40.6	85.7	46.3	30.8
Y-Index	0.35	0.29	0.13	0.15
Divalents fraction (mass fraction of TDS)	63%	72%	18%	20%

3.2.2. Summary of Data Used for Comparison

Several sources of data were utilized for this chapter. A combination of pilot study data, full scale operational data, manufacturer information were used in order to make a comparison of the CCRO, CERRO, and ZDD technologies. The data available for this chapter are summarized briefly in the following sections.

3.2.2.1. CERRO Data

The CERRO data available for this chapter are limited, but still allow for an evaluation of the technology. Batch CERRO data are taken from pilot studies at the KBH desalination plant and BGNDRF and are taken from Delgado [21] and Tarquin [13,19,22]. Semi-batch data from 2015 and 2016 were provided by the CERRO licensee, Industrial Water Services, for analysis and are summarized herewith.

In order to show repeatability of the semi-batch CERRO process, pilot data showing eight consecutive batch runs using water from Well 412 are shown in Figure 3.4a. The pilot system was

operated with 20-gallon (15-minute) batches and constant pressure (around 600 psi)[7]. Conductivity and flow data are shown in Figure 3.4b. In general, the data shows consistent operation. The final two runs had slightly lower flow (and higher pressure, not shown), but it seems to be related to an inadequate flush after Run 6.

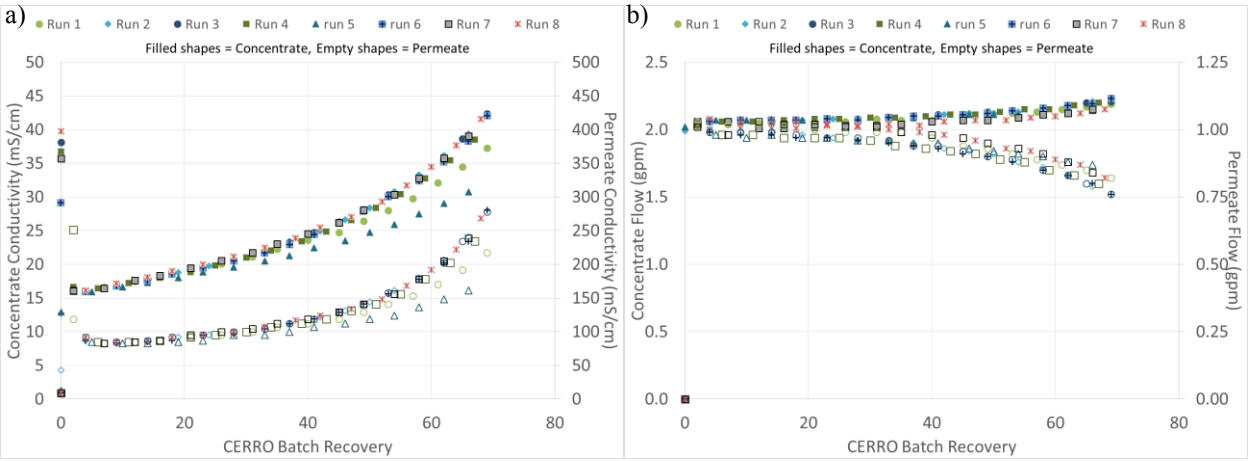

Figure 3.4 Batch CERRO pilot data u Well 412 BWRO showing a) Conductivity and b) Flow (April 2015)

The next set of data used for this study is obtained with the full size semi-batch CERRO system desalinating water from Well 412. Two sets of data were available for analysis, including the shakedown data in 2015 and operating data in early 2016. Even though the operational parameters were being studied and finalized in 2015, it can be seen that the flow and energy were consistent over the course of several weeks. The focus area for a deeper dive is September 1-8, 2015, and the overnight data on January 11-12, 2016. In September 2015, the semi-batch CERRO system was operating with 15-minute batches similar to the pilot system. The Well 412 concentrate is treated with sulfuric acid and antiscalant to mitigate scale formation. The system was started conservatively with acid addition and antiscalant set at pH 5.0 and 10 ppm, respectively. It was determined that these set points could be raised to pH 6.0 and 5 ppm antiscalant and is still operated in this manner. In January 2016, the semi-batch CERRO system was operated with 20-minute

[7] CERRO pilot systems have historically been run at high pressures. The main goal is usually to prove that high recovery is achievable and sustainable, and not necessarily to optimize energy consumption.

batches, and it is thought that longer batches will also be stable. Increased batch time improves system recovery since no (or minimal) permeate is produced during flush cycles. Data are not available for the flush cycles at the time of writing, so it is assumed that 240-second flushes at 60 gpm are used in both 2015 and 2016.

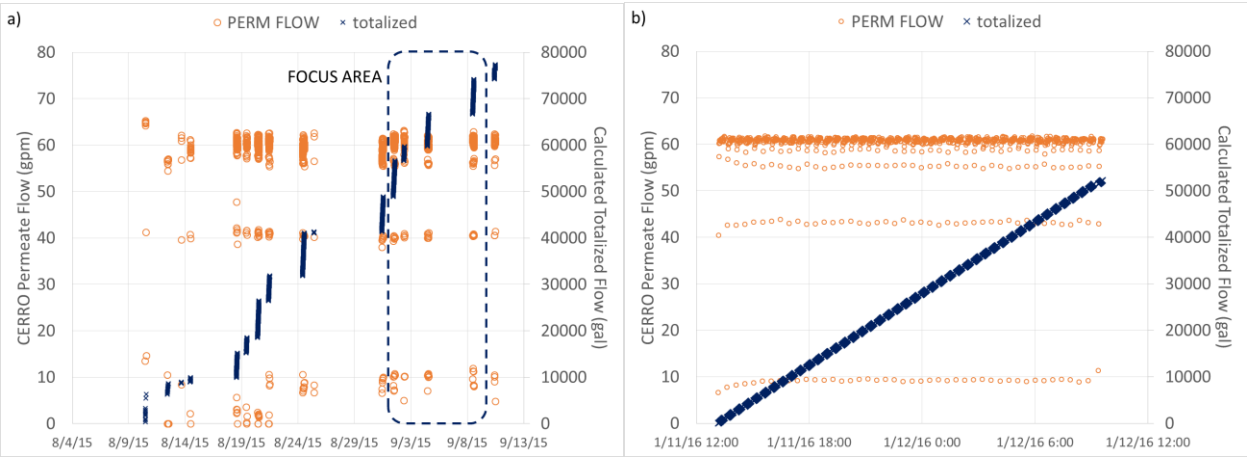

Figure 3.5 Semi-batch CERRO Full Scale Flow data at Well 412 BWRO (September 1-8, 2015 and January 11-12, 2016)

A power meter is installed on the semi-batch CERRO system. Energy consumption can easily be calculated from this information, however power data are only available with the 2015 data set (see Figure 3.6). The power and energy consumption data from 2015 (see Figure 3.6) includes the pumping energy for desalination as well as the flushing pump and other power consumption (lights, controls, chemical pumps, etc.). In order to compare the two sets of data, the pumping power (high pressure pump and booster pump) was calculated for the 2015 data. The flow and pressure data for the high pressure and booster pumps as well as assumptions for the pumping efficiency (75% motor/pump efficiency, 95% VFD efficiency) were used to approximate the pumping energy (see Figure 3.7). The pumping power accounts for approximately 90% of the total power, so use of this calculated value will yield useful information.

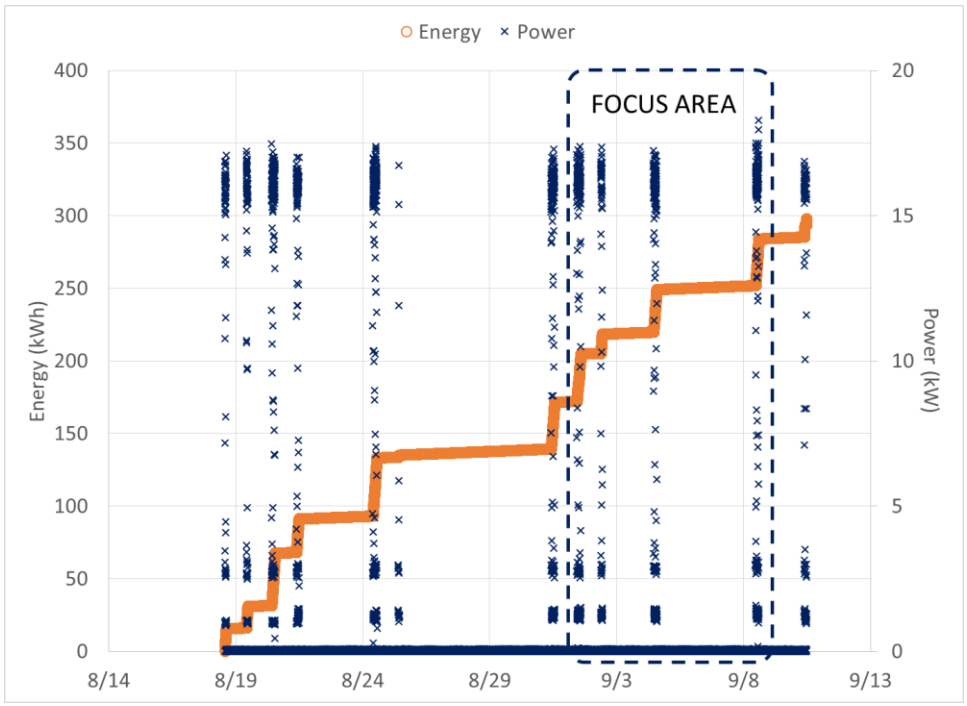

Figure 3.6 Semi-batch CERRO Full Scale Power Meter data (September 1-8, 2015)

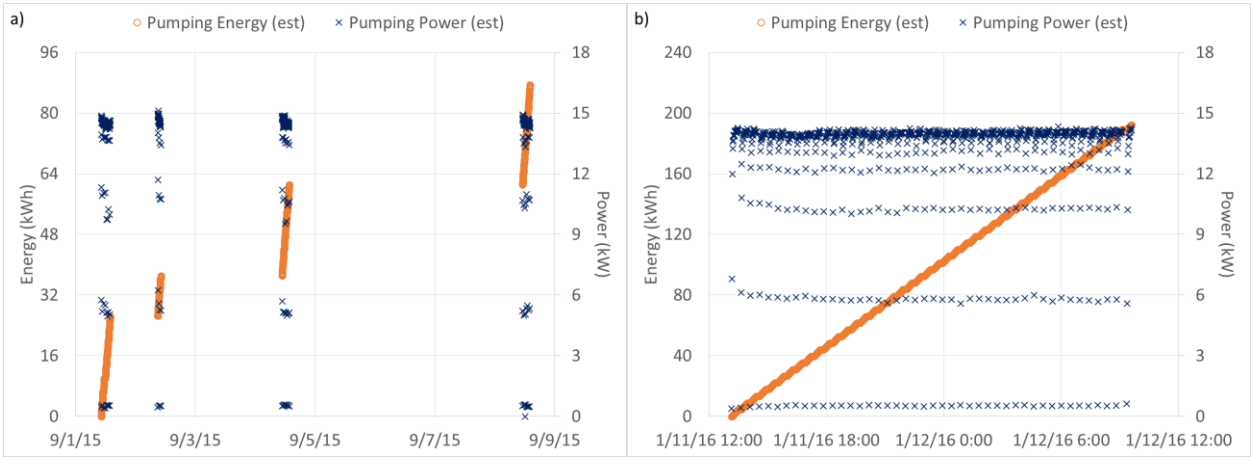

Figure 3.7 Semi-batch CERRO Calculated Pumping Values at Well 412 BWRO for a) 2015 and b) 2016 (September 1-8, 2015 and January 11-12, 2016)

Other online data available for analysis include the flow, pressure, and conductivity for the various CERRO streams. As can be seen, the semi-batch CERRO performance was nearly identical in the two data sets (see Figure 3.8). The CERRO system is designed to operate at approximately

74% recovery (permeate/feed) and since SWRO membranes are utilized, the conductivity is reduced by nearly 99%.

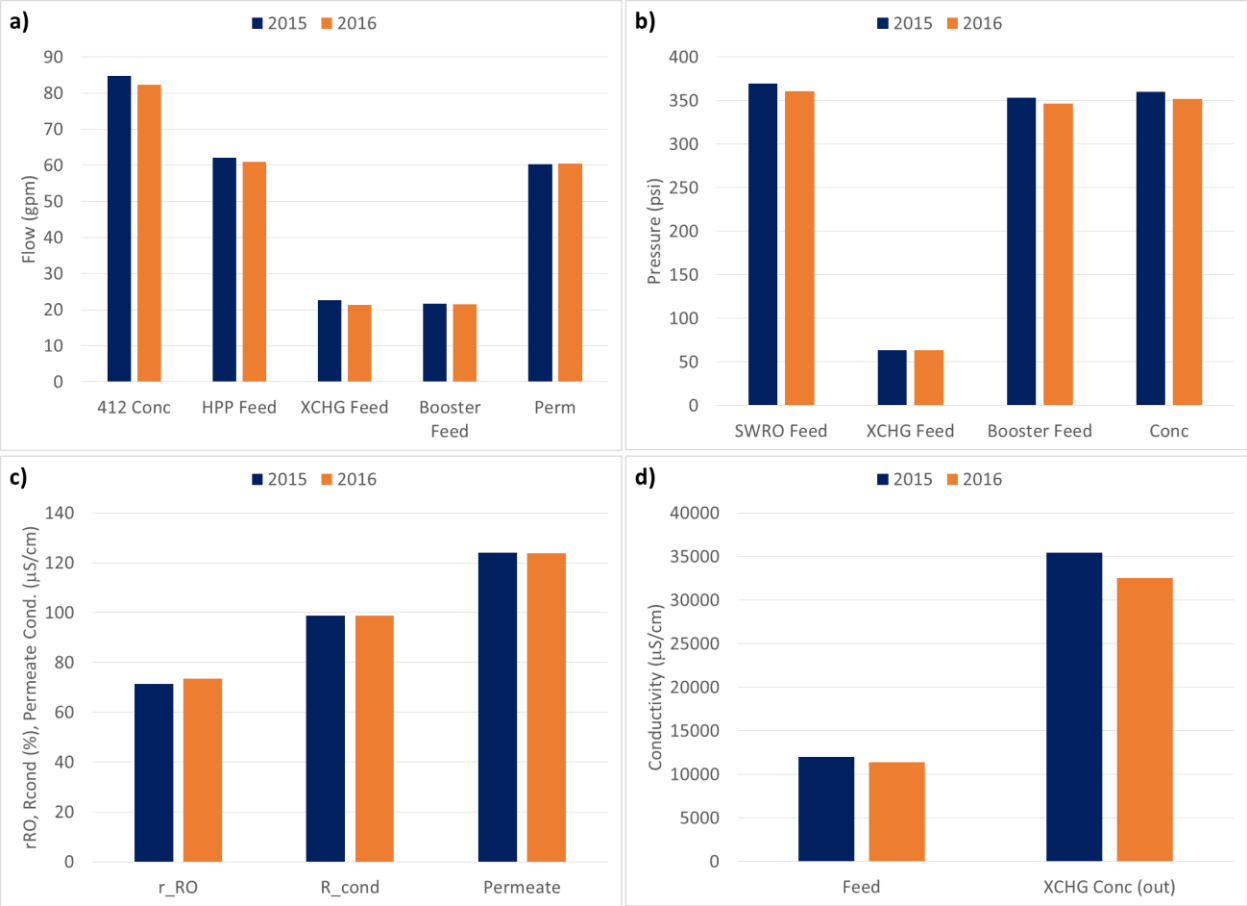

Figure 3.8 Semi-batch CERRO Full Scale Average Data at Well 412 BWRO showing a) Flow Rate, b) Pressure, c) Recovery, Conductivity Removal, and Permeate Conductivity, and d) Feed and Concentrate Conductivity (September 1-8, 2015 and January 11-12, 2016)

Water quality samples were obtained while the semi-batch system was operating in January and February 2016, but the online data were not available at the time of this writing. Because TDS removal (99%) is close to the conductivity reduction demonstrated in January 2016 (see Figure 3.8c), it is assumed that the later water quality samples reasonably describe the earlier performance. Table 3.2 summarizes average data for the samples taken between January 29 and February 15, 2016. The brackish feed water to the Well 412 desalination system has 1,854 mg/L

TDS. The reported values for silica in the CERRO brine were lower than the CERRO feed. This is likely because the water samples were not diluted in the field and the method for silica detection only detects reactive silica. It is possible that some of the silica precipitated prior to analysis. The difference between reactive silica (molybdate method) and total silica (found using ICP-OES) can be as much as 26% at high CERRO recovery [13]. The silica concentration reported in Table 3.2 was estimated based on a mass balance approach with an assumed value for the average permeate silica concentration (5 mg/L), CERRO instantaneous (perm/feed; excludes flush volume) recovery of 70%, and silica rejection of 96%.

Table 3.2. Average Water Quality for Various Semi-batch CERRO System Samples (January 29-February 16, 2016)

	412B Raw	412B Brine/ CERRO Feed	CERRO Permeate	CERRO Brine	CERRO +BWRO blend
Ca^{2+} (mg/L)	93	349	5.0	1400	24.5
Mg^{2+} (mg/L)	23	87.9	1.2	343	6.2
K^{+} (mg/L)	10.7	39.3	<2	155	3.3
Na^{+} (mg/L)	534	1901	28	7220	157
Cl^{+} (mg/L)	856	3100	33	12100	231
SO_4^{2-} (mg/L)	258	936	3.6	4280	59.9
Alkalinity (as $CaCO_3$)	87.3	314	5.0	578	92.0
TDS (mg/L)	1850	7010	43	27400	528
pH	7.5	7.8	5.2	6.5	5.6
SiO_2 (mg/L)	32	118	<5.0	342[8]	8.5

3.2.2.2. CCRO Data

CCRO data are available from pilot testing during Desalitech-sponsored research in 2015-2016. As mentioned above, piloting activities spanned three phases, but this chapter focuses on

[8] Estimated value based on average data for CERRO feed and permeate. Calculation estimates the silica concentration in the CERRO concentrate based on the mass balance approach ($C_{c,SiO2} = C_{f,SiO2}$ (1+ rR/(1-r), where r=70% and R=96%); silica rejection (R) is calculated assuming the concentration in the permeate is 5 mg/L. Lab reported values were 90-120 mg/L.

the portion of Phase 2 when the system was operated at 90% recovery (Figure 3.9a) and Phase 3 when operated at 94% recovery (Figure 3.9b).

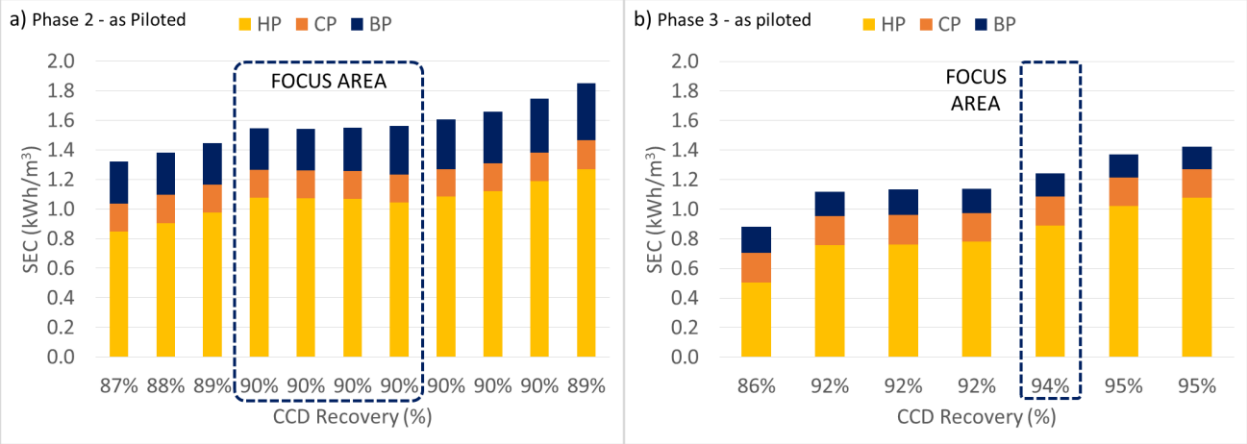

Figure 3.9 Phase 2 and Phase 3 CCRO Pilot Specific Energy Consumption Data for a) September 22-27, 2015 and b) February 21-23, 2016

As described earlier, CCRO systems have two distinct operating modes. Figure 3.10 shows how the conductivity and pressure changes during CCD and PFD operations. During the CCD cycle, no concentrate is leaving the system, so the concentrate conductivity continually increases until the system is flushed during the PFD cycle. Similarly, the CCRO permeate conductivity and feed pressure both increase during CCD and decrease during PFD. In order to simplify the data analysis, the available data are filtered to summarize the end of CCD and average PFD conditions. The end of CCD is defined as the module feed pressure being greater than 350 psi for Phase 2 and greater than 215 psi for Phase 3. PFD is defined as the period when P3 (concentrate recirculation) pump is off (0 rpm).

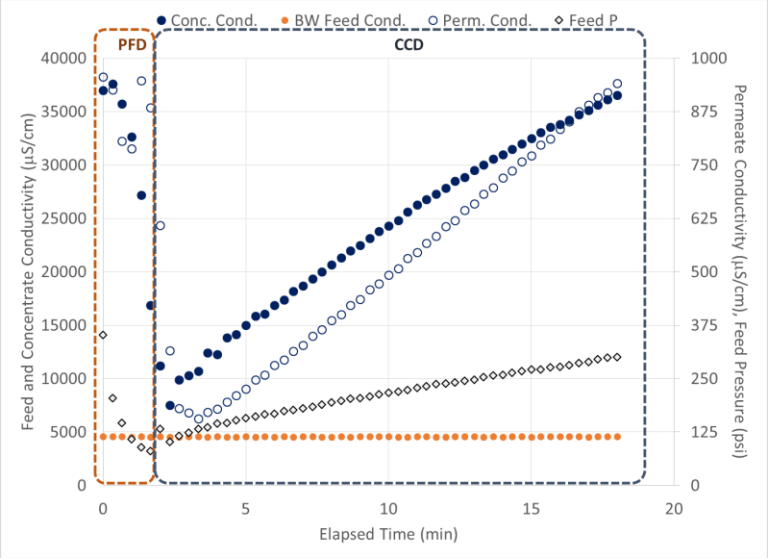

Figure 3.10 Representative PFD and CCD Operations during Phase 2 Operations (r =90%) at KBH

As shown in Figure 3.11a, the CCD permeate and concentrate flow and module recovery were nearly identical between Phases 2 and 3. Since the ESPA2 MAX membranes have a higher salt rejection, they require more feed pressure to produce the same amount of permeate flux (see Figure 3.11b). The PFD flows were also similar between Phase 2 and 3 (Figure 3.11c). There is a discernable difference between the pressures in Phases 2 and 3 (Figure 3.11d). It takes time for the high pressure pump speed to decrease, so since the pressure was higher in Phase 2, so was the average PFD feed pressure. The PFD cycle lasts two minutes, so even a few points with higher pressure will skew the average.

Water samples were taken from the brackish water feed (raw), as well as at the beginning and end of CCD and PFD cycles during Phase 2. PFD sampling was omitted in Phase 3. The results for both phases are summarized in Table 3.3 and Table 3.4.

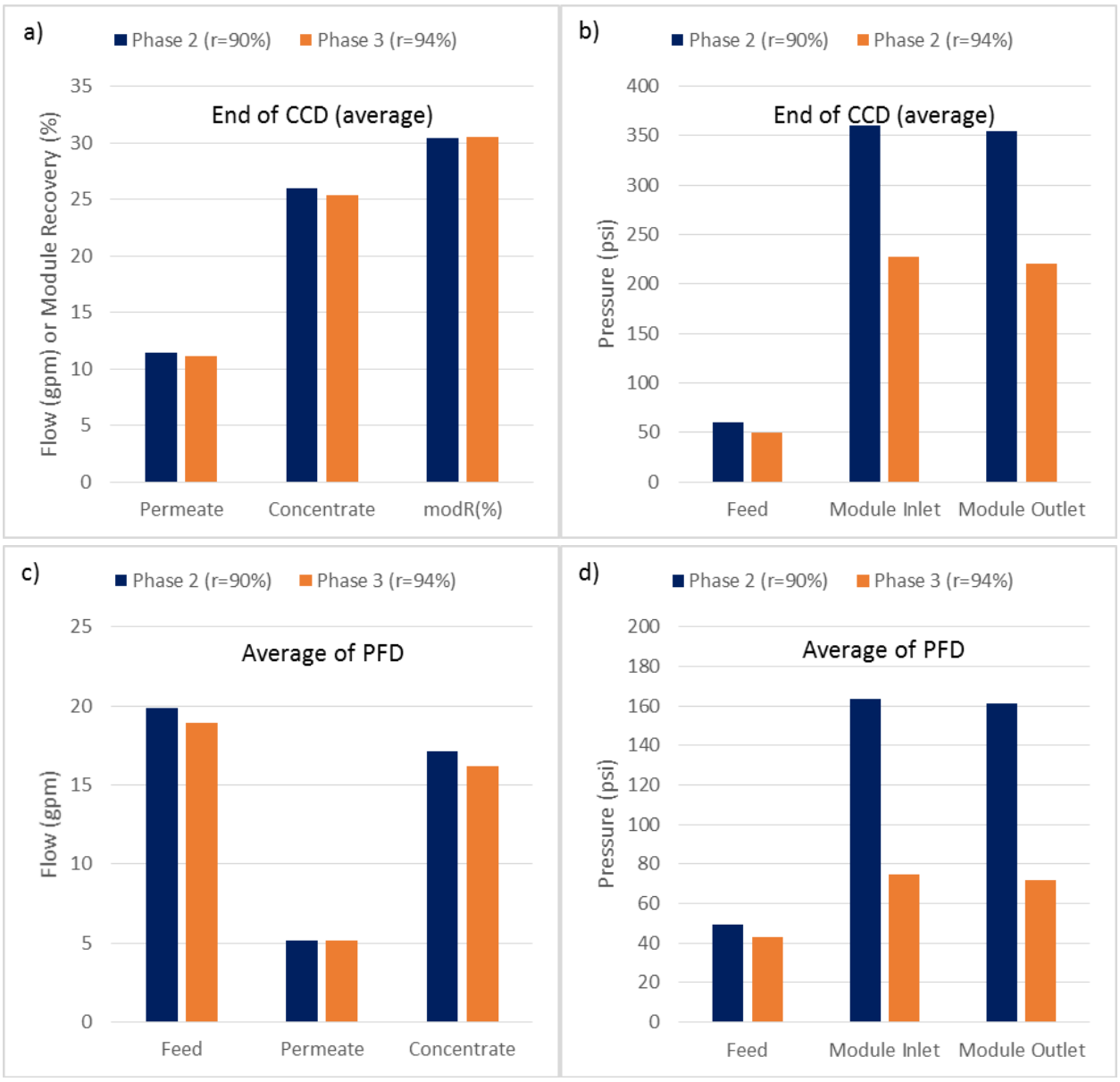

Figure 3.11 Phase 2 and Phase 3 CCRO Pilot Average Data at KBH Desalination Plant showing a) End of CCD Cycle Flow Rate and Module Recovery, b) End of CCD Cycle Pressure, c) PFD Flow, and d) PFD Pressure (September 22-27, 2015 and February 21-23, 2016)

Table 3.3. Water Quality for Phase 2 (r = 90%) CCRO System Samples (September 25, 2016)

	Raw	CCD-Perm-Beg	CCD-Perm-End	CCD-Conc-Beg	CCD-Conc-End	PFD-Perm-End	PFD-Conc-End
Conductivity (μS/cm)	4600	500	996	9940	32700	1130	2470
pH	7.8	5.9	5.9	7.9	7.8	6.1	7.9
Ca^{2+} (mg/L)	148	0.6	0.5	378	1540	0.9	1140
Mg^{2+} (mg/L)	35.7	<0.5	<0.5	91.9	370	0.0	272
Na^{+} (mg/L)	766	94.4	191	1790	6820	218	4940
Cl^{-} (mg/L)	1360	146	301	3090	12300	346	8990
SO_4^{2-} (mg/L)	274	0.1	0.3	692	2920	0.3	2180
HCO_3^{-} (mg/L)	97	12.8	17.1	342	836	18.3	689
SiO_2 (mg/L)	28.0	2.0	4.0	70	270	5.0	200
TDS (mg/L)	2930	302	518	7290	26890	587	20340

Table 3.4. Water Quality for Phase 3 (r = 94%) CCRO System Samples (September 25, 2016)

	Raw	CCD-Perm-Beg	CCD-Perm-End	CCD-Conc-Beg	CCD-Conc-End
pH	6.6	6.3	6.2	6.2	7.2
Ca^{2+} (mg/L)	176	13.2	21.8	373	3760
Mg^{2+} (mg/L)	47	2.5	7.7	108	964
Na^{+} (mg/L)	17.9	6.2	18.0	31	132
K^{+} (mg/L)	784	277	783	1270	5700
Cl^{-} (mg/L)	1420	455	1270	2420	12900
SO_4^{2-} (mg/L)	298	2.1	5.4	676	7260
HCO_3^{-} (mg/L)	91.5	18.3	36.6	567	1040
SiO_2 (mg/L)	26	8.0	20	50	290
TDS (mg/L)	3000	782	2140	5240	35030

3.2.2.4. ZDD Data

ZDD data are available from pilot testing during research in 2013. As described in Cappelle et al. (2017), there were several periods of operation [26]. The ZDD system included an NF system fitted with eight NF270 membranes that was operated at 50-55% recovery. The NF concentrate was fed to an EDM system with two 100-quad MEGA stacks. Earlier activities involved troubleshooting and optimization of operational set points. The ZDD model described in [1] and updated in Chapter 2 focused on the data obtained between June 3 and July 12, 2013. This chapter focuses on the four-day portion of piloting activities when the system achieved the highest ZDD system recovery (97.7%) as shown in Figure 3.13. Data from the pilot as well as ZDD modeling was used to compare performance with the CERRO and CCRO systems.

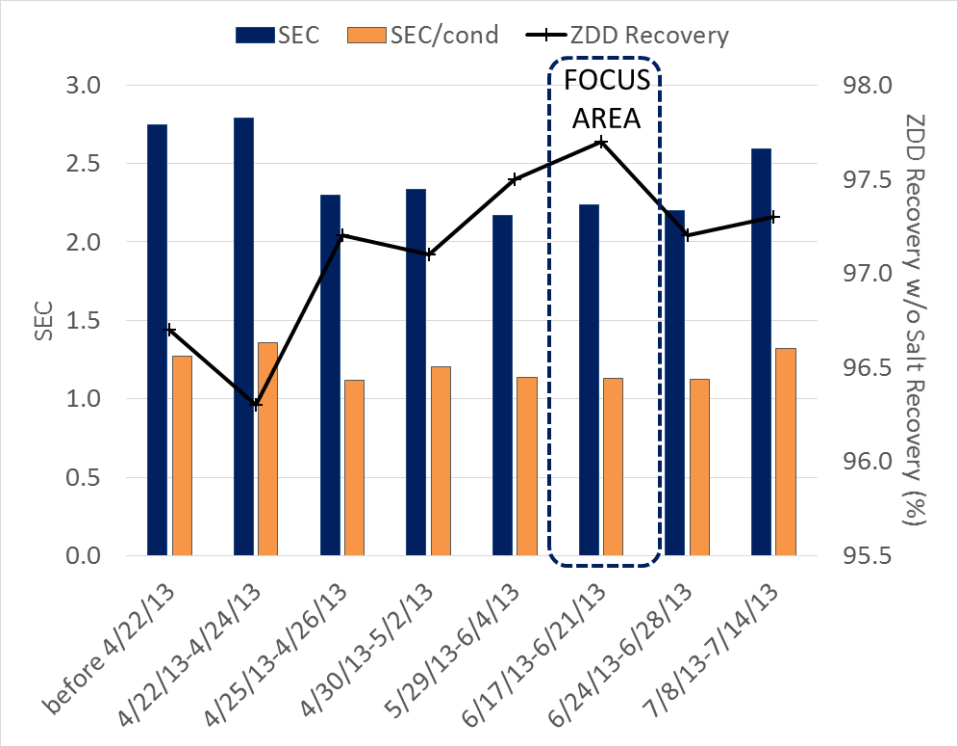

Figure 3.12. ZDD Calculated Specific Energy Consumption (SEC, kWh/m^3), SEC/cond (kWh/m^3 per mS/cm removed), and ZDD System Recovery During ZDD Pilot Testing

3.2.3. Performance Evaluation Assumptions and Calculations

Each of the data sets used to evaluate the technologies used in this chapter had different formats and content. In order to have the most consistent set of data for comparison, the individual data sets were processed with certain calculations. For example, power meter data were only available for the CCRO system and one portion of the CERRO (Well 412) system. CERRO and CCRO power and energy consumption calculations were performed using a similar methodology. For the CERRO batch experiments, data points were taken every 1-5 minutes, so the permeate production (V_{perm}) was calculated by taking an average of the recorded permeate flow (Q_{avg}), then multiplying by the elapsed time (t):

$$V_{perm}(gal) = Q_{avg}(gpm) \cdot t(min) \tag{3.1}$$

Next, the power required for desalination in each time step (P_t) is calculated using the permeate flow and pressure (P_{feed}) that have been converted to the units, m^3/s and Pa, respectively. For the batch CERRO processes, the combined pump/motor efficiency (η) is assumed to be 75%. For the semi-batch processes, it is assumed that a VFD with (95% efficiency) is used; the combined pump/motor efficiency is, therefore, assumed to be 71.25% (0.75 x 0.95).

$$P_t(kW) = \frac{Q_{avg}(m3) \cdot P_{feed}(Pa)}{\eta \cdot 1000 \left(\frac{W}{kW}\right)} \tag{3.2}$$

Finally, the energy at each time step is simply the multiplication of the power and the elapsed time with the appropriate conversion to allow for the units to be kWh. The permeate production during and energy required for the batch is the sum of the values at each of the time steps. By way of example, the batch data from Table B9 in [19] are used to show how they were used to calculate the permeate production, batch recovery, energy, and specific energy consumption (SEC). Similar calculations were used to process the remaining batch CERRO data used in this study. The semi-batch CERRO data were processed slightly differently in that the flow rates were not averaged, but otherwise the methodology was the same.

Table 3.5. Example Calculation Output for CERRO 30-gallon Batch (shaded cells have data directly or derived from Table B9 in [19])

Time (min)	Avg perm flow (lpm)	Perm. Prod. (gal)	avg flow (m^3/s)	Pressure (psi)	Pressure (MPa)	Power (kW)	Energy (kWh)
0				699			
5	2.2	11.1	3.69E-05	697	4.81	0.24	0.0197
10	2.2	10.9	3.63E-05	695	4.80	0.23	0.0193
15	2.1	10.6	3.53E-05	699	4.81	0.23	0.0189
20	2.0	10.2	3.41E-05	705	4.84	0.22	0.0183
25	1.9	9.6	3.19E-05	728	4.94	0.21	0.0175
30	1.6	8.0	2.68E-05	772	5.17	0.18	0.0154
35	1.1	5.7	1.89E-05	810	5.45	0.14	0.0115
40	0.6	3.1	1.04E-05	803	5.56	0.08	0.0064
43	0.3	0.9	5.05E-06	822	5.60	0.04	0.0019
45	0.2	0.4	3.15E-06	831	5.70	0.02	0.0008
	Total Permeate:	70.5	L			Energy (kWh)	0.130
		0.07	m^3			SEC (kWh/m^3)	2.16
	Batch Recovery	62%					

Since the power meter data for the CCRO study provided a breakdown by pump, the recorded data were simply converted using a ratio of the full scale pump efficiency values (provided by Desalitech) to the pilot pumps (assumption). Desalitech suggested that the efficiencies for the high pressure and concentrate circulating pumps would be 84% and 94% for the pump and motor, respectively. It was assumed that a VFD would be used and that its efficiency would be 95% to match the CERRO calculations. It was further assumed that the booster pump would also have the same efficiencies. (The combined efficiency of the motor, pump, and VFD ends up being 75%, but the process is described for clarity nonetheless).

The piloted and calculated full scale pumping SEC (units kWh/m^3) values were compared as-is amongst all of the technologies, but a normalized version was also calculated to see if a visible

trend could be seen for the SEC/cond, which is the SEC divided by the conductivity removed from the brackish water feed (units kWh/m^3 per mS/cm reduction). For example, Figure 3.13 compares the data for Phases 2 (r = 90%) and 3 (r = 94%) at the KBH desalination plant.

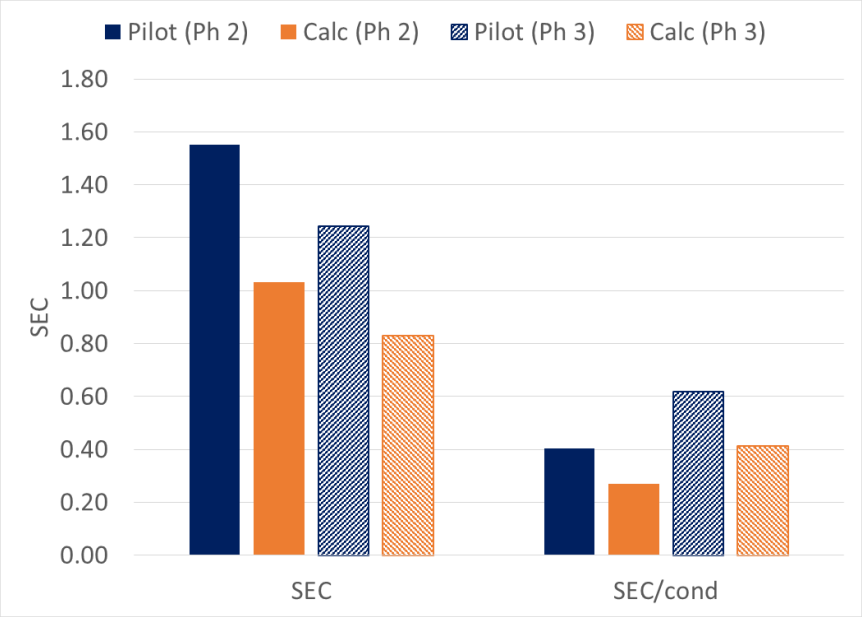

Figure 3.13. CCD Specific Energy Consumption (SEC, kWh/m^3) and SEC/cond (kWh/m^3 per mS/cm removed) as Piloted and Calculated at the KBH plant

3.2.4. Cost Performance Assumptions

The ZDD economic calculations made in Chapter 2 remained as-is, so there are slight differences in the assumptions for some items like the installation factor cost of antiscalant. However, attempts were made to have as close a comparison as possible between the three technologies. Assumptions used in the calculations are summarized in Table 3.6. All cases with evaporation ponds assume an evaporation rate of 14.8 cm/month and capital cost of $200,000 per acre. Deep well injection systems are assumed to be $5.28/gpd reject flow and are based on the KBH site [4]. All cases are amortized assuming a 6% borrowing rate for 20 years. Acid and antiscalant are assumed to cost $3.53 per gallon and $11 per 9-lb gallon, respectively [19]. CERRO acid dosages were calculated using Avista Advisor with the pilot water quality data and pH set point shown in Table 3.6. CCRO acid dosages were calculated using AWC Proton with the

modeled water quality and pH set point shown (even though Desalitech is assuming acid is not needed for the full scale 90% recovery design, it is included because it was piloted). The cost of energy is assumed to be $0.10/kWh in all cases. CERRO equipment cost is based on the cost as installed at the Well 412 site (containerized, small flow rate) and scaled according to permeate production. CCRO equipment-only costs were provided by Desalitech for a 3 MGD feed and scaled according to permeate production. It is possible that the CERRO capital costs are overestimated and the CCRO costs underestimated, but the estimations should be in the same order of magnitude. For the CERRO El Paso cases, El Paso Water reported costs for production at the KBH and Lower Valley desalination plants were used for the primary desalter capital cost estimate. It was assumed that the Well 412 energy consumption is the same as the KBH (0.5 kWh/m^3). The capital and operating costs reported for CERRO account for the relative portion of the permeate production of the primary RO and CERRO. For example, at the Well 412 site, 75% of the capital cost is from the primary RO and 15% (25% x 60%).

Table 3.6. Assumptions Used in Technology Comparison

Case	CERRO	CCRO (KBH)	ZDD
System Feed	18 MGD (KBH) 0.46 MGD (Well 412) 3.9 MGD (Well 2)	18 MGD	18 MGD (KBH) 3.1 MGD (Well2, Well 1/4)
CERRO Feed	3 MGD (KBH) 0.12 MGD (Well 412) 2 MGD (Well 2)	N/A	N/A
1º RO Recovery	82.5% (KBH) 75% (Well 412) 50% (Well 2)	N/A	70% (KBH) 75% (Well 1/4) 50% (Well 2)
System Recovery	96% (KBH) 90% (Well 412) 77% (Well 2)	90%	91% (KBH) 97-98% (Well 1/4) 94% (Well 2)
1º RO Capital Cost	$600/AF [27] (KBH) $503/AF[9] (Well 412)	N/A	$1.50/gpd feed [28]

[9] Used a ratio of 2010 Lower Valley Desalination to KBH Desalination costs in [30], then multiplied by 2014 KBH Desalination cost reported in [27] ($419/$500 x $600 = $502.8/AF)

Case	CERRO	CCRO (KBH)	ZDD
	$1.50/gpd (Well 2)		
CERRO/CCRO/ ZDD Capital Cost Estimate	$3.30/gpd permeate (based on 412 cost)	$1.5M for 3-MGD (equipment only)	$3-$4/gpd (KBH, Well 1/4) $6-7 (Well 2)
Installation Factor (desal equipment)	1.25	CCRO: 5[10]	1.5
Installation Factor (conc. management)	1.5	1.5	1.5
Sulfuric acid set point & dosage	pH 4.0; 228 mg/L (KBH) pH 6.0; 180 mg/L (Well 412) pH 4.0; 253 mg/L (Well 2)	pH 6.9 (90%) 15 mg/L pH 6.3 (94%) 50 mg/L	N/A
Antiscalant dosage	5 (KBH, Well 412) 20 (Well 2)	5	N/A[11]

3.3. Results and Discussion

3.3.1. Water Quality

A total of fourteen cases were developed to evaluate whether medium and high recovery desalination processes such as ZDD, CERRO, and CCRO would be capable of producing good quality drinking water. As shown in

Table 3.7, except for the Phase 3 CCD case, all technologies are expected to be able to produce water with a TDS less than 1000 mg/L, which is the TDS secondary standard in Texas and New Mexico. The ESPA4 MAX membranes were not chosen for their salt rejection, so the case is included for illustrative purposes only. Since the CERRO cases utilize SWRO membranes, the designs are able to produce water with 500 mg/L or lower TDS. Similarly, the CCD operated at 90% recovery is able to produce good quality water as well (410 mg/L TDS). Finally, the ZDD

[10] Desalitech suggested that standard RO bids are in the range of $0.40-$0.50/gpd permeate for equipment only. The ZDD model assumes that a RO will cost $1.50/gpd and has an installation factor of 1.5. In order to have more equivalent capital cost estimates, the value from Desalitech was multiplied by 5, which is calculated from $1.50/$0.50 x 1.5 = 4.5 (rounded to 5).

[11] The ZDD economic model assumed an antiscalant cost of $0.07/kgal feed [5]

designs are able to produce good quality water when higher salt rejection membranes are utilized, but the recovery decreases and/or specific energy consumption increases with increasing salt rejection of the RO/NF membranes. That said, the water shown in the case studies developed are of suitable quality in many locations. The updated ZDD model could be used to identify a design that produces a lower TDS permeate if a user so desires.

Table 3.7. Summary of Technology Comparison Case Studies and their Expected Permeate TDS

Case	System	Water Quality	Type	Feed TDS (mg/L)	Perm TDS (mg/L)
1	CERRO batch	EPW Well 412	Pilot	9,210	74.5
2	CERRO semi-batch	EPW Well 412	Pilot	7,010	75.5
3	BWRO alone	EPW Well 412	Full scale, estimations[12]	1,850	≤ 500
4	BWRO+CERRO	EPW Well 412	Full scale, estimations[13]	1,850	≤ 500
5	KBH alone	KBH	Full scale	11,800	378
6	CERRO batch	KBH	Pilot data + estimations[14]	2,790	468
7	BWRO+CERRO	KBH	Pilot	2,790	381
8	CCRO - Phase 2	KBH	Pilot	2,790	410
9	CCRO - Phase 3	KBH	Model	2,790	1,459
10	ZDD - NF90	KBH	Pilot	5,590	485
11	BWRO + CERRO	BGNDRF Well 2	Model	5,590	150
12	ZDD (NF90)	BGNDRF Well 2	Model	2,570	342
13	ZDD (NF270)	BGNDRF Well 1/4	Pilot	2,690	630
14	ZDD – low i (NF90-NF270)	BGNDRF Well 1/4	Model	2,690	801
15	ZDD – low i (NF90-NF270)	BGNDRF Well 1/4	Model	2,690	586

Another way to compare the case studies is shown in Figure 3.17, where the feed and concentrate TDS concentrations are shown along with the calculated Case Study System TDS removal. While CCRO and CERRO can produce a highly concentrated brine, the ZDD super-

[12] Calculations are based on pilot and full scale data with the assumption that BWRO operates at 75% recovery, CERRO operating at 60% recovery to account for estimated flushes (240 gallons per flush)

[13] Same calculations as for the design without an evaporation pond.

[14] Analysis assumes that Semi-batch CERRO will operate the same as the batch pilot data. The CERRO recovery used in the calculations (76%) is 10% lower than the batch recovery (86%) in order to account for flushing. EPWU assumed to operate at current recovery (82.5%) and SEC (0.5 kWh/m^3).

concentrates are several times more concentrated. This is an important consideration with high recovery processes such as ZDD. Disposal of the ZDD super-concentrate into a surface water supply or sewer system is likely infeasible. In some cases, the CERRO or CCRO concentrates might be allowed to be disposed of this manner. However, since the ZDD case studies involve salt recovery using a relatively small evaporation pond, there is no concern with liquid waste leaving the site. Again, the TDS removal is much higher for the CERRO and CCRO case studies as compared to the ZDD case studies because RO membranes are employed instead of NF membranes.

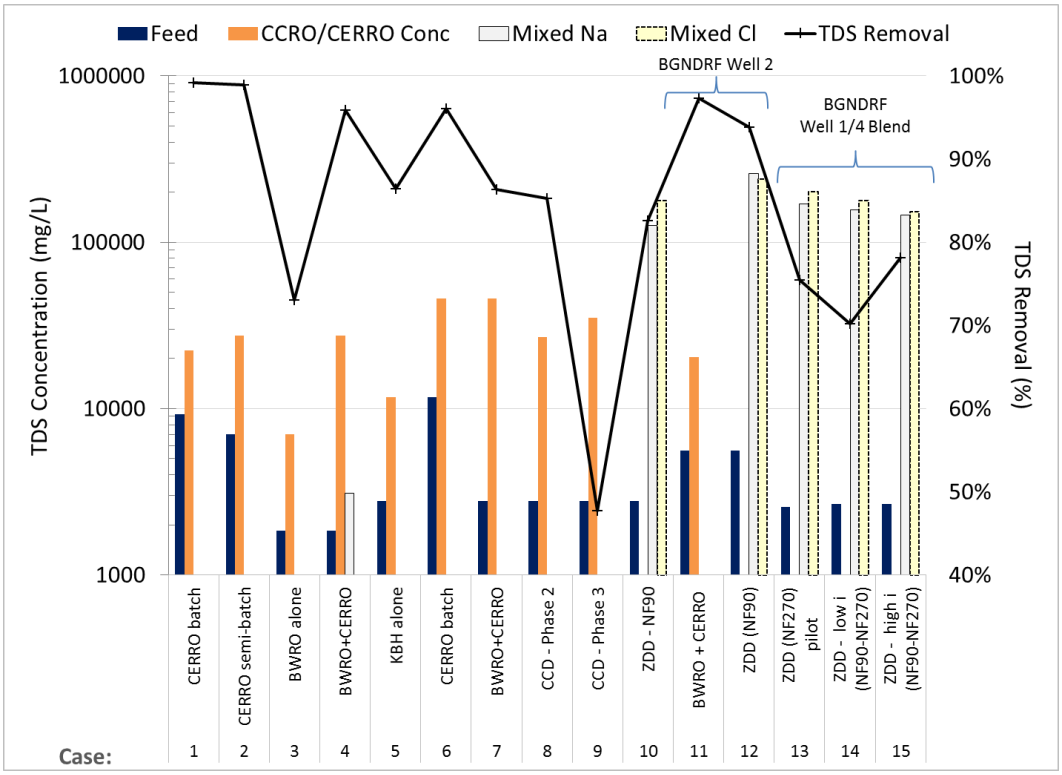

Figure 3.14. Comparison of Case Study Feed and Concentrate TDS with the Calculated TDS Removal

3.3.2. System Recovery & Specific Energy Consumption

The case studies summarized in Section 3.3.1 were further analyzed to evaluate the electrical efficiency and unit cost. As summarized in Figure 3.15, CERRO appears to be expensive when only looking at the unit cost. Part of the reason for this relatively higher capital cost is that

the CERRO system employs an isobaric energy recovery device (ERD). This type of energy recovery is the most efficient, but is also the most expensive. The isobaric ERD is reported to have 90-96% efficiency and cost $77 to $113 per gpm of brine feed, which is approximately 30-100% more expensive than the less efficient Pelton Wheel and Turbocharger ERDs [29]. The isobaric ERD does reduce the energy required for the feed pump by approximately 20%. The cost breakdown of the equipment was not available at the time of this writing, so it is not possible to determine whether the ERD is a net benefit in terms of cost savings. Two forms of concentrate disposal were considered and are summarized in Figure 3.15, namely evaporation ponds (evap) and surface water (SW) disposal.

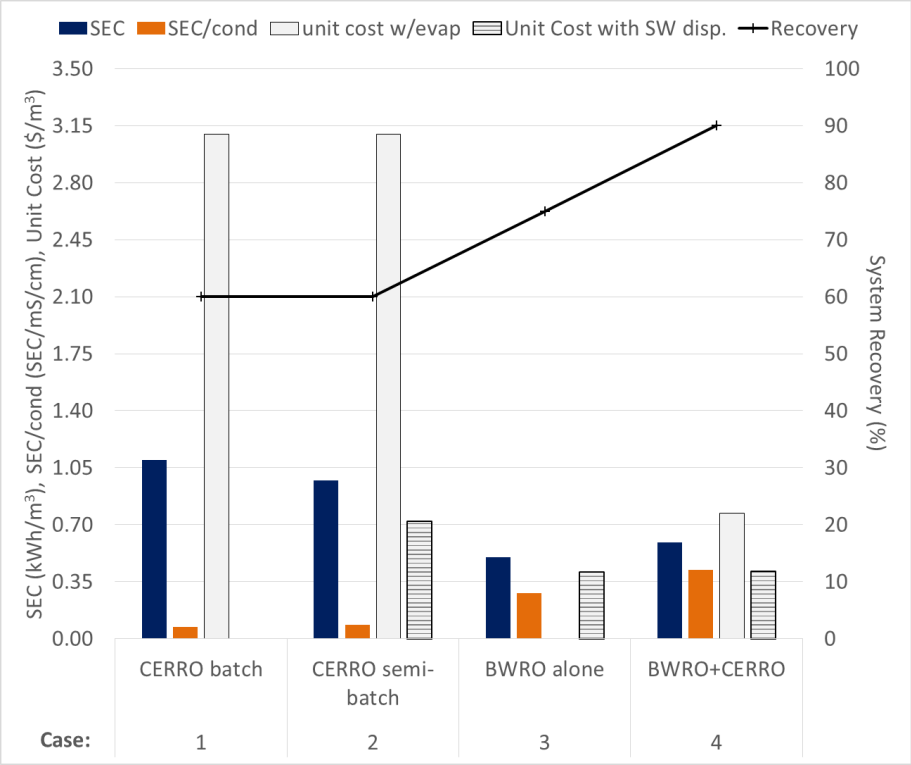

Figure 3.15. Comparison of Calculated Specific Energy Consumption (SEC), SEC/cond, Unit Cost, and System Recovery for Well 412 Location (320 gpm feed)

The KBH plant is the only location for which pilot (and model) data are available to compare all three technologies. Since only batch CERRO data was available for the KBH, the recovery was decreased to account for the flush volumes, but the system recovery is still near 96%.

Two types of concentrate management are summarized in Figure 3.16, namely evaporation ponds (evap) and deep well injection (DWI).

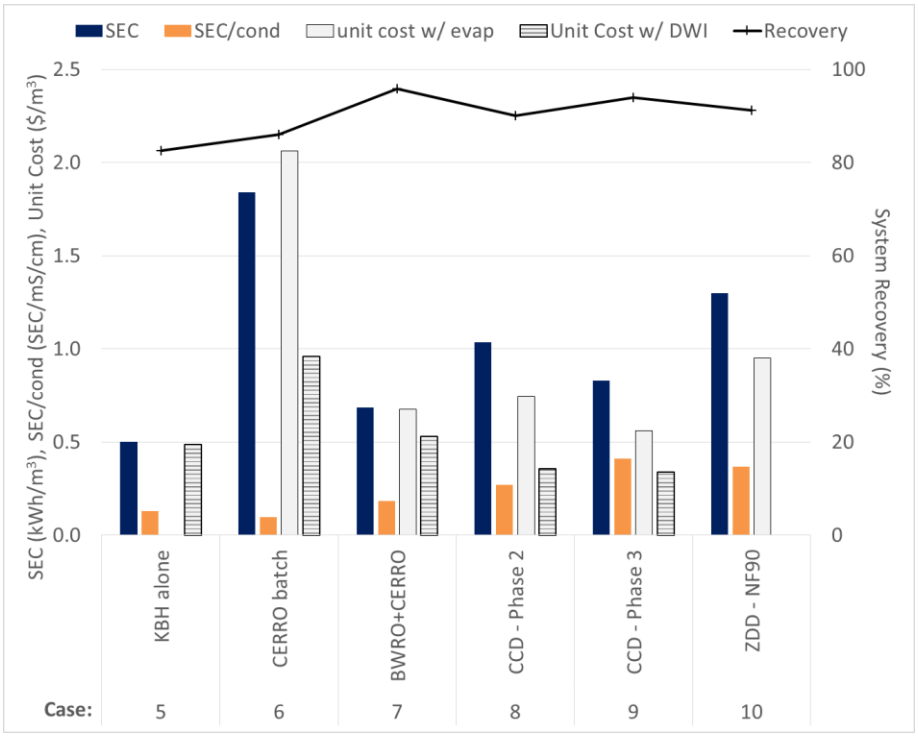

Figure 3.16. Comparison of Calculated Specific Energy Consumption (SEC), SEC/cond, Unit Cost, and System Recovery for KBH Desal Plant (18 MGD feed)

While an evaporation pond would not be feasible for either of the El Paso sites, it is included for the sake of comparing all sites. It is unknown whether the permit conditions or geology would support deep well injection at both of the sites. The KBH site has existing injection wells, but the super concentrate from both CCRO and CERRO would contain higher TDS concentrations than the existing concentrate. For the sake of comparison, cost estimates with both evaporation ponds and deep well injection are included for the KBH case study. Only evaporation ponds are included with the Well 2 study because the super-concentrate from the CERRO and ZDD are expected to be too scale-forming to be injected. With the assumptions used in this chapter (see Table 3.6) and built into the ZDD model, it appears that the lowest cost options for medium and high recovery at the KBH desalination plant are CCRO and ZDD with salt recovery. The ZDD

design still utilizes a 56-acre evaporation pond, which is 35% smaller than what either of the CERRO or CCRO would require.

The Alamogordo case studies are summarized in Figure 3.17. As described in the pilot report, CERRO was not able to achieve reasonable recovery without the addition of sodium chloride or high doses of antiscalant when treating the Well 2 water at the BGNDRF [19]. The 20 ppm antiscalant RO+CERRO case was reported to achieve an overall recovery of 76.5% (RO recovery = 50%, CERRO recovery = 53%) [19]. With this in mind, CERRO outperforms on the basis of specific energy consumption and unit cost (see Figure 3.17a). However, with a 27% increase in unit cost, there is a 23% increase in system recovery and 79% reduction in the size of the evaporation ponds. Again, a 177-acre evaporation pond may not be realistic, however it is not known whether the geology or permitting rules would allow for disposal of the CERRO concentrate. The final five ZDD case studies are shown in Figure 3.17b. The reason for inclusion is to show how the SEC can be relatively high with a reasonable cost for the recovery of the ZDD system. More power would be required in order to achieve a lower TDS product water.

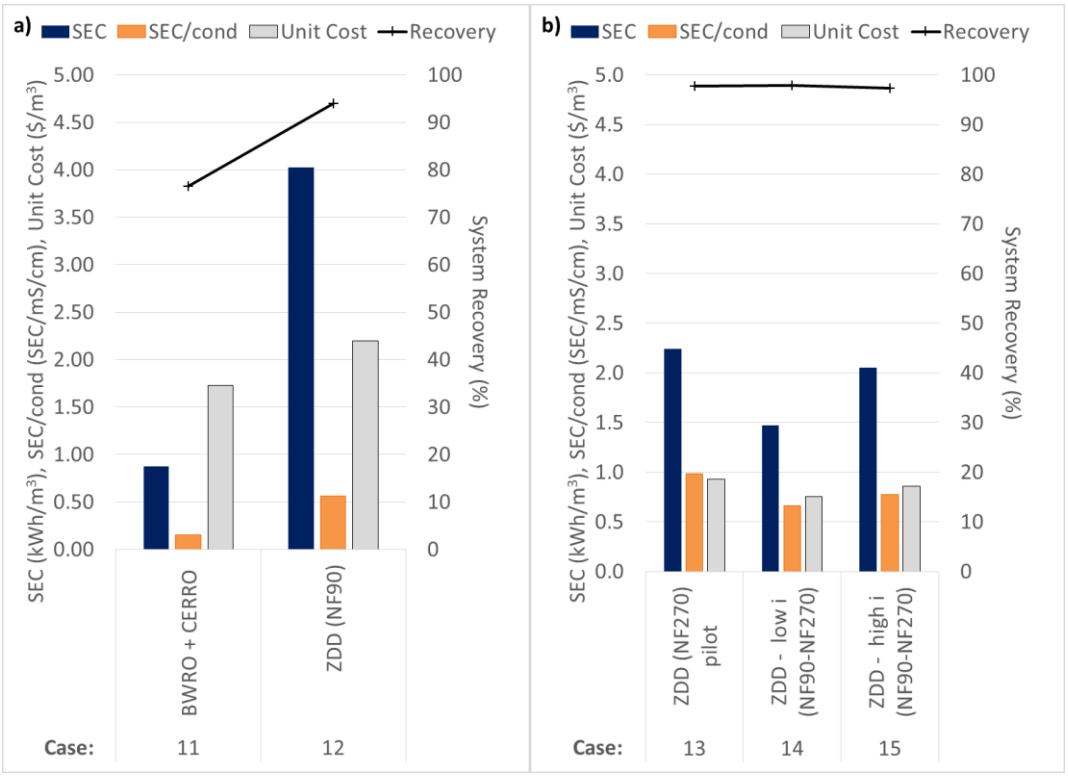

Figure 3.17. Comparison of Calculated Specific Energy Consumption, SEC/cond, Unit Cost, and System Recovery for a) BGNDRF Well 2 and b) BGNDRF Well 1/4 Blend

3.3.3. Relative Performance of Technologies

One way to compare the performance of desalination technologies relative to each other is to use a matrix with weighted factors. The matrix includes a ranking of each technology in order of performance in the categories of specific energy consumption, cost, system recovery, system complexity, and technology readiness. The first three categories utilize the numerical results from the pilot tests and economic calculations. The final two are subjective and based on the author's assessment of the technology. Different assumptions and weights could yield different results. A technology is rated as "better" than the others if its performance is better. For example, if ZDD has a recovery of 97% and CERRO 77%, ZDD would be assigned a value of one and CERRO a value of two. Since recovery is assumed to play a crucial role in whether a desalination plant is built, recovery is given a higher weight (30%) than the other four categories. Technology readiness is assumed to carry a higher weight, at least with respect to municipal facilities, so the assigned

weight is 25%. The remaining categories each have a 15% weight. In some cases, the performance was similar (*e.g.*, ZDD recovery = 91% and CCRO recovery = 90%[15]), so a tie is declared and each technology is given the same rank value. Evaluating the complexity was done for the system as a whole for each technology and is admittedly subjective. The readiness ranking was decided based on the number of customers. CCRO has sold more than 100 systems on six continents to different customers and has a developed marketing strategy. CERRO has been installed at one location and three more are planned in El Paso, Texas. No known installations exist for the ZDD technology. The CCRO and CERRO desalination processes themselves are considered to be less complex than the ZDD system since ZDD includes two desalination processes and salt recovery. The rank and weighted score are shown for each of the categories for the two site comparisons in Table 3.8 and Table 3.9. The order of the technology preference is the opposite of weighted scores (*i.e.*, low score = better performer). At the KBH, the technology preference is CCRO-90% (1.45) > CERRO (1.55) > ZDD (2.4). At the BGNDRF Well 2, the technology preference is CERRO (1.45) > ZDD (1.55). It is assumed that CCRO would perform similarly to CERRO at the Well 2 site.

Table 3.8. Relative Performance of CCRO and CERRO with Deep Well Injection, and ZDD with Evaporation Ponds at KBH

	CERRO	**CCRO**	**ZDD**
Cost	3	1	2
SEC	1	2	3
Recovery	1	2	2
Complexity	1	1	2
Readiness	2	1	3
Weighted Average	1.55	1.45	2.4

[15] While the CCRO is expected to be able to operate stably at 94% with high salt rejection membranes, since 90% recovery was the highest piloted with RO membranes, that case is used for comparison purposes.

Table 3.9. Relative Performance of CERRO and ZDD Technologies (both with Evaporation Ponds) at BGNDRF Well 2

	CERRO	ZDD
Cost	1	2
SEC	1	2
Recovery	2	1
Complexity	2	1
Readiness	1	2
Weighted Average	1.45	1.55

3.4. Conclusions

Several medium and high recovery technologies were compared for the desalination of brackish groundwater in the El Paso, Texas, and Alamogordo, New Mexico, areas. While better cost estimates and possibly additional piloting are needed to confirm the results obtained, some general statements can be made. There does seem to be a water quality factor that causes differentiation between the technologies, however more research is needed to quantify. At a first glance, it seems that waters similar to those in El Paso (relatively low *Y-Index*) are well-suited for semi-batch processes such as CERRO and CCRO and water similar to those in Alamogordo could benefit from ZDD with salt recovery.

Since costs are known for the KBH desalination plant, some specific observations can be made:

- Assuming the semi-batch CERRO system will operate the same as the batch system tested at the KBH, the CERRO option has the largest increase in recovery (16%), followed by ZDD with salt recovery (10.5%), and CCRO (9.1%).
- All technologies will increase the system recovery and consequently increase the specific energy consumption required to produce drinking water. The CERRO process would have the smallest increase in SEC relative to KBH (37%), followed by CCRO (107%), and ZDD with salt recovery (160%).

- Assuming the semi-batch CERRO system scales with permeate production and that evaporation ponds are an acceptable concentrate management solution, CCRO has the lowest increase in unit cost (39%), followed by CERRO (53%), then ZDD (95%). If the existing injection wells could not be utilized for the CERRO and CCRO concentrate, the unit increase would be higher because evaporation ponds would be required (and the cost of deep well injection has a relatively lower capital cost).
- ZDD with salt recovery offers the smallest evaporation pond size, but it is likely still infeasible at the KBH and Well 412 sites. The KBH plant is located near the airport, so ponds would not be good because of reflection, and they could attract birds. The Well 412 site is located near the Interstate Highway 10 in a congested area. The CERRO concentrate is currently sent to the sewer system at the Well 412 site, which is not a problem since there are minimal salts added (although locally the concentration may increase in the pipelines).

In cases where the brackish water contains relatively high proportions of divalent ions (high *Y-Index*), ZDD may have an advantage because it is able to achieve the highest recoveries. It is possible that there would be savings from pumping less groundwater to achieve the same production of drinking water and also that revenue from the sale of byproducts would lessen the cost increase from lower recovery desalination. In places where the geology or permitting rules do not allow for deep well injection, ZDD may be an attractive option.

General Conclusions

Desalination is being considered by many cities, regions, and industry as a way to augment their existing water supplies. Electrodialysis, reverse osmosis, and nanofiltration systems have been installed in many locations throughout the US and rest of the world, however these technologies are generally limited to 75-80% recovery for brackish feed water. This means that 20-25% of the initial volume of water pumped from a deep aquifer must now be managed as a waste stream. Desalination concentrate can be disposed of in surface water supplies (river, lake), evaporation ponds, deep well injection, pipelines to the ocean (as in southern California), or thermal zero liquid discharge processes. In most cases, the cost and land requirement for evaporation ponds will eliminate this evaporation ponds. Regulations and availability of suitable geological formations for disposal can limit high recovery processes will limit where deep well injection is feasible. And disposal into surface water supplies is generally limited to low volume, low salinity concentrate streams. Finally, thermal processes can be expensive, both in terms of capital and operating cost.

High recovery desalination technologies such as ZDD, CCRO, and CERRO can reduce the volume of concentrate that would need to be disposed of and, assuming a fixed product flow, could also reduce the amount of brackish water that would have to be pumped from an aquifer in the first place. Of course, each site will have its own challenges and requirements that will affect the choice of desalination method and its unit cost.

A mathematical process model was used to evaluate the technical performance of ZDD for the desalination of eight brackish groundwaters in Texas, New Mexico, Colorado, and California. The model combines proprietary software output, ZDD pilot data from the BGNDRF and the KBH Desalination plant, mass and energy balances, and theoretical calculations. The model allows for user-selection of a range of membranes (loose NF, tight NF, hybrid NF, low-energy RO, standard RO) and manual input of EDM characteristics (membrane resistance, current efficiency, etc.). The model output suggests that an optimum ZDD design will balance the capital cost of EDM stacks

with the ZDD system specific energy consumption. The lowest cost designs evaluated in this research included ZDD systems that maximized the RO/NF recovery, minimized the EDM current density and recycle ratio, and incorporated salt recovery. The choice of membrane for the primary desalter is driven by the desired product water quality. If high rejection membranes are chosen, lower ZDD recovery can be expected. The predicted sodium chloride solution purity may not be pure enough to use directly in the EDM, however pilot studies have shown different results.

A comparison of three desalination technologies capable of achieving medium (>90%) and high (>95%) recoveries for the desalination of brackish groundwater at four locations (two El Paso desalination plants and two Alamogordo, New Mexico, well waters). While additional research is necessary in order to fine tune the economic analyses and further optimize the system designs, some general observations were made. The type of groundwater being desalinated does seem to have an impact on the choice of technology. Brackish groundwater similar to that of El Paso Water's KBH and Well 412 are well-suited for semi-batch processes such as CERRO and CCRO. Brackish groundwater with relatively high concentrations of calcium and sulfate relative to TDS could benefit from ZDD with salt recovery, because it can achieve very high recovery (93%-98%) even with relatively high TDS (3,500 mg/L). A numerical matrix ranking approach was developed to compare the relative performance of ZDD, CERRO, and CCRO with respect to specific energy consumption, cost, system recovery, and system complexity. The relative performance for desalinating brackish water with relatively low divalent ion concentrations is: CERRO > CCRO > ZDD. The relative performance for the desalination of brackish water with relatively high concentrations of divalent ions is: ZDD > CERRO = CCRO, although this is subject to the assumptions made in the chapter. Site-specific details such as the feasibility of deep-well injection can change the order of technology preference.

Future Work

The results of the ZDD modeling effort suggest that a design different (75% RO recovery versus 55% recovery, lower EDM ion removal) from what was piloted could have substantial energy and cost savings. A pilot test that evaluates the performance of ZDD as a function of design choices would allow for better cost estimates to be made. Additionally, a field test that demonstrates the feasibility of salt recovery using precipitation and evaporation processes would be useful to evaluate the purity of the recovered solid products and sodium chloride solution.

More models should be built to evaluate whether the CERRO and CCRO designs could be further optimized to reduce energy and capital cost savings. Simple models that are commercially available could be used for this process. In the case of CCRO, some of the antiscalant software models have actually built in the CCRO concept, which will allow for detailed analysis of concentrate stability with chemical treatment. If possible, additional testing with a 3:2:1 semi-batch CERRO should be tested at new El Paso Water wellhead desalination systems prior to the full scale systems being installed.

Several agencies and other entities have published maps of brackish groundwater chemistries of the United States. Linking the database values to desalination technologies may be of interest to design engineers working to design desalination plants.

References

[1] M. Cappelle, W.S. Walker, T.A. Davis, Improving Desalination Recovery Using Zero Discharge Desalination (ZDD): A Process Model for Evaluating Technical Feasibility, Ind. Eng. Chem. Res. 56 (2017) 10448–10460. doi:10.1021/acs.iecr.7b02472.

[2] M.C. Mickley, Treatment of Concentrate, US Department of the Interior, Bureau of Reclamation, Technical Service Center, Denver, CO, 2009. www.usbr.gov/pmts/water/publications/reports.html.

[3] E.G. Archuleta, R.S. Raucher, J. Clements, J. Oxenford, M. Mickley, W. Dugat, M. Cappelle, T.A. Davis, A. Tarquin, W. Hargrove, A. Michelson, Z. Sheng, R. Lacewell, A. Fernald, Desalination Concentrate Management Policy Analysis for the Arid Southwest, WateReuse, Alexandria, VA, 2015.

[4] M. Cappelle, T.A. Davis, L.M. Camacho, P.J. Brandhuber, B. Biagini, B. Mack, A. Yetayew, Mining for salts: Recovering useful by-products from BWRO Brine, in: Proc. from 2013 AWWA/AMTA Membr. Technol. Conf., n.d.

[5] R. Bond, T.A. Davis, J. DeCarolis, M. Dummer, Demonstration of a new electrodialysis technology to reduce energy required for salinity management: Treatment of RO concentrate with EDM, California Energy Commission, Energy Research and Development Division, Sacramento, CA, 2015.

[6] R. Bond, B. Klayman, C. Spencer, V. Veerapaneni, T.A. Davis, B. Batchelor, Zero Liquid Discharge Desalination, Water Research Foundation, Denver, CO, 2011. http://www.waterrf.org/Pages/Projects.aspx?PID=4163.

[7] P.J. Brandhuber, A. Vieira, K. Kinser, J. Gelmini, Pilot testing of membrane zero liquid discharge for drinking water systems, IWA Publishing, London, 2014. http://www.werf.org/a/ka/Search/ResearchProfile.aspx?ReportId=WERF5T10.

[8] A.H. Galama, M. Saakes, H. Bruning, H.H.M. Rijnaarts, J.W. Post, Seawater predesalination with electrodialysis, Desalination. 342 (2014) 61–69.

[9] W.S. Walker, Y. Kim, D.F. Lawler, Treatment of model inland brackish groundwater reverse osmosis concentrate with electrodialysis—Part I: sensitivity to superficial velocity, Desalination. 344 (2014) 152–162. doi:10.1016/j.desal.2014.03.035.

[10] N. Kabay, O. Ipeck, H. Kahveci, M. Yuksel, Effect of salt combination on separation of monovalent and divalent salts by electrodialysis, Desalination. 198 (2006) 84–91.

[11] H.J. Lee, F. Sarfert, H. Strathmann, S.H. Moon, Designing of an electrodialysis desalination plant, Desalination. 142 (2002) 267–286. doi:10.1016/S0011-9164(02)00208-4.

[12] H.J. Lee, H. Strathmann, S.H. Moon, Determination of the limiting current density in

electrodialysis desalination as an empirical function of linear velocity, Desalination. 190 (2006) 43–50. doi:10.1016/j.desal.2005.08.004.

[13] R.K. McGovern, S.M. Zubair, J.H. Lienhard, The cost effectiveness of electrodialysis for diverse salinity applications, Desalination. 348 (2014) 57–65.

[14] J.M. Ortiz, J. a. Sotoca, E. Expósito, F. Gallud, V. García-García, V. Montiel, a. Aldaz, Brackish water desalination by electrodialysis: Batch recirculation operation modeling, J. Memb. Sci. 252 (2005) 65–75. doi:10.1016/j.memsci.2004.11.021.

[15] Dow Water & Process Solutions, ROSA System Design Software, (n.d.). http://www.dow.com/en-us/water-and-process-solutions/resources/design-software/rosa-software (accessed January 2, 2017).

[16] E. Mancha, D. DeMichele, W.S. Walker, T.F. Seacord, J. Sutherland, A. Cano, Part II: Performance Evaluation of Reverse Osmosis Membrane Computer Models, Texas Water Development Board, 2014. https://www.twdb.texas.gov/innovativewater/desal/projects/carollo2/doc/Part II. Performance Evaluation of Reverse Osmosis Membrane Computer Models.pdf.

[17] D.R. Helsel, R.M. Hirsch, Chapter 2 Graphical Data Analysis, in: Stat. Methods Water Resour. Tech. Water Resour. Investig., US Geological Survey, 2002: pp. 17–64. http://pubs.usgs.gov/twri/twri4a3/pdf/chapter2new.pdf.

[18] MEGA, Technical Documentation: Electrodialyser ED-II/4x, MEGA a.s., Straz pod Ralskem, Czech Republic, 2010.

[19] H. Strathmann, Ion-Exchange Membrane Separation Processes, Elsevier B.V., 2004.

[20] A.J. Bard, L.R. Faulkner, Electrochemical Methods: Fundamentals and Applications, 2nd ed., Wiley, 2001.

[21] T.A. Davis, J.D. Genders, D. Pletcher, A first course in ion permeable membranes, The Electrochemical Company, Lancaster, New York, 1997.

[22] J.J. Krol, M. Wessling, H. Strathmann, Concentration polarization with monopolar ion exchange membranes: current-voltage curves and water dissociation, J. Memb. Sci. 162 (1999) 145–154. doi:10.1016/S0376-7388(99)00133-7.

[23] N. Káňavová, L. Machuča, D. Tvrzník, Determination of limiting current density for different electrodialysis modules, Chem. Pap. 68 (2013) 324–329. doi:10.2478/s11696-013-0456-z.

[24] F.B. Leitz, M.A. Accomazzo, H.I. Viklund, A.D. Jha, High temperature electrodialysis: Phase V, US Department of Commerce, National Technical Information Service, Springfield, VA, 22151, 1974.

[25] N. Ortega-Corral, High-recovery inland desalination: Concentrate treatment by

electrodialysis and batch reverse osmosis, The University of Texas at El Paso, 2013. http://digitalcommons.utep.edu/dissertations/AAI3682476/.

[26] M. Cappelle, T.A. Davis, E. Gilbert, Demonstration of Zero Discharge Desalination (ZDD), US Department of the Interior, Bureau of Reclamation, 2014. https://www.usbr.gov/research/dwpr/reportpdfs/report165.pdf.

[27] A. Seidell, Solubilities of inorgainic and organic substances: A handbook of the most reliable quantitative solubility determinations, D. Van Nostrand Company, New York, 1911.

[28] C.L. Bellona, A. Waldron, J. Min, L. Jin, Selection of Salt, Metal, Radionuclide, and Other Valuable Material Recovery Approaches, WateReuse Research Foundation, Alexandria, VA, 2015.

[29] D.H. Kim, A review of desalting process techniques and economic analysis of the recovery of salts from retentates, Desalination. 270 (2011). doi:10.1016/j.desal.2010.12.041.

[30] J. Goldman, Selective Salt Recovery from Reverse Osmosis Concentrate Using Inter-stage Ion Exchange, The University of New Mexico, 2012.

[31] Enviro Water Materials, Enviro Water Minerals Company Celebrates Completion of Innovative Water Project in El Paso, (2017). http://envirowaterminerals.com/press/RibbonCut.pdf (accessed March 24, 2018).

[32] L. Katzir, Y. Volkmann, N. Daltrophe, E. Korngold, R. Mesalem, Y. Oren, J. Gilron, WAIV - Wind aided intensified evaporation for brine volume reduction and generating mineral byproducts, Desalin. Water Treat. 13 (2010) 63–73. doi:10.5004/dwt.2010.772.

[33] M. Cappelle, B. Alspach, J. Gilron, C. Russell, T.A. Davis, N. Asaf, G. Trejo, High recovery desalination with enhanced evaporation: Achieving Zero Liquid Discharge sustainably, in: AMTA Membr. Technol. Conf., AMTA, 2015.

[34] J.P. Gustafsson, Visual MINTEQ ver. 3.1, (2016). https://vminteq.lwr.kth.se/ (accessed April 8, 2018).

[35] ASTOM, Comparison Table for Detailed Specifications of Cation/Anion Exchange Membranes, (n.d.). http://www.astom-corp.jp/en/product/images/astom_hyo.pdf (accessed March 24, 2018).

[36] W.S. Walker, Y. Kim, D.F. Lawler, Treatment of Model Inland Brackish Groundwater Reverse Osmosis Concentrate with Electrodialysis — Part II: Sensitivity to Voltage Application and Membranes, Desalination. 345 (2014) 128–135. doi:10.1016/J.DESAL.2014.04.026.

[37] A. Campione, L. Gurreri, M. Ciofalo, G. Micale, A. Tamburini, A. Cipollina, Electrodialysis for water desalination: A critical assessment of recent developments on

process fundamentals, models and applications, Desalination. 434 (2018) 121–160. doi:10.1016/J.DESAL.2017.12.044.

[38] H. Jaroszek, P. Dydo, Potassium nitrate synthesis by electrodialysis-metathesis: The effect of membrane type, J. Memb. Sci. 549 (2018) 28–37. doi:10.1016/J.MEMSCI.2017.11.062.

[39] R.K. McGovern, A.M. Weiner, L. Sun, C.G. Chambers, S.M. Zubair, J.H. Lienhard V, On the cost of electrodialysis for the desalination of high salinity feeds, Appl. Energy. 136 (2014) 649–661. doi:10.1016/J.APENERGY.2014.09.050.

[40] J.C. Crittenden, R. Rhodes Trussell, David W. Hand, K.J. Howe, G. Tchobanoglous, J.H. Borchardt, 20: Removal of Selected Constituents, in: MWH's Water Treat. Princ. Des., 3rd ed., John Wiley & Sons, Inc., Hoboken, New Jersey, 2012: p. 1574.

[41] K.M. Chehayeb, D.M. Farhat, K.G. Nayar, J.H. Lienhard, Optimal design and operation of electrodialysis for brackish-water desalination and for high-salinity brine concentration, Desalination. 420 (2017) 167–182. doi:10.1016/J.DESAL.2017.07.003.

[42] R. Bond, V. Veerapaneni, Zero Liquid Discharge for Inland Desalination, AWWA Research Foundation, 2007.

[43] G. Juby, A. Zacheis, W. Shih, P. Ravishanker, B. Mortazavi, M.D. Nusser, Evaluation and Selection of Available Processes for a Zero-Liquid Discharge System for the Perris, California, Ground Water Basin, 2008. http://www.usbr.gov/pmts/water/publications/reportpdfs/report149.pdf.

[44] Y. Oren, E. Korngold, N. Daltrophe, R. Messalem, Y. Volkman, L. Aronov, M. Weismann, N. Bouriakov, P. Glueckstern, J. Gilron, Pilot studies on high recovery BWRO-EDR for near zero liquid discharge approach, Desalination. 261 (2010) 321–330. doi:10.1016/j.desal.2010.06.010.

[45] N. Ghaffour, T.M. Missimer, G.L. Amy, Technical review and evaluation of the economics of water desalination: Current and future challenges for better water supply sustainability, Desalination. 309 (2013) 197–207. doi:10.1016/j.desal.2012.10.015.

[46] USGS, Average Value of Salt, by Product Form and Type, 2015 USGS Miner. Yearb. (2017). https://minerals.usgs.gov/minerals/pubs/commodity/salt/index.html#mcs (accessed January 1, 2017).

[47] USGS, Lime Prices in the United State, By Type, 2015 USGS Miner. Yearb. (Advance Data Release). (2016). https://minerals.usgs.gov/minerals/pubs/mcs/#C.

[48] M. Mickley, Membrane Concentrate Disposal: Practices and Regulation, U.S. Department of the Interior, Bureau of Reclamation, 2006.

[49] USGS, Salient Gypsum Statistics, 2016. https://minerals.usgs.gov/minerals/pubs/commodity/gypsum/index.html#mcs.

[50] USGS, 20, 2016. https://minerals.usgs.gov/minerals/pubs/commodity/magnesium/index.html#mcs.

[51] D. Brown, T. Rynders, C. Stillwell, C. Douglas, S. Niebur, Brackish Water Reverse Osmosis: A Proven Cost-Effective Renewable Water Supply, J. AWWA. 109 (2017) 28–39. doi:10.5942/jawwa.2017.109.0020.

[52] S.H. Shirazi, E. Harrah, D. Timmermann, J. Hudkins, J.K. Kinslow, Initial Performance of Membrane and Remineralization Processes for the SAWS Brackish Groundwater Desalination Plant, in: AMTA Membr. Technol. Conf., San Antonio, 2013.

[53] P.J. Gorder, Development of Brackish Groundwater as a Sustainable Supply to Support Growth and Military Base Expansion in El Paso, in: Ninth Annu. Natl. Salin. Summit, Multi-State Salinity Coalition, 2009. http://multi-statesalinitycoalition.com/storage/summit/2009/Summit2009_gorder.pdf (accessed January 15, 2018).

[54] G.W. Carpenter, Recovery & Concentrate Management: A Quick Look at Three Local Projects, in: WRRC Annu. Conf., WRRC, Yuma, AZ, 2011.

[55] Snehal Desai, Steve Rosenberg, Nanette Hermsen, Minimal Liquid Discharge Adopting A "Less Is More" Mindset, Water Online. (2016). https://www.wateronline.com/doc/minimal-liquid-discharge-adopting-a-less-is-more-mindset-0001 (accessed March 29, 2018).

[56] M. Cappelle, T.A. Davis, L.M. Camacho, P. Brandhuber, B. Biagini, B.R. Mack, A.A. Yetayew, Mining for salts: Recovering useful by-products from bwro brine, in: AMTA/AWWA Membr. Technol. Conf. Expo. 2013, 2013.

[57] J. Morillo, J. Usero, D. Rosado, H. El Bakouri, A. Riaza, F.-J. Bernaola, Comparative study of brine management technologies for desalination plants, Desalination. 336 (2014) 32–49. doi:10.1016/J.DESAL.2013.12.038.

[58] B. Alspach, G. Juby, Cost-Effective ZLD Technology for Desalination Concentrate Management, J. Am. Water Works Assoc. 110 (2018) 37–47. doi:10.5942/jawwa.2018.110.0005.

[59] A. Tarquin, High tech methods to reduce concentrate volume prior to disposal, Final Rep. (TWDB Contract #0704830769). (2010). http://www.twdb.texas.gov/publications/reports/contracted_reports/doc/0704830769_ConcentrateVolume.pdf (accessed March 29, 2018).

[60] R.L. Stover, Permeate recovery and flux maximization in semibatch reverse osmosis, IDA J. Desalin. Water Reuse. 5 (2013). doi:DOI 10.1179/2051645213Y.0000000002.

[61] A. Efraty, Z. Gal, Closed circuit desalination series No 7: retrofit design for improved performance of conventional BWRO system, Desalin. Water Treat. 41 (2012) 301–307.

doi:10.1080/19443994.2012.664716.

[62] A. Subramani, J.G. Jacangelo, Emerging desalination technologies for water treatment: A critical review, Water Res. 75 (2015) 164–187. doi:10.1016/J.WATRES.2015.02.032.

[63] J.R. Werber, A. Deshmukh, M. Elimelech, Can batch or semi-batch processes save energy in reverse-osmosis desalination?, Desalination. 402 (2017) 109–122. doi:10.1016/J.DESAL.2016.09.028.

[64] D.M. Warsinger, E.W. Tow, K.G. Nayar, L.A. Maswadeh, J.H. Lienhard V, Energy efficiency of batch and semi-batch (CCRO) reverse osmosis desalination, Water Res. 106 (2016) 272–282. doi:10.1016/J.WATRES.2016.09.029.

[65] A. Tarquin, High Recovery of RO Concentrate Using a Batch-Treatment Seawater RO System, Denver, CO, 2012. https://www.usbr.gov/research/dwpr/reportpdfs/Report 159-Final with Appendices_508.pdf (accessed March 29, 2018).

[66] A. Efraty, R.N. Barak, Z. Gal, Closed circuit desalination - A new low energy high recovery technology without energy recovery, Desalin. Water Treat. 31 (2011) 95–101. doi:doi: 10.5004/dwt.2011.2402.

[67] G.G. Delgado, An evaluation of the CERRO process as an efficient RO concentrate mangement system, ETD Collection for University of Texas, El Paso, 2013. https://digitalcommons.utep.edu/dissertations/AAI3609478 (accessed March 31, 2018).

[68] A. Tarquin, Continuous Flow Seawater RO System for Recovery of Silica-Saturated RO Concentrate, Texas Water Development Board, 2011. http://www.twdb.texas.gov/innovativewater/desal/projects/elpaso/doc/elpaso_final_report_0711.pdf (accessed March 29, 2018).

[69] A. Tarquin, W.S. Walker, G.G. Delgado, Sea Water Reverse Osmosis System to Reduce Concentrate Volume Prior to Disposal, US 2017/0203979, 2017.

[70] US Bureau of Reclamation, FY 2014 WaterSMART Water and Energy Efficiency Grants, WaterSmart. (n.d.). https://www.usbr.gov/watersmart/weeg/docs/FY2014WaterSMARTWaterandEnergyEfficiency Grants.pdf (accessed March 30, 2018).

[71] A. Efraty, CCD series no-22: Recent advances in RO, FO and PRO and their hybrid applications for high recovery desalination of treated sewage effluents, Desalination. 389 (2016) 18–38. doi:10.1016/J.DESAL.2016.01.009.

[72] T. Nading, S. Alt, WRF-08-14, Selecting the Best Energy Recovery Device at RO Plants, in: Webinar, Water Research Foundation, 2013. https://watereuse.org/wp-content/uploads/2015/11/Energy-Recovery-Device-WRF-Webinar-Presentation.pdf (accessed April 6, 2018).

[73] J. Balliew, Why Desalination in El Paso?, in: WRRC Annu. Conf., WRRC, Yuma, AZ,

2011.

[74] J. Balliew, Overview of the El Paso Kay Bailey Hutchison Desalination Plant, in: Texas Water Dev. Board Work Sess., El Paso, TX, 2014.

Appendices

This section includes two documents included with the supporting information for Chapter 1 of this dissertation and as published in the IECR article [1].

- Appendix A: ZDD Model details with supporting piloting data (as submitted to the IECR [1], which describes sections 1-5 in the model shown in Appendix B)
- Appendix B: ZDD MathCad 14.0 Model (version as of April 8, 2018)
- Appendix C: Sample ZDD Model Output and Cost Calculations

Appendix A. ZDD Model Details with Supporting Piloting Data

This appendix[16] provides supplemental details to the manuscript and additional context to the Mathcad model (Appendix B). As described in Chapter 1 of this manuscript, the ZDD model was developed to simulate ZDD system performance using mass balance, desalination design equations, and experimental data. This appendix is organized to match each of the sections in Chapter 1, as well as the Mathcad ZDD model.

1. Input Water Chemistry & Fixed Input Parameters

1.1 Input Design

A total of five cases were developed in order to evaluate the technical performance of ZDD designs with different RO and NF membranes. The input design parameters for the five cases are shown in Tables S.1 and S.2. In the ZDD Model, modeling parameters that are highlighted yellow in the ZDD model indicate a place that requires user input or choice. The model mostly employs US customary units (*e.g.,* gpm, psi); however, Mathcad allows the user to modify units as desired.

[16] This appendix was published in Industrial & Engineering Chemistry Research (I&ECR) with co-authors W. Shane Walker, and Thomas A. Davis. Some slight edits were made to fix typographical errors and to fulfill UTEP formatting requirements:
Ind. Eng. Chem. Res., 2017, 56 (37), pp 10448–10460, DOI: 10.1021/acs.iecr.7b02472

Table S.1. Input Parameters for Dow FILTMEC ROSA Designs

	Cases 1-4				**Case 5**
Membranes	NF270	NF90	XLE	BW30	NF-90 & NF270
Staging by r_{RO}	1-stage: 50-60%, 2-stage: 70-80%				
Pressure Vessels (PVs) [a]	1-stage: 78 PVs 2-stage: 52 x 26 PVs		1-stage: 71 PVs 2-stage: 47x24 PVs	1-stage: 78 PVs [b] 2-stage: 52 x 26 PVs [c]	
Permeate Flow	2083 gal/min				
RO/NF Feed T	25°C				
Average Flux	13.7 $gal \cdot ft^{-2} \cdot day^{-1}$ (gfd)				
Permeate Back P (2-stage only)	40 psi	30 psi	40 psi	30 psi	0 psi

Notes: [a] All designs have seven 8"x40" membranes per pressure vessel

[b] The NF90-NF270 design has four NF90 membranes followed by three NF270 membranes

[c] The NF90-NF270 model for two stage has NF90 membranes in the first stage and NF270 in the second stage

Table S.1. MEGA EDM Stack Design Parameters [1]

Parameter	**Value**
Number of Quads per Stack	100
Membranes in a Quad	(2) AEM-PES and (2) CEM-PES
Thickness of Main Spacers	0.8 mm
Thickness of Electrode Rinse Spacers	1 mm (two at each electrode)
Electrodes	Ti/Pt at anode, 316 Stainless steel at cathode
Spacer Dimensions	1610mm x 410mm x 0.8mm
Membrane Sheet area	0.660 m^2
Sealing & Channel rake off	36.4%
Active Membrane Area	0.420 m^2
Linear Velocity	5-11 cm/s

1.2 Choose Feed Water Composition

This section of the model includes eight different water chemistries (listed in Table 1 of Chapter 1) that can be used in the model. Several of these waters are from the Brackish

Groundwater National Desalination Research Facility (BGNDRF), and others are from locations where ZDD has been tested by UTEP or other researchers.

Additional information for each source:

- $c_{Well1and4\_2013}$: Pilot testing research sponsored by the U.S. Bureau of Reclamation (USBR) Desalination and Water Purification Research (DWPR) program was performed by the authors from 2011 through 2013. A blend of BGNDRF Wells 1 and 4 (about 40% of Well 1 and 60% of Well 4) was tested in order to approximate the chemistry of water from the Snake Tank wells available to the City of Alamogordo. The concentrations reported in Table 1 of the manuscript are the average of 2013 ZDD pilot data at the BGNDRF.
- c_{well1}, c_{well2}, c_{well3}, c_{well4} are Wells 1-4 at the BGNDRF and are based on the analyses listed on the BGNDRF website for 6/27/2016.
- c_{raw_KBH} is typical brackish water chemistry at the Kay Bailey Hutchison desalination plant in El Paso, Texas.
- c_{raw_Alamo} is the average of the three Snake Tank wells, as provided in 2003 (personal communication with Livingston Associates).
- $c_{raw\_LaJunta}$ is the average of the raw water samples taken by others and analyzed by UTEP during pilot operations at the desalination plant in La Junta, Colorado.
- $c_{raw\_Brighton}$ is the average of the raw water samples taken by and analyzed by UTEP during pilot operations at the desalination plant in Brighton, Colorado.
- c_{raw_BH} is the water chemistry for the Beverly Hills, California as reported by Bond, et al. in a California Energy Commission report, CEC-PIR-11-020

Prior to performing any calculations, the chosen feedwater is adjusted for electroneutrality. The ZDD model includes a function that calculates the error in electroneutrality and then adjusts the concentration of each ion by the magnitude of the error. The function $EN(c_i)$ is also defined here because it is used in later calculations in the model.

1.3 Input Parameters: Flow Balances

This section of the ZDD model defines the flow balances summarized in Figure 4 of the manuscript. Most of the equations should be self-explanatory, as they are algebraic. The DI water sizing and EDM concentrate flows may require more explanation. When ions are transported into each of the EDM concentrate streams, a volume of water is also transported. This transported water is called the "water of hydration" and was estimated from ZDD piloting. During startup research tests in April 2013, the waste flows for the Mixed Na and Mixed Cl were measured when no DI dilutions were being added, and average flows were measured. Ratios were calculated for each of the concentrate streams to the total waste flow. The average values for the ratios obtained are shown in the Mathcad model (approximately 52% for Mixed Cl and 48% Mixed Na). DI water consumption is approximated as 1.0% of the product water in the model and is apportioned equally between the DI for NaCl pellet dissolution and Mixed Na dilutions. These values were chosen by entering pilot flows and adjusting the fractions in Q_{DI_NaCl} and Q_{DI_mNa} until the calculated concentrate flows (Q_{mNa} and Q_{mCl}) were similar to what was observed during the pilot activities.

2. ZDD Design Parameters

2.1 RO/NF Design and Membrane Choice

Feed water composition and product water quality requirements also drive membrane choice and RO/NF design. If brackish water contains nitrate, boron, arsenic, or other uncharged and small dissolved constituents, a high rejection RO membrane or a multiple-pass configuration may be required to meet product water goals. Brackish water composition is important in terms of membrane choice and RO/NF design because sparingly soluble salts will dictate the maximum recovery and the presence of fouling constituents will dictate the maximum flux. The goal of the RO/NF design is to maximize the production of permeate (maximize flux) while optimizing the energy consumption (minimize pressure, cross-flow velocity) and mitigating precipitation and fouling (optimal flux and cross-flow velocity).

The RO/NF membrane used must be designed strategically to optimize the performance of the entire ZDD system. Otherwise, improper design and membrane choice can increase cost and reduce the overall efficiency of the process. For example, RO and most NF membranes are very effective at rejecting silica. Silica can limit RO and NF recovery, even with the use of antiscalants. Also, there is a feedback loop between the RO/NF and EDM systems. Electrodialysis metathesis only removes charged species. Since silica (silicic acid) has a $pKa_1 = 9.8$ [2], silica is less than 1% ionized in a near-neutral RO concentrate with pH of 7-8. Hence, silica is essentially not removed by the EDM. This means that silica will concentrate in the RO/NF-EDM loop over time and could precipitate in one or both systems if an RO/NF membrane with high silica rejection is employed. Silica can be removed in a pre-treatment step by co-precipitation with magnesium and filtration or electrocoagulation, but these methods are typically relatively expensive. Another option is to have a constant bleed to maintain a constant silica concentration in the RO/NF-EDM loop, but this reduces the efficiency of ZDD. Some membrane manufacturers have developed low rejection NF membranes (*e.g.*, Dow FILMTEC NF-270) that allow silica to pass through to the permeate. This option allows for the highest ZDD recovery and mitigation of silica precipitation.

Dow FILMTEC NF270 membranes were used for two phases of ZDD piloting in 2011-2013. The Phase 1 pilot tested a ZDD system with 76 L/min (20 gallons per minute, gpm) of permeate in which the primary desalter was a three-stage RO/NF array (4:2:1 ratio) with four NF270-4040 (4 inch nominal diameter, 40 inch length) membranes in each pressure vessel. The Phase 2 pilot tested a ZDD system with 151 L/min (40-gpm) of permeate in which the primary desalter had a two-stage 2:2 array with eight NF270-400 (diameter: 201-mm, or 7.9-in) membranes in total, which mimics a single 8-element pressure vessel in a full scale design. Pilot tests performed by others [3] with UTEP equipment included combinations of Dow FILMTEC NF90 and NF270 membranes to achieve lower product water TDS while still mitigating silica scale in the ZDD process.

2.2 RO/NF Salt Rejection

The salt rejection (*i.e.*, removal) of each ion was calculated using individual linear regressions were developed for each ion for each membrane type. To accomplish this, the average water quality from ZDD piloting ($c_{Well1and4\_2013}$) was entered into the Dow ROSA program to generate models for 50-80% recovery. The designs for recoveries of 50% and 60% for the 37 m^2 (400 ft^2) membrane elements (NF270, NF90, and BW30) included a single stage of 78 pressure vessels, and the 70% and 80% models were two-stage, 52x26 arrays. All designs assume seven elements per pressure vessel. The XLE membranes have 41-m^2 (440-ft^2) available surface area, so the two-stage designs were modified slightly to match the flux in the other three membrane designs (*i.e.*, the 50% and 60% design had 71 pressure vessels, and 70% and 80% designs had 47x24 arrays). The temperature was fixed at 25°C and the water type was chosen to be "Well Water" for all models. The resulting permeate concentrations for Cases 1-5 are summarized in Table S.3.

Table S.3. ROSA Predicted RO/NF Permeate Water Concentrations (all in mg/L except pH)

	Recovery (%)	**Na**	**Mg**	**Ca**	**HCO_3**	**Cl**	**SO_4**	**SiO_2**	**TDS**	**pH**
Feed	N/A	379	121	288	248	342	1298	20.0	2698	7.6
NF270	50	186	18.8	59	148	332	37	15.4	797	7.5
	60	194	19.9	61	159	340	43	15.8	834	7.5
	70	199	20.2	62	167	342	48	16.2	855	7.6
	80	209	21.4	65	183	349	59	16.7	904	7.6
NF90-NF270	55	126	12.0	37	97	215	31	9.6	527	7.3
	70	117	12.1	36	96	196	36	8.8	503	7.3
	75	130	13.5	40	108	218	41	9.8	560	7.4
	80	144	15.1	45	121	240	46	10.8	623	7.4
NF90	50	34.8	1.9	4.4	26.2	35.8	21.7	1.2	126	6.6
	60	39.6	2.2	5.1	29.9	40.6	25.2	1.3	144	6.6
	70	42.7	2.4	5.5	32.0	44.0	27.0	1.4	155	6.6
	80	52.8	3.0	7.0	39.7	54.1	34.4	1.8	193	6.7
XLE	50	16.9	2.0	4.7	12.4	16.0	23.1	0.5	75.6	6.3
	60	19.2	2.3	5.4	14.1	18.2	26.5	0.6	86.3	6.3
	70	21.6	2.6	6.0	15.7	20.4	29.4	0.7	96.3	6.3
	80	26.7	3.2	7.5	19.5	25.2	36.9	0.8	120	6.4
BW30	50	5.0	0.6	1.4	3.8	4.8	6.8	0.2	22.5	5.8
	60	5.8	0.7	1.6	4.4	5.4	7.9	0.2	26.0	5.8
	70	6.3	0.7	1.7	4.8	6.0	8.5	0.2	28.3	5.8
	80	7.8	0.9	2.2	5.9	7.3	10.6	0.3	34.9	5.9

There are many choices in RO and NF membranes from several manufacturers. In general, RO membranes will have higher rejection of dissolved constituents as compared to NF membranes. However, there is some variation among the individual types. ROSA automatically balances for electroneutrality and the user can choose the ions to add for balancing. Since the BGNDRF water contains mostly calcium and sulfate, those ions were chosen for electroneutrality balancing in the ROSA models used. All of the membranes had lower salt rejection as the recovery was increased, but the effect was most pronounced with the nanofiltration membranes, especially the NF270.

The rejection of each species was calculated at each recovery and then graphs were produced for each membrane type at 50% and 80% recovery (see Figure S.1). Finally, linear

regression was used to describe the salt rejection as a function of RO/NF recovery. Table S.4 summarizes the regression equations and R^2 values for the NF270, NF90, XLE, and BW30 membrane models used in Cases 1-4.

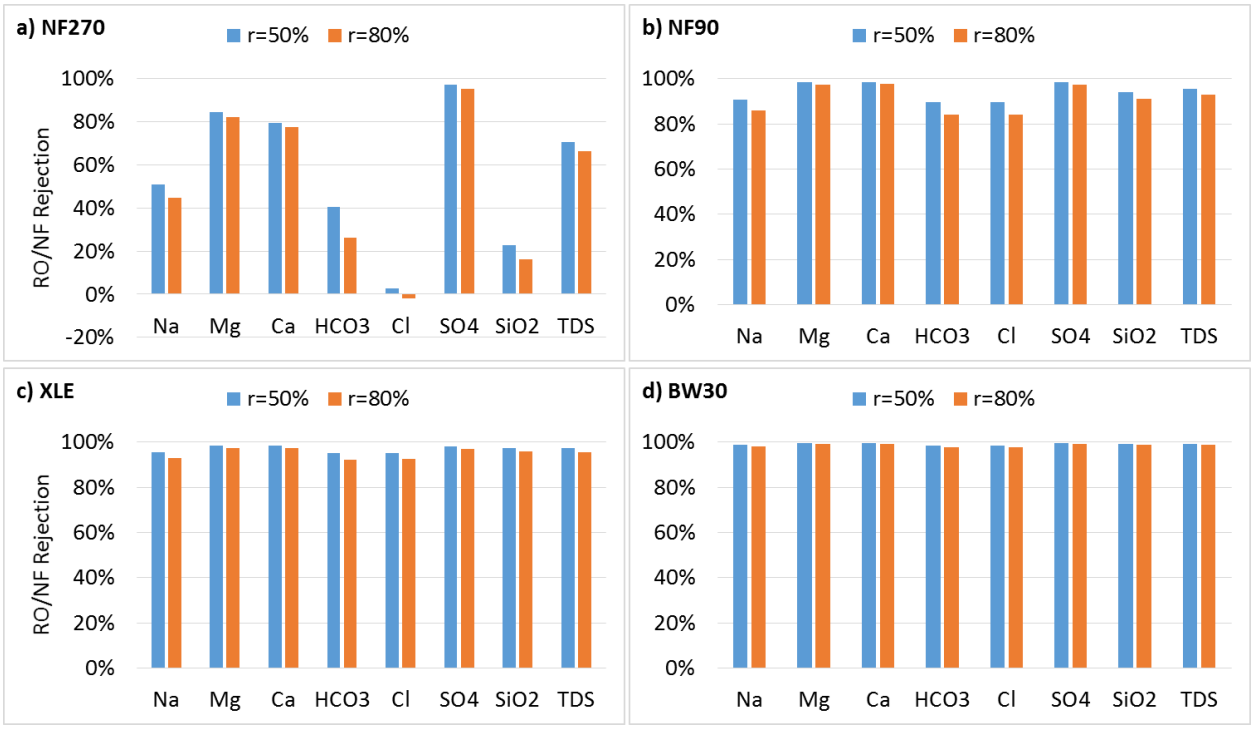

Figure S.1. Comparison of RO and NF Rejection with the BGNDRF wells 1&4 blend (Table 1.1 in Chapter 1) and an average flux of 22.3 lmh (13.7 gfd).

Table S.4. Salt Rejection (Ri) vs RO/NF Recovery (rRO) for Cases 1 – 4 (based on ROSA)

R_i	NF270 Rejection	NF90Rejection	XLE Rejection	BW30 Rejection
R_{Ca}	$-0.0655*r_{RO} + 0.8284$ ($R^2 = 0.96$)	$-0.0282*r_{RO} + 0.9992$ ($R^2 = 0.92$)	$-0.0316*r_{RO} + 1.0001$ ($R^2 = 0.95$)	$-0.0085*r_{RO} + 0.9996$ ($R^2 = 0.95$)
R_{Mg}	$-0.0673*r_{RO} + 0.8781$ ($R^2 = 0.96$)	$-0.0288*r_{RO} + 0.9991$ ($R^2 = 0.92$)	$-0.032*r_{RO} + 1$ ($R^2 = 0.95$)	$-0.0088*r_{RO} + 0.9997$ ($R^2 = 0.94$)
R_{Na}	$-0.1939*r_{RO} + 0.606$ ($R^2 = 0.98$)	$-0.1504*r_{RO} + 0.9857$ ($R^2 = 0.94$)	$-0.0833*r_{RO} + 0.9985$ ($R^2 = 0.95$)	$-0.0233*r_{RO} + 0.9987$ ($R^2 = 0.95$)
R_{Cl}	$-0.1507*r_{RO} + 0.1011$ ($R^2 = 0.95$)	$-0.1703*r_{RO} + 0.9832$ ($R^2 = 0.94$)	$-0.0872*r_{RO} + 0.9983$ ($R^2 = 0.96$)	$-0.0243*r_{RO} + 0.9986$ ($R^2 = 0.96$)
R_{HCO3}	$-0.4616*r_{RO} + 0.6381$ ($R^2 = 0.98$)	$-0.1719*r_{RO} + 0.983$ ($R^2 = 0.94$)	$-0.0923*r_{RO} + 0.9978$ ($R^2 = 0.95$)	$-0.026*r_{RO} + 0.9979$ ($R^2 = 0.95$)
R_{SO4}	$-0.0536*r_{RO} + 0.9989$ ($R^2 = 0.96$)	$-0.0307*r_{RO} + 0.9991$ ($R^2 = 0.92$)	$-0.0343*r_{RO} + 1$ ($R^2 = 0.95$)	$-0.0093*r_{RO} + 0.9995$ ($R^2 = 0.95$)
R_{SiO2}	$-0.2175*r_{RO} + 0.3393$ ($R^2 = 0.99$)	$-0.1015*r_{RO} + 0.9944$ ($R^2 = 0.94$)	$-0.0485*r_{RO} + 0.9982$ ($R^2 = 0.95$)	$-0.0145*r_{RO} + 0.9996$ ($R^2 = 0.94$)

The hybrid model used in Case 5 employs two types of NF membranes (NF90 and NF270). Only one single-stage model was developed for 55% recovery and three were made for a range of recoveries (70-80%). One ROSA model was created for a 55% recovery option with a single stage with 78 pressure vessels, each with four NF90 membranes followed by three NF270 membranes. A second ROSA model was developed for a two-stage design and 70-80% recovery; this had the same staging as the previous designs (52x26, 7 membranes per pressure vessel), but had different membranes in each stage (1st stage: 52 vessels with NF90, 2nd stage: 26 vessels with NF270). Table S.5 summarizes the regression equations and R^2 values for the NF90-NF270 membranes models used in Case 5.

Table S.5. NF90-NF270 Salt Rejection for 55% Recovery Design (from ROSA)[1]

	r_{RO}=55%	r_{RO}=70-80%
Constituent	Rejection (%)	Rejection (%)
Ca	87.1	-0.3104* r_{RO}+1.0933 (R^2 = 1.0)
Mg	90.1	-0.2521* r_{RO} + 1.0771 (R^2 = 1.0)
Na	66.9	-0.7055* r_{RO} + 1.1851 (R^2 = 1.0)
Cl	37.2	-1.2819* r_{RO} + 1.3238 (R^2 = 1.0)
HCO_3	61.0	-1.0125* r_{RO} + 1.322 (R^2 = 1.0)
SO_4	97.6	-0.0784* r_{RO} + 1.0267 (R^2 = 1.0)
SiO_2	52.0	-1.005* r_{RO} + 1.2649 (R^2 = 1.0)

[1]Note: R^2 values ranged from 0.9987-1.0, all are rounded to two significant figures

2.3 EDM Membrane Choice and Design

Electrodialysis equipment (called "stacks") are built with alternating cation- and anion-exchange membranes. Commercial stacks can include hundreds of cell pairs. An aqueous solution, such as brackish water, is fed into alternating feed compartments. As an electrical potential (voltage) is applied, anions move towards the positively charged anode and cations move towards the negatively charged cathode [4]. This leads to changes in the salt content of alternating streams; one is a diluted stream (called diluate) and the other is a concentrated stream (called concentrate). Oxidation and reduction reactions occur and gasses are generated at each of the electrodes. An electrode rinse stream flows across each electrode to provide a path for current to flow from the electrodes into the rest of the stack, as well as to cool both electrodes and sweep gases out of the stack. Gases generated in the electrode rinse compartments are vented to the atmosphere.

EDM was first described in US Patent 2,721,171, which was issued in 1955 and assigned to DuPont. Several other researchers have used EDM for a variety of uses [5-8]. An electrodialysis metathesis (EDM) stack is built similarly to an ED stack, but instead of a single diluting and single concentrating stream, EDM has two diluting streams and two concentrating streams. The combination of the four streams and associated membranes is called a "quad"; commercial EDM stacks may include 100 or more quads. Figure S.2 shows a single quad and how that quad is incorporated in the rest of the EDM stack. Brackish water or desalination concentrate is fed to the

EDM feed compartments. Cations from the EDM feed combine with chloride from the NaCl to produce a mixed chloride salt concentrate stream (called Mixed Cl). Anions from the EDM feed combine with sodium from the NaCl to produce a mixed sodium salt concentrate stream (called Mixed Na). This metathesis, or changing of partners, produces highly soluble sodium and chloride salts such as calcium chloride and sodium sulfate from sparingly soluble salts like calcium sulfate. NaCl is added to the EDM at a rate equivalent to the rate of ions removed from the EDM feed.

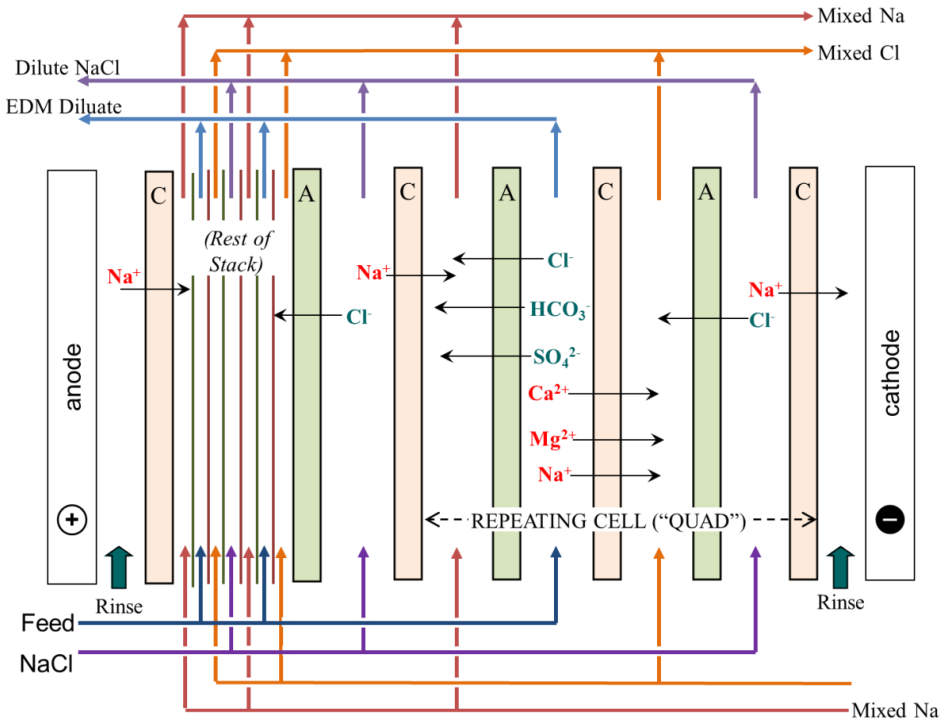

Figure S.2. Flow of Ions in Electrodialysis Metathesis (C=cation exchange membrane, A=anion exchange membrane)

Similar to RO/NF design, care must be taken to optimize the design of electrodialysis systems, EDM included. However, unlike RO/NF, the electrodialysis (ED) industry has not standardized the geometry of equipment used for desalination. In RO/NF, the size of the pressure vessels is such that any membrane can be used with minimal changes required. However, in ED systems, one must purchase the stack and membranes together. In general, membranes are not interchangeable and manufacturers require use of their membranes in their equipment. The cost of

ED is largely driven by the cost of the equipment and membranes, but also by the operating cost related to the electrical resistance of the membranes. There are many ED membrane manufacturers located around the world (see appendix in [4]) and there is a wide variety of performance characteristics and cost. Piloting activities at the BGNDRF were carried out with stacks and RALEX membranes made by MEGA. Laboratory and small pilot experiments have been performed by UTEP using both RALEX and a variety of Neosepta membranes, supplied by ASTOM, including some with special characteristics such as oxidation resistance and the ability to selectively transport monovalent ions. RALEX membranes are heterogeneous (*i.e.*, ion exchange material bound to a structural mesh/fabric) and generally have higher electrical resistance as compared to the (homogeneous) Neosepta membranes. However, RALEX membranes are also more durable since they are thicker and, at the time of piloting, were significantly less expensive than the Neosepta membranes.

2.4 EDM Ion Removal

The EDM feed and diluate concentrations are calculated using data obtained during ZDD pilot research. The extraction (removal) of ions within the EDM were calculated as a ratio of the EDM extraction (removal) of calcium, E_{Ca}. The relative removal of each ion (RRR_i) is based on a user-input value for the EDM removal of calcium (E_{Ca}) from the EDM feed:

$$RRR_i = \frac{[(C_{E,i} - C_{d,i})/C_{E,i}]}{E_{Ca}} \quad (3)$$

The extraction of the rest of the ions are calculated using the product of the relative removal ratio (RRR_i) and calcium removal. The RRR values were approximated by dividing the removal of the ion ($R_{EDM,i}$) by the calcium removal ($R_{EDM,\,Ca}$) observed in BGNDRF 2013 pilot results. The average values for each of the ZDD streams during pilot activities is shown in Table S.6. As mentioned above, silica is poorly ionized at neutral pH, so the EDM was conservatively assumed to remove no silica. The resulting EDM diluate concentration is adjusted to be electroneutral. Table S.7 summarizes the average and range of ion removal (calculated from ZDD pilot results shown in Table S.7), the relative removal of each ion, and model removal equations for each ion.

Table S.6. Water Quality for ZDD Streams during 2013 BGNDRF Piloting (all are in mg/L except pH and conductivity)

	Raw	NF feed	NF permeate	NF reject	EDM feed	EDM diluate	Mixed Cl	Mixed Na
	Average (Standard Deviation)							
pH	7.8 (0.1)	6.8 (0.2)	6.8 (0.2)	6.8 (0.2)	6.6 (0.2)	6.4 (0.2)	4.7 (1.7)	7.8 (0.2)
Conductivity (μS/cm)	3546 (135)	3558 (153)	1259 (63)	8259 (438)	4950 (330)	3765 (377)	170171 (5196)	115186 (4526)
TDS	2641 (149)	2740 (192)	640 (45)	8471 (744)	4287 (368)	3006 (363)	185338 (14646)	164980 (6730)
Ca	264 (20)	246 (19)	26 (2.6)	835 (90)	355 (39)	206 (38)	20976 (2047)	661 (250)
Mg	112 (13)	108 (11)	8.9 (1.4)	371 (47)	172 (19)	108 (19)	9218 (829)	243 (137)
Na	369 (19)	396 (23)	191 (11)	947 (63)	617 (56)	507 (67)	18492 (1948)	55713 (6483)
Cl	310 (17)	241 (30)	289 (16)	151 (11)	108 (5)	94 (9)	93266 (9234)	11194 (1050)
HCO3	238 (27)	129 (45)	100 (17)	150 (38)	90 (29)	76 (36)	58 (54)	2735 (917)
SO4	1208 (90)	1661 (929)	38 (10)	4973 (476)	2444 (134)	1770 (250)	808 (295)	96549 (11417)
SiO2	20.9 (0.7)	23.0 (1.5)	21. (0.6)	26.5 (1.4)	27.5 (1.5)	28.1 (2)	5.5 (1.3)	11.1 (5.8)

Table S.7. 2013 BGNDRF Pilot Results and Calculated Relative Removal Ratios (RRRs)

	Average removal of ion (range of values)	Relative removal, (Ca as basis)	EDM Removal used in model (RRR_i)
$R_{EDM,Ca}$	43% (32-50%)	100%	E_{Ca}
$R_{EDM,Mg}$	38% (27-47%)	90%	$0.9*E_{Ca}$
$R_{EDM,Na}$	17% (11-27%)	40%	$0.4*E_{Ca}$
$R_{EDM,Cl}$	13% (11-19%)	30%	$0.3*E_{Ca}$
$R_{EDM,SO4}$	28% (24-39%)	70%	$0.7*E_{Ca}$
$R_{EDM,HCO3}$	16% (13-60%)	40%	$0.4*E_{Ca}$

2.5 Concentration Calculation Iterations

The initial calculation assumes that the RO/NF feed concentration is equal to the brackish water feed quality. The concentration of each constituent in the permeate (c_{ROp_i}) is calculated

based on the salt passage (SP_i) of the constituent using the constituent's salt rejection (Tables S.4 and S.5). The concentration of each constituent in the RO/NF concentrate (c_{ROc}) is calculated using the concentration factor, *CF*. The resulting concentration is then balanced for electroneutrality similar to the process described for the permeate.

Similarly, the initial calculation assumes the EDM feed is solely comprised of RO concentrate. The diluate quality is then calculated based on the salt passage from the EDM feed to concentrate streams (SP_{EDM}) using the relative removal for each ion (Table S.7). Next, the EDM feed is calculated as a blend of the EDM diluate and RO concentrate using the ratio of each stream's flow to the total EDM feed flow.

The while loop shown in the model iterates until the maximum change in the calculated ion concentrations is less than 0.1% from the previous iteration:

1. The RO/NF feed water quality is calculated using a volumetric blend of the brackish water and EDM diluate.
2. The RO/NF permeate water quality is calculated using the salt passage (based on salt rejections shown in Tables S.4 and S.5), then balanced for electroneutrality.
3. The RO/NF concentrate water quality is calculated using the concentration factor, then balanced for electroneutrality.
4. The EDM feed is calculated based on a volumetric, the previous iteration's EDM diluate water quality, and the current iteration's RO/NF concentrate, then is balanced for electroneutrality.
5. The EDM diluate water quality is calculated based on the relative removal ratios (Table S.6), then is balanced for electroneutrality.

3. Check RO/NF Concentrate Stability

3.1 Data output & graphing: Use to check solubility, other, externally

In order to evaluate ZDD as a function of RO/NF recovery, EDM recycle ratio, EDM ion removal, and Silica bleed from the RO/NF concentrate, four tables are produced from the extracted

information produced during the iterations. This allows the model to run several iterations keeping all parameters constant except for the parameter of interest. These four data tables output for analysis are summarized as:

- DATA_r_RO: The RO/NF recovery (r_{RO}) is varied from 50 to 98%
- DATA_RR: The EDM recycle ratio (RR_{EDM}) is varied from 0.20 to 2 for RO/NF recovery less than 70% and 2 to 4 for RO/NF recovery of 70-80% (requires manual adjustment of RREDM assignment).
- DATA_cut: The EDM calcium removal fraction (E_{Ca}) is varied from 0.2 to 0.6.
- DATA_Silica_bleed: the silica removal fraction (p_{silica}) is varied from 0 to 0.30.

3.2 Final Concentrations

The final result of the iterations is shown and variables are assigned to the results. Electroneutrality is checked and several summary calculations are also shown.

4. EDM Design, Concentrate Quality, and Power

4.1 Calculate Mixed Na and Mixed Cl Concentrations

The concentration of the ions transferred into the Mixed Na and Mixed Cl streams is calculated in a stepwise manner:

1. The equivalent concentrations in the EDM feed and diluate are calculated based on the cation concentrations ($N_{EDMfCat}$, $N_{EDMdCat}$) and anion concentrations (N_{EDMfAn}, N_{EDMdAn}).
2. The total volume of each ZDD stream produced each day is calculated.
3. The number of Ca, Mg, and Na equivalents transferred are calculated by subtracting the equivalents in the diluate from the EDM feed. The chloride equivalents are assumed to be equal to the sum of the cation equivalents removed from the EDM feed.
4. The number of Cl, HCO_3, and SO_4 equivalents is calculated by subtracting the equivalents in the diluate from the EDM feed. The sodium equivalents are assumed to be equal to the sum of the anion equivalents removed from the EDM feed.

5. The concentrations (in mg/L) for the Mixed Cl (c_{mCl}) and Mixed Na (c_{mNa}) streams are then calculated by dividing the results in Step 4 by the volume of Mixed Cl (V_{mCl}) and Mixed Na (V_{mNa}) and multiplying by each ion's equivalent weight.

4.2 NaCl Consumption and Evaporation Pond Sizing

The theoretical amount of Na required each day is the first row in the Eq_{mNa} array and is

$$M_{Na} := \left(\sum N_{EDMfAn} \cdot V_{EDMf} - \sum N_{EDMdAn} \cdot V_{EDMd} \right) \cdot EW_2$$

calculated as:

The theoretical amount of Cl required each day is the fourth row in the Eq_{mCl} array and is calculated as:

$$M_{Cl} := \left(\sum N_{EDMfCat} \cdot V_{EDMf} - \sum N_{EDMdCat} \cdot V_{EDMd} \right) \cdot EW_3$$

The mass of NaCl is therefore the sum of M_{Na} and M_{Cl}.

The minimum area required to evaporate the ZDD waste is calculated from the daily volume ($V_{evap\_no\_rec}$) and evaporation rate (r_{evap}).

As described earlier, two concentrate streams are produced by the EDM (Mixed Na and Mixed Cl). These streams can be considered super-concentrates, as the concentration is very high (generally more than 100,000 mg/L TDS). This concentration would likely be too high for disposal by deep well injection. However, useful byproducts can be recovered and sold to reduce the amount of (and cost associated with) NaCl purchased. Pilot tests performed by UTEP and others indicate that NaCl purchases account for about 40% of the operating cost (*e.g.* chemicals, power, maintenance by ZDD (or, about 90% of the cost of non-power operating expenses see Figure 8 in [9]).

If the Mixed Cl (calcium-rich) and Mixed Na (sulfate-rich) concentrate streams are combined in stoichiometric proportions gypsum will precipitate. Gypsum may be used by farmers to improve soil quality [10], as well as to produce drywall and other products (see Appendix 3 in [11]). If magnesium is present in sufficient concentration in the brackish water feed, it may be

advantageous to add lime to the Mixed Cl stream to precipitate magnesium hydroxide prior to mixing with the Mixed Na stream [12]. Replacing magnesium ions with calcium ions can allow for a better stoichiometric balance of calcium and sulfate, which will allow for maximum recovery of gypsum and minimize the residual sulfate in the remaining fluid, which is mostly NaCl. This NaCl can be purified using ED with monovalent-selective membranes or using evaporation ponds [12].

4.3 EDM Sizing & Power Calculations

The model uses a manual iteration method to identify the EDM design and operating parameters. The first step involves calculating the EDM membrane area and number of stacks required to achieve the calculated ion removal (Eq_{rem}) given a range of current density values (i_{edm} array). The EDM design is assumed to be based on the MEGA EDM stacks used in the ZDD piloting activities. The calculated number of stacks is rounded to the next integer (N_{stack_r}) and the user can choose which design is preferred. More stacks offer more flexibility for changes in water quality, but also cause higher cost; fewer stacks offer lower capital cost, but minimal flexibility for changes in water quality.

The next step involves identifying the appropriate velocity in the EDM stack. The EDM stacks operated with fewer problems when the EDM feed-diluate velocity was above 5.2 cm/s. The MEGA manual indicates that the maximum velocity is 11 cm/s. Programming conditional-if statements are used to determine if the number of stacks and velocity are acceptable for the design (N_{stack_des} and v_{stack}). The model allows for a manual adjustment to the number of stacks. New values for the design velocity (v_{stack_adj}) and membrane area (A_{mem_des}) are calculated based on the entered value for N_{stack_adj}.

Strathmann described the concept of limiting current density using a current density vs. voltage drop graph [4]. This graph includes three regions (ohmic, plateau, and overlimiting). A linear regression can be used to describe each of the regions. The limiting current density is located at the point where the slope changes dramatically between the ohmic and plateau regions and can

be determined graphically [4,13]. Piloting results from BGNDRF were used to identify limiting current density as a function of velocity to use in the ZDD model. As the current density increases, the rate of removal of ions through the exchange membranes increases, and the concentration gradients increase at the membrane surfaces. In general, cations diffuse towards the membrane more slowly than anions, so the concentration gradient is steeper at the surface of the cation-exchange membrane than at the anion-exchange membrane [14], which leads to operational limitations of limiting current density (LCD) in the diluting cells and mineral scaling in the concentrate cells. When there is an insufficient concentration of ions available in the diluate solution at the membrane surface, the difference is made up by dissociation of water into H^+ and OH^- ions, which are transported through the cation- and anion-exchange membranes, respectively. This effect causes the pH to increase at the anion exchange membrane and decrease at the cation-exchange membrane[4].

In Figure S.3, piloting results from the limiting current density experiments for three velocities are shown. The change in color depicts where the slope changes, indicating the limiting current density. The stack should be operated in the range shown in blue, the ohmic region, as described in the manuscript. The limiting current density for each velocity was then plotted to derive an equation that can be used to calculate the limiting current density as a function of velocity (shown in part (d) of Figure S.3).

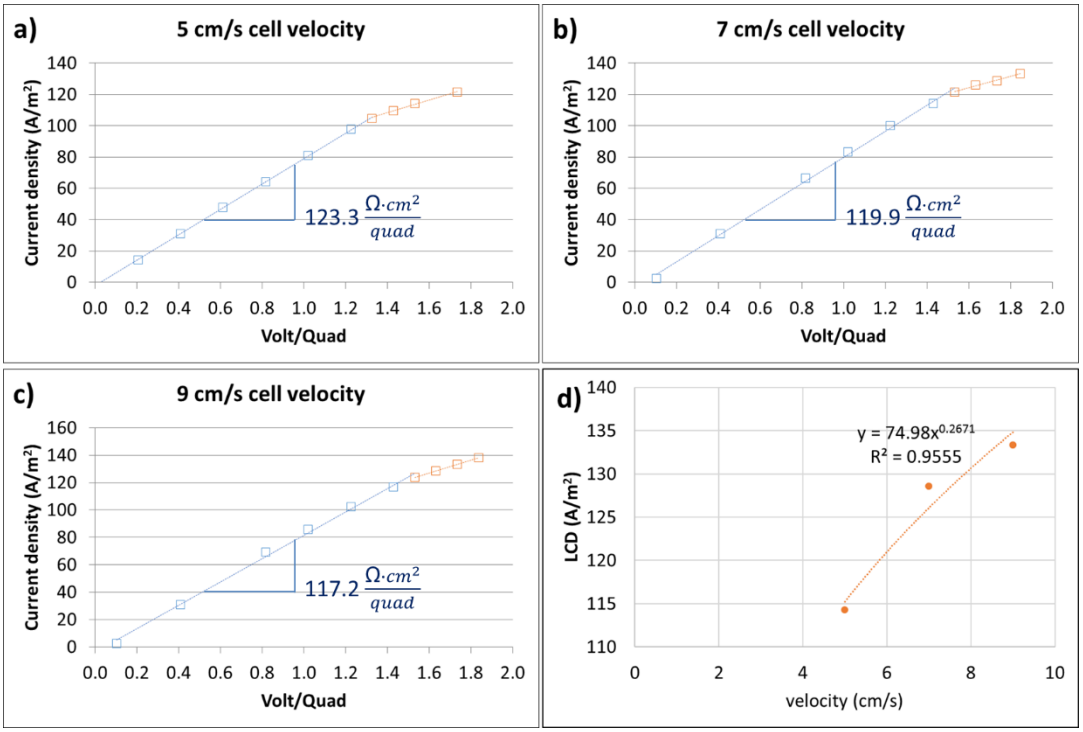

Figure S.4. Limiting Current Density tests and Equation from 2013 BGNDRF Piloting

The voltage required to achieve the calculated current density is a sum of the electrode voltage (V_{elec}) and the voltage associated with the solutions and membranes. The minimum voltage drop for an EDM quad (V_{quad}) is estimated using physical parameters (e.g. spacer thickness) and field measurements (e.g. stream conductivities). The electric potential loss across each quad is split into two components. The first voltage loss is associated with liquid junction potentials between cells (ΔV_{dp}), and the second voltage loss is associated with ohmic resistance through the membranes and solutions (ΔV_{IR}). Deviations from the predicted voltage drop using this approximation method can be associated with difference in stream temperatures, and scaling or fouling of the membranes.

The electrode rinse conductivity and NaCl stream conductivity are fixed at 30 mS/cm and 50 mS/cm, respectively. The remaining stream conductivities (EDM feed, Mixed Cl, Mixed Na)

are estimated using a relationship between concentration in TDS and conductivity derived from water quality analyses (see Figure S.4).

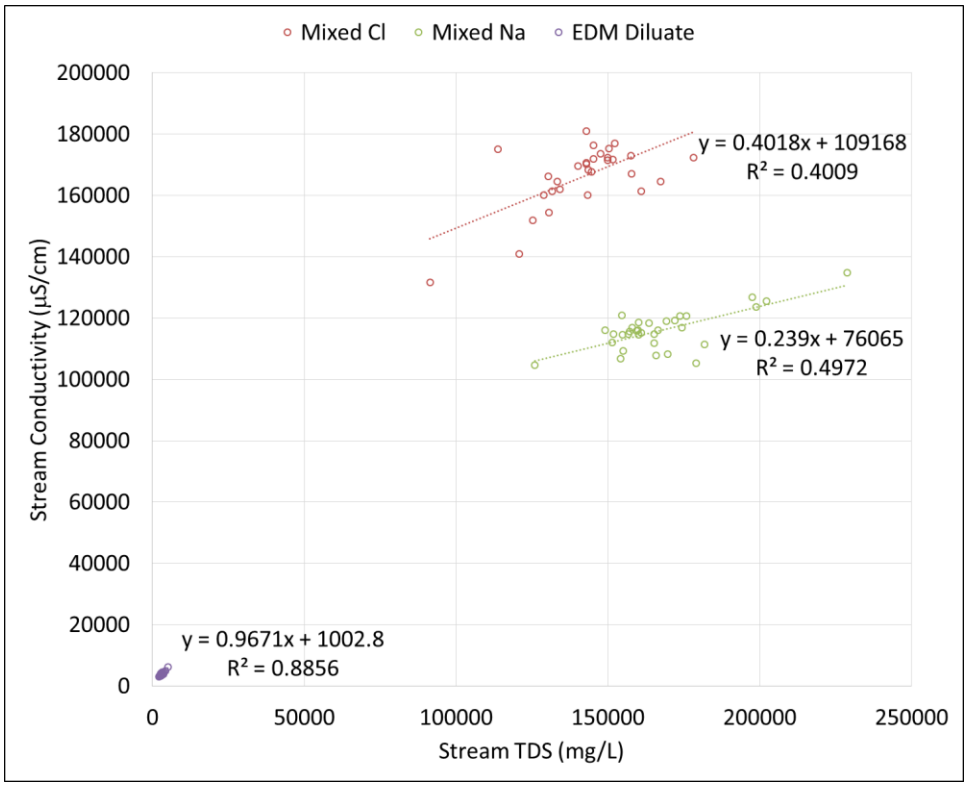

Figure S.4. Estimation of EDM Stream Conductivity from BGNDRF Pilot (2013)

The terms used in the Mathcad model are summarized as follows. T is the EDM feed temperature in Kelvin, and the conductivities (κ) are converted to S/cm (see Section 4.3 in Appendix B). β is the shadow factor, which takes into account how the spacer material reduces the active area of the membrane available for transport. A value of 0.65 is used in this model for the shadow factor. Additional terms include the spacer thickness (Δ = 0.08 cm) and membrane resistance (ρ_{CEM}=10 $\Omega \cdot cm^2$, ρ_{AEM}=7.5 $\Omega \cdot cm^2$) for the cation-exchange membrane (CEM) and anion exchange membrane (AEM). Each EDM quad contains two CEMs and two AEMs.

An EDM stack has five pumped streams (EDM feed, NaCl, Mixed Na, Mixed Cl, and Electrode Rinse). The EDM is generally designed for a desired EDM feed flow and is operated in a way to minimize internal leaks by adjusting the other stream flows to ensure the pressures in

each stream are equal. For the purpose of the ZDD model, the flow of the NaCl, Mixed Na, and Mixed Cl are assumed to be equal to the calculated EDM feed (related to recycle ratio, RR_{EDM}) and the Electrode Rinse flow is assumed to be 20% of the EDM feed based on BGNDRF piloting. A relationship between the EDM feed velocity and pressure (P_{EDM}) was derived from experimental data from BGNDRF piloting (see Figure S.5). The pumping energy required for the EDM is then calculated using the calculated feed pressure, EDM feed flow, and an assumed pumping efficiency.

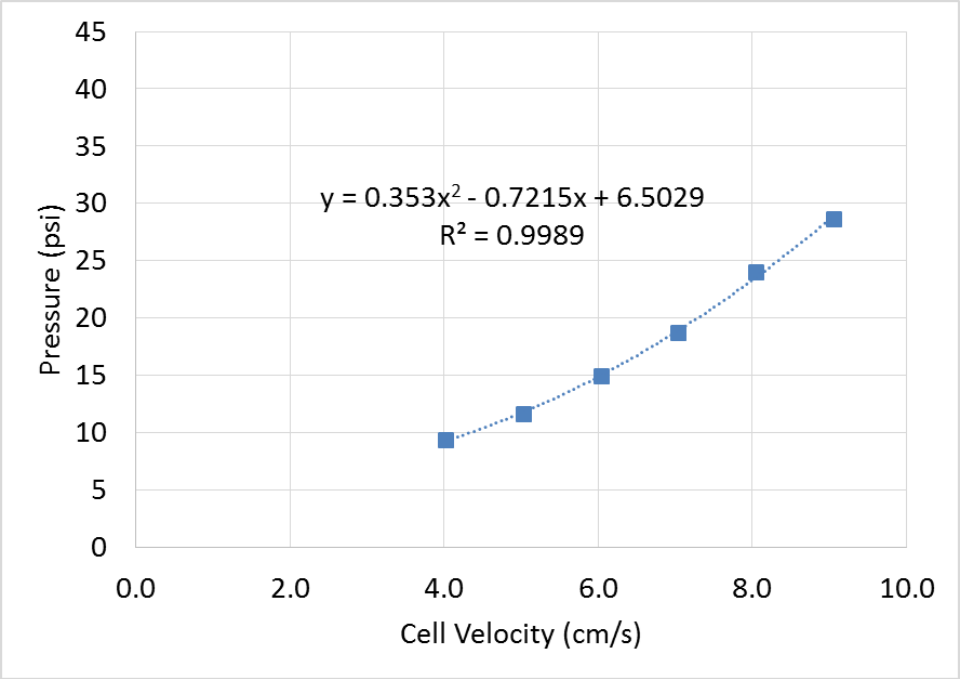

Figure S.5. EDM Pressure and Superficial Cell Velocity

4.4 RO/NF System Power Calculations

ROSA model output includes the estimated feed pressure required for a specific design. It accounts for membrane characteristics, osmotic pressure, permeate back pressure, and other factors, but it is not evident how each of the factors is considered. Permeate back pressure is required to balance permeate flux (and eliminate error messages in ROSA) in the two-stage models. In order to estimate the feed pressure required in the ZDD model, empirical equations were developed to approximate the RO/NF feed pressure. The process involves several steps:

1. Run models with and without any permeate back pressure and record estimated feed pressure values from ROSA.
2. Calculate the osmotic pressure for the concentrate based on the ROSA-predicted concentrations: $\Pi_c = R_{ideal} \cdot T_{ROf} \cdot C_{ROc}$
3. Graph the difference between the RO/NF pressure without back pressure (*Difference*) against the concentrate osmotic pressure (Π_{conc}).
   $Difference = \frac{P_{ROf,without\ BP} - \Pi_{conc}}{\Pi_{conc}}$
4. Develop equations to describe the difference as a function of the concentrate stream osmotic pressure.
   $\%\ Difference = \frac{\Delta Difference}{\Delta \Pi_{conc}} \cdot \Pi_{conc} + Constant$
5. Develop equations that include the relationship from Step 3 and add in a portion of the permeate back pressure, P_{BP}, (a calibration factor, f_{BP}, was determined manually):
   $P_{ROf} = f_{BP} \cdot P_{BP}(1 + Differenc)) \cdot \Pi_{conc}$

This multi-step process is shown in detail here for the NF270 membranes and the other membrane's results are summarized in Table S.8. The highlighted columns are graphed and shown in Figure 2.6. The energy required for desalination is calculated using the calculated RO/NF feed pressure (P_{ROf}), RO/NF feed flow (Q_{ROf}), and assumed pumping efficiency (ξ_{pump}).

Table S.8. NF270 Pressure Information (ROSA and ZDD model)

$r_{RO/NF}$	Permeate back P (psi)	Feed P w/ back P (psi)	Feed P (w/o back P) (psi)	Calculated Π_c (psi)	Diff between Feed P values (%)	Est. RO/NF Feed P (psi)
0.5	0	70	67	32	1.1	64
0.6	0	67	64	38	0.7	70
0.7	40	110	82	47	0.7	105
0.8	40	106	79	65	0.2	108

The ROSA output for each simulation, along with the calculated concentrate stream osmotic pressure (Π_c), % difference between the RO/NF feed pressures with and without permeate back pressure, and estimated RO/NF feed pressure are shown in Table S.9.

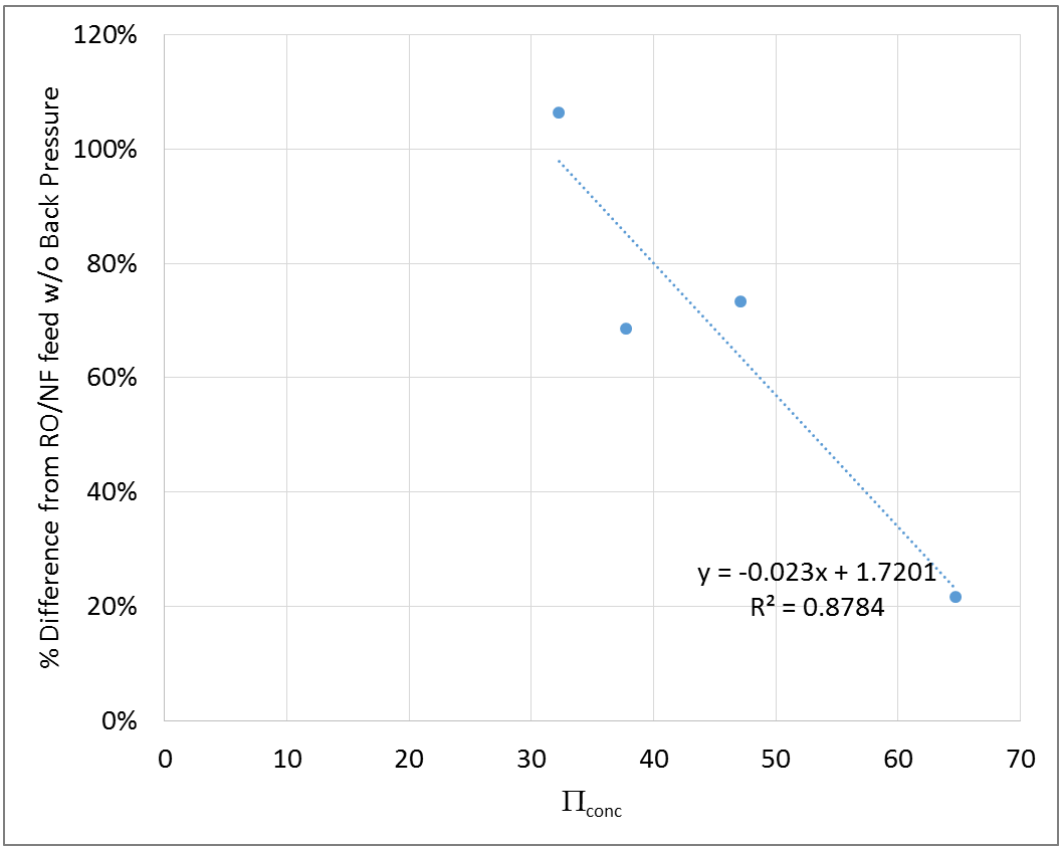

Figure S.6. Relationship between Feed Pressure Difference and Concentrate Stream Osmotic Pressure

Table S.9. Summary of Pressure Equations used in ZDD Model

Membrane	Back P (psi) – *Two stage models only*	% Difference Equation (R^2)	RO/NF Feed P Equation
NF270	40	-0.023*Π_c + 1.7201 (0.8784)	1-stage: (1 + %Diff)*Π_c 2-stage: (1 + %Diff)*Π_c + 0.7*BackP
NF90	30	-0.0157*Π_c + 1.4816 (0.9523)	1-stage: (1 + %Diff)*Π_c 2-stage: (1 + %Diff)*Π_c + 0.4*BackP
NF270-NF90	0	-0.0181*Π_c + 1.5003 (0.9903)	All models: (1 + %Diff)*Π_c
XLE	40	-0.0201*Π_c + 2.2132 (0.9305)	1-stage: (1 + %Diff)*Π_c 2-stage: (1 + %Diff)*Π_c + 0.6*BackP
BW30	30	-0.0294*Π_c + 3.849 (0.9437)	1-stage: (1 + %Diff)*Π_c 2-stage: (1 + %Diff)*Π_c + 0.5*BackP

ZDD Specific Energy Consumption

The power for the RO and EDM (summarized in sections 4.4 and 4.5 of this Appendix and the model in Appendix B) is divided by the ZDD product flow (Qprod) to calculate the subsystem specific energy consumption (SEC). As shown in the manuscript (Section 2.6), the SEC for the ZDD system is simply the sum of the sub-systems' SEC values.

Additional References

[1] MEGA. Technical Documentation: Electrodialyser ED-II/4x; MEGA a.s.: Straz pod Ralskem, Czech Republic, 2010.

[2] Belton, D. J.; Deschaume, O.; Perry, C. C. An Overview of the Fundamentals of the Chemistry of Silica with Relevance to Biosilicification and Technological Advances. FEBS J. 2012, 279 (10), 1710.

[3] Brandhuber, P. J.; Vieira, A.; Kinser, K.; Gelmini, J. Pilot Testing of Membrane Zero Liquid Discharge for Drinking Water Systems; IWA Publishing: London, 2014.

[4] Strathmann, H. Ion-Exchange Membrane Separation Processes; Elsevier B.V., 2004.

[5] Winger, A. Membrane Processes-Ion Exchange. Chem. Eng. Prog. 1957, 53 (12).

[6] Ochoa G., J. R.; Santa-Olalla G., J.; de Diego Z., A.; Martin R., J. L. Isolation and Purification of Iminodiacetic Acid from Its Sodium Salt by Electrodialysis. J. Appl. Electrochem. 1993, 23 (1), 56.

[7] Alhéritière, C.; Ernst, W. R.; Davis, T. A. Metathesis of Magnesium and Sodium Salt Systems by Electrodialysis. Desalination 1998, 115 (2), 189.

[8] Genders, J. D.; Hartsough, D. Electrodialysis of Multivalent Metal Salts. U.S. Patent 6,712,946, 2004.

[9] Cappelle, M.; Alspach, B.; Gilron, J.; Russell, C.; Davis, T. A.; Asaf, N.; Trejo, G. High Recovery Desalination with Enhanced Evaporation: Achieving Zero Liquid Discharge Sustainably. In AMTA Membrane Technology Conference; AMTA, 2015.

[10] Fisher, M. Amending Soils with Gypsum. Crops & Soils Magazine. 2011.

[11] Goldman, J. Selective Salt Recovery from Reverse Osmosis Concentrate Using Inter-Stage Ion Exchange, The University of New Mexico, 2012.

[12] Cappelle, M.; Davis, T. A.; Camacho, L. M.; Brandhuber, P. J.; Biagini, B.; Mack, B.; Yetayew, A. Mining for Salts: Recovering Useful by-Products from BWRO Brine. In Proceedings from the 2013 AWWA/AMTA Membrane Technology Conference.

[13] Krol, J. J.; Wessling, M.; Strathmann, H. Concentration Polarization with Monopolar Ion Exchange Membranes: Current-Voltage Curves and Water Dissociation. J. Memb. Sci. 1999, 162 (1–2), 145.

[14] Benjamin, M. M.; Lawler, D. F. Water Quality Engineering; Wiley, 2013.

Appendix B: ZDD MathCad 14.0 Model (version as of May 2, 2018)

1. Input Water Chemistry & Fixed Input Parameters

1.1 Input Design Parameters

Product Flow Rate

$Q_{prod} := 3\,mgd$

DI for Dissolving NaCl Pellets

$Q_{DI\_NaCl} := 0.005 \cdot Q_{prod} = 1.5 \times 10^{4} \cdot \frac{gal}{day}$

M.Na Dilutions

$Q_{DI\_mNa} := 0.005 \cdot Q_{prod} = 1.5 \times 10^{4} \cdot \frac{gal}{day}$

M. Cl Dilutions

$Q_{DI\_mCl} := 0 \cdot \frac{gal}{day}$

EDM Diluate Recovery

$r_{EDM} = \frac{Q_d}{Q_E}$ $r_{EDM} := 99\%$

RO/NF and EDM feed temperatures

$T_{ROf} := 25\,°C$ $T_{EDMf} := 30\,°C$

Ideal Gas Constant

$R_{ideal} := 0.08206 \frac{L \cdot atm}{mol \cdot K}$

1.2 Choose Feed Water Concentration

Avg raw feed, ZDD
pilot data at BGNDRF

$$Comp := \begin{pmatrix} "Ca" \\ "Mg" \\ "Na" \\ "Cl" \\ "HCO3" \\ "SO4" \\ "SiO2" \end{pmatrix} \quad c_{well1and4\_2013} := \begin{pmatrix} 288 \\ 121 \\ 379 \\ 342 \\ 248 \\ 1281 \\ 20 \end{pmatrix} \cdot \frac{mg}{L}$$

BGNDRF Well Water Chemistry (6/27/16 sample from https://www.usbr.gov/research/bgndrf/water.html)

$$c_{well1} := \begin{pmatrix} 129 \\ 34.9 \\ 450 \\ 36.1 \\ 140.3 \\ 1360 \\ 22.0 \end{pmatrix} \frac{mg}{L} \quad c_{well2} := \begin{pmatrix} 479 \\ 347 \\ 696 \\ 537 \\ 307.4 \\ 3290 \\ 19.6 \end{pmatrix} \frac{mg}{L} \quad c_{well3} := \begin{pmatrix} 387 \\ 204 \\ 377 \\ 630 \\ 228.1 \\ 1640 \\ 17.9 \end{pmatrix} \frac{mg}{L}$$

Other Well Water Chemistry

$$c_{raw\_KBH} := \begin{pmatrix} 162 \\ 40 \\ 792 \\ 1392 \\ 93 \\ 295 \\ 26 \end{pmatrix} \frac{mg}{L} \quad c_{raw\_Alamo} := \begin{pmatrix} 413 \\ 88 \\ 164 \\ 133 \\ 132 \\ 1433 \\ 28 \end{pmatrix} \cdot \frac{mg}{L} \quad c_{raw\_LaJunta} := \begin{pmatrix} 173 \\ 63 \\ 115 \\ 44 \\ 263 \\ 581 \\ 16 \end{pmatrix} \frac{mg}{L} \quad c_{raw\_Brighton} := \begin{pmatrix} 108 \\ 22.3 \\ 118.8 \\ 133.4 \\ 294.33 \\ 176.9 \\ 20.8 \end{pmatrix} \frac{mg}{L}$$

Choose raw chemistry
(type into equation)

$c_{raw\_in} := c_{raw\_Alamo}$

$TDS_{raw\_in} := \sum c_{raw\_in} = 2391 \cdot \frac{mg}{L}$

1.3 Input Parameters: Flow Balances

Dilution Flow

$$Q_{DI} := Q_{DI\_NaCl} + Q_{DI\_mNa} + Q_{DI\_mCl} = 3 \times 10^{4} \cdot \frac{gal}{day}$$

Permeate Flow

$$Q_{ROp} := Q_{prod} + Q_{DI} = 2104.17 \cdot gpm$$

RO Recovery

$$r_{RO} = \frac{Q_{ROp}}{Q_{ROf}} \qquad r_{RO} := 70\%$$

RO Feed Flow Rate

$$Q_{ROf}(r_{RO}) := \frac{Q_{ROp}}{r_{RO}}$$

RO Concentrate Flow

$$Q_{ROc}(r_{RO}) := Q_{ROf}(r_{RO}) - Q_{ROp}$$

Silica Purge Ratio

$$p_{silica} = \frac{Q_{Si}}{Q_{ROc}} \qquad p_{silica} := 0\%$$

Silica Purge Flow

$$Q_{Si}(r_{RO}, p_{silica}) := p_{silica} \cdot Q_{ROc}(r_{RO}) \qquad Q_{Si}(r_{RO}, p_{silica}) = 0 \cdot gpm$$

EDM Recycle Ratio

$$RR_{EDM} = \frac{Q_{d2F}(r_{RO}, RR_{EDM}, p_{silica})}{Q_{ROc}(r_{RO}) - Q_{Si}(r_{RO}, p_{silica})} \qquad RR_{EDM} := 2.5$$

EDM Diluate Recycle Flow

$$Q_{d2F}(r_{RO}, RR_{EDM}, p_{silica}) := RR_{EDM} \cdot \left(Q_{ROc}(r_{RO}) - Q_{Si}(r_{RO}, p_{silica})\right)$$

EDM feed flow

$$Q_{E}(r_{RO}, RR_{EDM}, p_{silica}) := \left(Q_{ROc}(r_{RO}) - Q_{Si}(r_{RO}, p_{silica})\right) \cdot \left(1 + RR_{EDM}\right)$$

Fraction of EDM feed that is Diluate:

$$frac_{EDM} := \frac{Q_{d2F}(r_{RO}, RR_{EDM}, p_{silica})}{Q_{E}(r_{RO}, RR_{EDM}, p_{silica})}$$

EDM Diluate Flow

$$Q_{d}(r_{RO}, r_{EDM}, RR_{EDM}, p_{silica}) := r_{EDM} \cdot Q_{E}(r_{RO}, RR_{EDM}, p_{silica})$$

EDM Diluate Return to RO feed:

$$Q_{d2R}(r_{RO}, RR_{EDM}, r_{EDM}, p_{silica}) := Q_{d}(r_{RO}, r_{EDM}, RR_{EDM}, p_{silica}) - Q_{d2F}(r_{RO}, RR_{EDM}, p_{silica})$$

Raw Flow

$$Q_{b}(r_{RO}, RR_{EDM}, r_{EDM}, p_{silica}) := Q_{ROf}(r_{RO}) - Q_{d2R}(r_{RO}, RR_{EDM}, r_{EDM}, p_{silica})$$

EDM Concentrate Flows. Assuming the water of hydration is equally spread to both Mixed Na & Mixed Cl streams. Adding all dilution volume to Mixed Na

$eq := mol \quad meq := \frac{eq}{1000} \quad Far := 96485\frac{C}{eq} \quad MW_{H2O} := 18\frac{gm}{mol} \quad \rho_{H2O} := 1000\frac{kg}{m^3}$

Use assumed ratio of ratio of water of hydration from EDM feed and NaCl streams to Mixed Na & Mixed Cl. Fixed amount of dilution water is added to each stream. Adjusted DI flows until EDM concentrate overflows matched what was seen in Alamogordo.

$hyd_{mCl} := 0.52 \quad hyd_{mNa} := 1 - hyd_{mCl} = 0.48$

$Q_{mCl}(r_{RO}, RR_{EDM}, r_{EDM}, p_{silica}) := hyd_{mCl}\cdot\left[(1 - r_{EDM})\cdot Q_E(r_{RO}, RR_{EDM}, p_{silica}) + Q_{DI\_NaCl}\right] + Q_{DI\_mCl}$

$Q_{mNa}(r_{RO}, RR_{EDM}, r_{EDM}, p_{silica}) := hyd_{mNa}\cdot\left[(1 - r_{EDM})\cdot Q_E(r_{RO}, RR_{EDM}, p_{silica}) + Q_{DI\_NaCl}\right] + Q_{DI\_mNa}$

$Q_{waste} := Q_{mNa}(r_{RO}, RR_{EDM}, r_{EDM}, p_{silica}) + Q_{mCl}(r_{RO}, RR_{EDM}, r_{EDM}, p_{silica}) + Q_{Si}(r_{RO}, p_{silica}) = 52.4\cdot gpm$

$Q_{outlet} := Q_{waste} + Q_{prod} = 2135.73\cdot gpm$

$Q_{mCl}(r_{RO}, RR_{EDM}, r_{EDM}, p_{silica}) = 3.14\times 10^4\cdot\frac{gal}{day}$

$Q_{ROout} := Q_{ROp} + Q_{ROc}(r_{RO}) = 3005.95\cdot gpm \quad Q_{mNa}(r_{RO}, RR_{EDM}, r_{EDM}, p_{silica}) = 4.4\times 10^4\cdot\frac{gal}{day}$

$Q_{ROin} := Q_{ROf}(r_{RO}) = 3005.95\cdot gpm$

$Q_{EDMin} := Q_{ROc}(r_{RO}) - Q_{Si}(r_{RO}, p_{silica}) + Q_{DI} = 922.62\cdot gpm$

$Q_{EDMout} := Q_{d2R}(r_{RO}, RR_{EDM}, r_{EDM}, p_{silica}) + Q_{mNa}(r_{RO}, RR_{EDM}, r_{EDM}, p_{silica}) + Q_{mCl}(r_{RO}, RR_{EDM}, r_{EDM}, p_{silica})$

Correct brackish feed for electroneutrality:

Molecular Weight, meq/mg

$$EW := \begin{pmatrix} 20 \\ 12.15 \\ 23 \\ 35.45 \\ 61 \\ 48 \\ 60 \end{pmatrix} \cdot \frac{mg}{meq} \qquad z := \begin{pmatrix} 2 \\ 2 \\ 1 \\ -1 \\ -1 \\ -2 \\ 0 \end{pmatrix} \qquad MM := \begin{pmatrix} 40 \\ 24.3 \\ 23 \\ 35.45 \\ 61 \\ 96 \\ 60 \end{pmatrix} \cdot \frac{gm}{mol}$$

Electroneutrality function:

$$EN(c_i) := \frac{\overrightarrow{\sum\left(\frac{c_i}{MM} \cdot z\right)}}{\overrightarrow{\sum\left(\frac{c_i}{MM} \cdot |z|\right)}}$$

Electroneutrality of the raw: $EN(c_{raw\_in}) = -1.05 \cdot \%$

$$EN\_correct(c_i) := \begin{bmatrix} (1 - EN(c_i)) \cdot c_{i_0} \\ (1 - EN(c_i)) \cdot c_{i_1} \\ (1 - EN(c_i)) \cdot c_{i_2} \\ (1 + EN(c_i)) \cdot c_{i_3} \\ (1 + EN(c_i)) \cdot c_{i_4} \\ (1 + EN(c_i)) \cdot c_{i_5} \\ c_{i_6} \end{bmatrix}$$

$$c_{raw} := EN\_correct(c_{raw\_in}) = \begin{pmatrix} 417.4 \\ 88.9 \\ 165.7 \\ 131.6 \\ 130.6 \\ 1417.9 \\ 28 \end{pmatrix} \cdot \frac{mg}{L}$$

$$EN(c_{raw}) = 0$$

Equivalent Concentration, raw

$$C_{raw} := \overrightarrow{\left(\frac{c_{raw}}{EW}\right)} = \begin{pmatrix} 20.9 \\ 7.3 \\ 7.2 \\ 3.7 \\ 2.1 \\ 29.5 \\ 0.5 \end{pmatrix} \cdot \frac{meq}{L}$$

2. ZDD Design Parameters

2.1. RO/NF Membrane Choice

$$\text{MembraneChoice} = \begin{pmatrix} \text{"1 = NF270"} \\ \text{"2 = NF90"} \\ \text{"3 = XLE"} \\ \text{"4 = BW30"} \\ \text{"5 = NF90-NF270 (55\%)"} \\ \text{"6 = NF90-NF270 (70-80\%)"} \end{pmatrix}$$

MembraneChoice := 6

2.2 RO/NF Salt Rejection

Equations are from ROSA output for 50-80% recovery. Enter number for corresponding membrane choice.

$$R_{RO\_NF270}(r_{RO}) := \begin{pmatrix} -0.0655 \cdot r_{RO} + 0.8284 \\ -0.0673 \cdot r_{RO} + 0.8781 \\ -0.1939 \cdot r_{RO} + 0.606 \\ -0.1507 \cdot r_{RO} + 0.1011 \\ -0.4616 \cdot r_{RO} + 0.6381 \\ -0.0536 \cdot r_{RO} + 0.9989 \\ -0.2175 \cdot r_{RO} + 0.3393 \end{pmatrix} \quad R_{RO\_NF90}(r_{RO}) := \begin{pmatrix} -0.0282 \cdot r_{RO} + 0.9992 \\ -0.0288 \cdot r_{RO} + 0.9991 \\ -0.1504 \cdot r_{RO} + 0.9857 \\ -0.1703 \cdot r_{RO} + 0.9832 \\ -0.1719 \cdot r_{RO} + 0.983 \\ -0.0307 \cdot r_{RO} + 0.9991 \\ -0.1015 \cdot r_{RO} + 0.9944 \end{pmatrix}$$

$$R_{RO\_NF90NF270\_55} := \begin{pmatrix} 0.871 \\ 0.901 \\ 0.669 \\ 0.372 \\ 0.61 \\ 0.976 \\ 0.52 \end{pmatrix} \quad R_{RO\_NF90NF270\_70\_80}(r_{RO}) := \begin{pmatrix} -0.3104 \cdot r_{RO} + 1.0933 \\ -0.2521 \cdot r_{RO} + 1.0771 \\ -0.7055 \cdot r_{RO} + 1.1851 \\ -1.2819 \cdot r_{RO} + 1.3238 \\ -1.0125 \cdot r_{RO} + 1.322 \\ -0.0784 \cdot r_{RO} + 1.0267 \\ -1.005 \cdot r_{RO} + 1.2649 \end{pmatrix}$$

$$R_{RO\_XLE}(r_{RO}) := \begin{pmatrix} -0.0316 \cdot r_{RO} + 1.0001 \\ -0.032 \cdot r_{RO} + 1 \\ -0.0833 \cdot r_{RO} + 0.9985 \\ -0.0872 \cdot r_{RO} + 0.9983 \\ -0.0923 \cdot r_{RO} + 0.9978 \\ -0.0343 \cdot r_{RO} + 1 \\ -0.0485 \cdot r_{RO} + 0.9982 \end{pmatrix} \quad R_{RO\_BW30}(r_{RO}) := \begin{pmatrix} -0.0085 \cdot r_{RO} + 0.9996 \\ -0.0088 \cdot r_{RO} + 0.9997 \\ -0.0233 \cdot r_{RO} + 0.9987 \\ -0.0243 \cdot r_{RO} + 0.986 \\ -0.026 \cdot r_{RO} + 0.9979 \\ -0.0093 \cdot r_{RO} + 0.9995 \\ -0.0145 \cdot r_{RO} + 0.9996 \end{pmatrix}$$

$$R_{RO}(r_{RO}) := \begin{cases} R_{RO\_NF270}(r_{RO}) & \text{if MembraneChoice} = 1 \\ R_{RO\_NF90}(r_{RO}) & \text{if MembraneChoice} = 2 \\ R_{RO\_XLE}(r_{RO}) & \text{if MembraneChoice} = 3 \\ R_{RO\_BW30}(r_{RO}) & \text{if MembraneChoice} = 4 \\ R_{RO\_NF90NF270\_55} & \text{if MembraneChoice} = 5 \\ R_{RO\_NF90NF270\_70\_80}(r_{RO}) & \text{if MembraneChoice} = 6 \end{cases}$$

If desired, can manually input RO/NF rejection values (requires disabling previous assignment calculation)

$$R_{RO}(r_{RO}) := \begin{pmatrix} 89\% \\ 91\% \\ 62\% \\ -4\% \\ 38\% \\ 97\% \\ 26\% \end{pmatrix}$$

$$CF(r_{RO}) := 1 + \frac{r_{RO} \cdot R_{RO}(r_{RO})}{1 - r_{RO}} \qquad CF(r_{RO}) = \begin{pmatrix} 3.04 \\ 3.1 \\ 2.61 \\ 2 \\ 2.43 \\ 3.27 \\ 2.31 \end{pmatrix} \qquad R_{RO}(r_{RO}) = \begin{pmatrix} 88 \\ 90 \\ 69 \\ 43 \\ 61 \\ 97 \\ 56 \end{pmatrix} \cdot \%$$

$$TDS(c_i) := \sum c_i$$

$$TDS(c_{raw}) = 2380.11 \cdot \frac{mg}{L}$$

2.3 EDM Membrane Choice and Design

Membrane Resistance: $\rho_{CEM} := 10\Omega \cdot cm^2$ $\rho_{AEM} := 7.5\Omega \cdot cm^2$

Stack & Spacer Information $A_{stack} := 4200cm^2$ $Quad_{stack} := 100$ $W_{stack} := 320mm$ $t_{spacer} := 0.8mm$

Shadow Factor (<1.0) $\beta := 0.65$ Current Efficiency $\xi := 75\%$

Inverter Efficiency $Conv_{AC\_DC} := 85\%$

2.4 EDM Ion Removal

Starting with fixed numbers based on the reduction in concentration from the EDM feed to diluate in Alamogordo (Year 2). E signifies removal rate. RRRs are relative removal ratios as compared to Calcium. Only input desired calcium removal (ECa), remaining ones are calculated from it.

$E_{Ca} := 0.25$ $RRR_{HCO3} := 0.4$ $RRR_{Cl} := 0.3$

$RRR_{Mg} := 0.9$ $RRR_{SO4} := 0.7$

$RRR_{Na} := 0.4$ $E_{SiO2} := 0$

2.5 Concentration Calculation Iterations

This section combines the RO/NF and EDM system desalination peformance and tracks the silica and calcium concentrations in the RO/NF concentrate and permeate.

$$\begin{aligned}
&\mathrm{EDM}(r_{RO}, RR_{EDM}, E_{Ca}, p_{silica}) := \\
&\quad c_{ROf} \leftarrow c_{raw} \\
&\quad SP_{RO} \leftarrow 1 - R_{RO}(r_{RO}) \\
&\quad c_{ROp} \leftarrow \overrightarrow{(SP_{RO} \cdot c_{ROf})} \\
&\quad c_{ROp} \leftarrow \mathrm{EN_correct}(c_{ROp}) \\
&\quad c_{ROc} \leftarrow \overrightarrow{(CF(r_{RO}) \cdot c_{ROf})} \\
&\quad c_{ROc} \leftarrow \mathrm{EN_correct}(c_{ROc}) \\
&\quad R_{EDM} \leftarrow \begin{pmatrix} E_{Ca} \\ RRR_{Mg} \cdot E_{Ca} \\ RRR_{Na} \cdot E_{Ca} \\ RRR_{Cl} \cdot E_{Ca} \\ RRR_{HCO3} \cdot E_{Ca} \\ RRR_{SO4} \cdot E_{Ca} \\ E_{SiO2} \end{pmatrix} \\
&\quad SP_{EDM} \leftarrow 1 - R_{EDM} \\
&\quad c_d \leftarrow \overrightarrow{(SP_{EDM} \cdot c_{ROc})} \\
&\quad c_d \leftarrow \mathrm{EN_correct}(c_d) \\
&\quad c_E \leftarrow \frac{Q_{d2F}(r_{RO}, RR_{EDM}, p_{silica})}{Q_E(r_{RO}, RR_{EDM}, p_{silica})} \cdot c_d + \frac{Q_{ROc}(r_{RO}) - Q_{Si}(r_{RO}, p_{silica})}{Q_E(r_{RO}, RR_{EDM}, p_{silica})} \cdot c_{ROc} \\
&\quad c_d \leftarrow \overrightarrow{(SP_{EDM} \cdot c_E)} \\
&\quad c_d \leftarrow \mathrm{EN_correct}(c_d) \\
&\quad EDM_{0,0} \leftarrow c_{ROf} \\
&\quad EDM_{1,0} \leftarrow c_{ROp} \\
&\quad EDM_{2,0} \leftarrow c_{ROc} \\
&\quad EDM_{3,0} \leftarrow c_E \\
&\quad EDM_{4,0} \leftarrow c_d \\
&\quad \varepsilon_{max} \leftarrow 1 \\
&\quad i \leftarrow 0 \\
&\quad \text{while } \varepsilon_{max} > .001 \\
&\qquad i \leftarrow i + 1 \\
&\qquad c_{ROf} \leftarrow \frac{Q_{d2R}(r_{RO}, RR_{EDM}, r_{EDM}, p_{silica})}{Q_{ROf}(r_{RO})} \cdot c_d + \frac{Q_b(r_{RO}, RR_{EDM}, r_{EDM}, p_{silica})}{Q_{ROf}(r_{RO})} \cdot c_{raw}
\end{aligned}$$

$$c_{ROp} \leftarrow \overrightarrow{\left(SP_{RO} \cdot c_{ROf}\right)}$$

$$c_{ROp} \leftarrow EN\_correct\left(c_{ROp}\right)$$

$$c_{ROc} \leftarrow \overrightarrow{\left(CF\left(r_{RO}\right) \cdot c_{ROf}\right)}$$

$$c_{ROc} \leftarrow EN\_correct\left(c_{ROc}\right)$$

$$c_E \leftarrow \frac{Q_{d2F}\left(r_{RO}, RR_{EDM}, p_{silica}\right)}{Q_E\left(r_{RO}, RR_{EDM}, p_{silica}\right)} \cdot c_d + \frac{Q_{ROc}\left(r_{RO}\right) - Q_{Si}\left(r_{RO}, p_{silica}\right)}{Q_E\left(r_{RO}, RR_{EDM}, p_{silica}\right)} \cdot c_{ROc}$$

$$c_d \leftarrow \overrightarrow{\left(SP_{EDM} \cdot c_E\right)}$$

$$c_d \leftarrow EN\_correct\left(c_d\right)$$

$$EDM_{0,i} \leftarrow c_{ROf}$$

$$EDM_{1,i} \leftarrow c_{ROp}$$

$$EDM_{2,i} \leftarrow c_{ROc}$$

$$EDM_{3,i} \leftarrow c_E$$

$$EDM_{4,i} \leftarrow c_d$$

for $j \in 0..4$

$$\varepsilon_j \leftarrow \frac{\left|EDM_{j,i} - EDM_{j,i-1}\right|}{EDM_{j,i}}$$

$$\varepsilon_{max} \leftarrow \max\left(\varepsilon_0, \varepsilon_1, \varepsilon_2, \varepsilon_3, \varepsilon_4\right)$$

$$results_0 \leftarrow c_{ROf}$$

$$results_1 \leftarrow c_{ROp}$$

$$results_2 \leftarrow c_{ROc}$$

$$results_3 \leftarrow c_E$$

$$results_4 \leftarrow c_d$$

return results

3. Check RO/NF Concentrate Stability

3.1 Data output & graphing: Use to check solubility, other, externally

$result := EDM(r_{RO}, RR_{EDM}, E_{Ca}, p_{silica})$ $N_{it} := 300$ $i := 1 .. N_{it}$

$DATA\_r\_RO :=$ for $i \in 0 .. 24$

$r_{RO} \leftarrow \frac{50 + 2 \cdot i}{100}$

$result \leftarrow EDM(r_{RO}, RR_{EDM}, E_{Ca}, p_{silica})$

$results_{i,0} \leftarrow r_{RO}$

for $j \in 0 .. 4$

for $k \in 0 .. 6$

$results_{i, 1+7 \cdot j+k} \leftarrow \frac{(result_j)_k}{\frac{mg}{L}}$

results

$DATA\_RR :=$ for $i \in 0 .. 40$

$RR_{EDM} \leftarrow \frac{20 + 2 \cdot i}{100}$

$result \leftarrow EDM(r_{RO}, RR_{EDM}, E_{Ca}, p_{silica})$

$results_{i,0} \leftarrow RR_{EDM}$

for $j \in 0 .. 4$

for $k \in 0 .. 6$

$results_{i, 1+7 \cdot j+k} \leftarrow \frac{(result_j)_k}{\frac{mg}{L}}$

results

DATA_cut :=
for $i \in 0..20$
$E_{Ca} \leftarrow \frac{20 + 2 \cdot i}{100}$
$result \leftarrow EDM(r_{RO}, RR_{EDM}, E_{Ca}, p_{silica})$
$results_{i,0} \leftarrow E_{Ca}$
for $j \in 0..4$
for $k \in 0..6$
$results_{i,1+7 \cdot j+k} \leftarrow \frac{(result_j)_k}{\frac{mg}{L}}$
results

DATA_Silica_bleed :=
for $i \in 0..30$
$p_{silica} \leftarrow \frac{0 + i}{100}$
$result \leftarrow EDM(r_{RO}, RR_{EDM}, E_{Ca}, p_{silica})$
$results_{i,0} \leftarrow p_{silica}$
for $j \in 0..4$
for $k \in 0..6$
$results_{i,1+7 \cdot j+k} \leftarrow \frac{(result_j)_k}{\frac{mg}{L}}$
results

3.2 Final Concentrations

RO/NF feed: RO/NF permeate: RO/NF concentrate:

$$c_{ROf} := \text{result}_0 = \begin{pmatrix} 529 \\ 122 \\ 293 \\ 158 \\ 173 \\ 2012 \\ 60 \end{pmatrix} \cdot \frac{mg}{L} \quad c_{ROp} := \text{result}_1 = \begin{pmatrix} 48.62 \\ 8.99 \\ 66.98 \\ 114.17 \\ 83.96 \\ 71.34 \\ 26.26 \end{pmatrix} \cdot \frac{mg}{L} \quad c_{ROc} := \text{result}_2 = \begin{pmatrix} 1652 \\ 388 \\ 785 \\ 307 \\ 408 \\ 6400 \\ 138 \end{pmatrix} \cdot \frac{mg}{L} \quad R_{RO\_act} := 1 - \frac{c_{ROp}}{c_{ROf}} = \begin{pmatrix} 0.91 \\ 0.93 \\ 0.77 \\ 0.28 \\ 0.51 \\ 0.96 \\ 0.56 \end{pmatrix}$$

EDM feed: EDM diluate: Check Electroneutrality:

$$c_{EDMf} := \text{result}_3 = \begin{pmatrix} 1045 \\ 256 \\ 655 \\ 247 \\ 313 \\ 4306 \\ 138 \end{pmatrix} \cdot \frac{mg}{L} \quad c_{EDMd} := \text{result}_4 = \begin{pmatrix} 802 \\ 203 \\ 604 \\ 223 \\ 275 \\ 3469 \\ 138 \end{pmatrix} \cdot \frac{mg}{L} \quad Check_{EN} := \begin{pmatrix} EN(c_{ROf}) \\ EN(c_{ROp}) \\ EN(c_{ROc}) \\ EN(c_{EDMf}) \\ EN(c_{EDMd}) \end{pmatrix} = \begin{pmatrix} 0 \\ 0 \\ 0 \\ 0 \\ 0 \end{pmatrix}$$

Summary Calculations

ZDD Recovery

$$Q_{prod} = 2083.33 \cdot gpm$$

$$Q_b(r_{RO}, RR_{EDM}, r_{EDM}, p_{silica}) = 2135.73 \cdot gpm$$

$$r_{ZDD} := \frac{Q_{prod}}{Q_b(r_{RO}, RR_{EDM}, r_{EDM}, p_{silica})} = 97.5 \cdot \%$$

ZDD Overall Salt Rejection

$$TDS_b := \sum c_{raw} = 2380.11 \cdot \frac{mg}{L}$$

$$TDS_{prod} := \sum \text{result}_1 = 420 \cdot \frac{mg}{L}$$

ZDD Recovery - 2nd method (permeate & waste)

$$r_{ZDD2} := \frac{Q_{ROp} - Q_{waste}}{Q_{ROp}} = 97.5 \cdot \%$$

$$R_{ZDD} := 1 - \frac{TDS_{prod}}{TDS_b} = 82 \cdot \%$$

4. EDM Design, Concentrate Quality, and Power

4.1 Calculate Mixed Na and Mixed Cl Concentrations

$$N_{EDMfCat} := \frac{\begin{pmatrix} c_{EDMf_0} \\ c_{EDMf_1} \\ c_{EDMf_2} \end{pmatrix}}{\begin{pmatrix} EW_0 \\ EW_1 \\ EW_2 \end{pmatrix}} \qquad N_{EDMfAn} := \frac{\begin{pmatrix} c_{EDMf_3} \\ c_{EDMf_4} \\ c_{EDMf_5} \end{pmatrix}}{\begin{pmatrix} EW_3 \\ EW_4 \\ EW_5 \end{pmatrix}} \qquad N_{EDMdCat} := \frac{\begin{pmatrix} c_{EDMd_0} \\ c_{EDMd_1} \\ c_{EDMd_2} \end{pmatrix}}{\begin{pmatrix} EW_0 \\ EW_1 \\ EW_2 \end{pmatrix}} \qquad N_{EDMdAn} := \frac{\begin{pmatrix} c_{EDMd_3} \\ c_{EDMd_4} \\ c_{EDMd_5} \end{pmatrix}}{\begin{pmatrix} EW_3 \\ EW_4 \\ EW_5 \end{pmatrix}}$$

Flow in one day:

$gpd := gpm \qquad gpd = 1440 \cdot \frac{gal}{day}$

$V_{EDMf} := Q_E(r_{RO}, RR_{EDM}, p_{silica})(1 \cdot day) = 5 \times 10^6 \cdot gal$

$V_{EDMd} := Q_d(r_{RO}, r_{EDM}, RR_{EDM}, p_{silica}) \cdot (1 \cdot day) = 4 \times 10^6 \cdot gal$

$V_{d2F} := Q_{d2F}(r_{RO}, RR_{EDM}, p_{silica}) \cdot (1 \cdot day) = 1 \times 10^7 \, L$

$V_{d2R} := Q_{d2R}(r_{RO}, RR_{EDM}, r_{EDM}, p_{silica}) \cdot 1day = 4.74 \times 10^6 \, L$

$V_{Sid} := Q_{Si}(r_{RO}, p_{silica}) \cdot (1 \cdot day) = 0$

$V_{DId} := Q_{DI} \cdot (1 \cdot day) = 1.14 \times 10^5 \, L$

$V_b := Q_b(r_{RO}, RR_{EDM}, r_{EDM}, p_{silica}) \cdot (1 \cdot day) = 1.16 \times 10^7 \, L$

$V_{ROf} := Q_{ROf}(r_{RO}) \cdot (1 \cdot day) = 2 \times 10^7 \, L$

$V_{ROc} := Q_{ROc}(r_{RO}) \cdot (1 \cdot day) = 5 \times 10^6 \, L$

$V_{ROp} := Q_{ROp} \cdot (1 \cdot day) = 1 \times 10^7 \, L$

$V_{mCl} := Q_{mCl}(r_{RO}, RR_{EDM}, r_{EDM}, p_{silica}) \cdot (1 \cdot day) = 1.2 \times 10^5 \, L$

$V_{mNa} := Q_{mNa}(r_{RO}, RR_{EDM}, r_{EDM}, p_{silica}) \cdot (1 \cdot day) = 1.7 \times 10^5 \, L$

$V_{prod} := Q_{prod} \cdot (1 \cdot day) = 1 \times 10^7 \, L$

$$Eq_{mCl} := \begin{bmatrix} \left(N_{EDMfCat_0} \cdot V_{EDMf} - N_{EDMdCat_0} \cdot V_{EDMd}\right) \\ \left(N_{EDMfCat_1} \cdot V_{EDMf} - N_{EDMdCat_1} \cdot V_{EDMd}\right) \\ \left(N_{EDMfCat_2} \cdot V_{EDMf} - N_{EDMdCat_2} \cdot V_{EDMd}\right) \\ \left(\sum N_{EDMfCat} \cdot V_{EDMf} - \sum N_{EDMdCat} \cdot V_{EDMd}\right) \end{bmatrix} \qquad Eq_{mNa} := \begin{pmatrix} \sum N_{EDMfAn} \cdot V_{EDMf} - \sum N_{EDMdAn} \cdot V_{EDMd} \\ N_{EDMfAn_0} \cdot V_{EDMf} - N_{EDMdAn_0} \cdot V_{EDMd} \\ N_{EDMfAn_1} \cdot V_{EDMf} - N_{EDMdAn_1} \cdot V_{EDMd} \\ N_{EDMfAn_2} \cdot V_{EDMf} - N_{EDMdAn_2} \cdot V_{EDMd} \end{pmatrix}$$

$$c_{mCl} := \overrightarrow{\left[\frac{Eq_{mCl}}{V_{mCl}} \cdot \begin{pmatrix} EW_0 \\ EW_1 \\ EW_2 \\ EW_3 \end{pmatrix}\right]} \qquad TDS_{mCl} := \frac{Eq_{mCl}}{V_{mCl}} \cdot \begin{pmatrix} EW_0 \\ EW_1 \\ EW_2 \\ EW_3 \end{pmatrix} \qquad c_{mNa} := \overrightarrow{\left[\frac{Eq_{mNa}}{V_{mNa}} \cdot \begin{pmatrix} EW_2 \\ EW_3 \\ EW_4 \\ EW_5 \end{pmatrix}\right]} \qquad TDS_{mNa} := \frac{Eq_{mNa}}{V_{mNa}} \cdot \begin{pmatrix} EW_2 \\ EW_3 \\ EW_4 \\ EW_5 \end{pmatrix}$$

4.2 NaCl consumption & Evaporation Pond Sizing

Na, per day $$M_{Na} := \left(\sum N_{EDMfAn} \cdot V_{EDMf} - \sum N_{EDMdAn} \cdot V_{EDMd}\right) \cdot EW_2 = 7745.31\ kg$$

Cl, per day $$M_{Cl} := \left(\sum N_{EDMfCat} \cdot V_{EDMf} - \sum N_{EDMdCat} \cdot V_{EDMd}\right) \cdot EW_3 = 1.19 \times 10^4\ kg$$

NaCl, lb/day $$M_{NaCl} := M_{Na} + M_{Cl} = 4.34 \times 10^4 \cdot lb$$

Evaporation pond sizing assumes No Salt Recovery

$$V_{evap\_no\_rec} := V_{mNa} + V_{mCl} + V_{Sid} = 2.86 \times 10^5\ L$$

$$r_{evap} := 177.6 \frac{cm}{yr}$$

$$A_{evap} := \frac{Q_{waste}}{r_{evap}} = 14.51 \cdot acre$$

4.3 EDM Sizing & Power Calculations

Calculate potential EDM stack membrane areas using fixed current efficiency & vary current density

Choose stack design & current density (pilot results used for this model)

Choose current density range for initial calculations:

$$i_{edm} := \begin{pmatrix} \frac{30A}{A_{stack}} \\ \frac{40A}{A_{stack}} \\ \frac{50A}{A_{stack}} \end{pmatrix} \qquad i_{edm} = \begin{pmatrix} 71.43 \\ 95.24 \\ 119.05 \end{pmatrix} \frac{A}{m^2}$$

Calculate equivalents removed:

$$N_E := \frac{{}^{c}EDMf_0}{EW_0} + \frac{{}^{c}EDMf_1}{EW_1} + \frac{{}^{c}EDMf_2}{EW_2} \qquad N_d := \frac{{}^{c}EDMd_0}{EW_0} + \frac{{}^{c}EDMd_1}{EW_1} + \frac{{}^{c}EDMd_2}{EW_2} \qquad Eq_{rem} := Q_E\left(r_{RO}, RR_{EDM}, p_{silica}\right)\cdot\left(N_E - N_d\right)$$

Calculate range of membrane area required:

Round to next integer:

$$A_{mem} := Eq_{rem}\cdot\frac{Far}{i_{edm}\cdot\xi} \qquad N_{quads} := \frac{A_{mem}}{A_{stack}} \qquad N_{stack} := \frac{N_{quads}}{Quad_{stack}} \qquad N_{stack\_r} := ceil\left(N_{stack}\right) = \begin{pmatrix} 161 \\ 121 \\ 97 \end{pmatrix}$$

Choose number of stacks. Max would allow for flexibility, Minimum reduces Capital Cost.

$N_{stack\_des\_area} := N_{stack\_r_2} = 97$

$v_{min} := 5.2\frac{cm}{s}$ $\qquad Q_{min} := v_{min}\cdot\left(N_{stack\_des\_area}\cdot Quad_{stack}\cdot t_{spacer}\cdot W_{stack}\right)$

$$Q_{stack} := \frac{Q_E\left(r_{RO}, RR_{EDM}, p_{silica}\right)}{N_{stack\_des\_area}} \qquad N_{stack\_min\_v} := \frac{Q_E\left(r_{RO}, RR_{EDM}, p_{silica}\right)}{\left(v_{min}\cdot Quad_{stack}\cdot t_{spacer}\cdot W_{stack}\right)}$$

$$v_{stack\_in} := \frac{Q_E\left(r_{RO}, RR_{EDM}, p_{silica}\right)}{N_{stack\_des\_area}\cdot Quad_{stack}\cdot t_{spacer}\cdot W_{stack}} \qquad v_{max} := 11\frac{cm}{s} \qquad Q_{max} := v_{max}\cdot\left(N_{stack\_des\_area}\cdot Quad_{stack}\cdot t_{spacer}\cdot W_{stack}\right)$$

$v_{stack\_in} = 8.02\cdot\frac{cm}{s}$ $\qquad N_{stack\_max\_v} := \frac{Q_E\left(r_{RO}, RR_{EDM}, p_{silica}\right)}{\left(v_{max}\cdot Quad_{stack}\cdot t_{spacer}\cdot W_{stack}\right)} = 70.71$

$$N_{stack\_des} := \begin{cases} round\left(N_{stack\_des\_area}\right) & \text{if } v_{stack\_in} > v_{min} \\ round\left(N_{stack\_max\_v}\right) & \text{if } v_{stack\_in} > v_{max} \\ round\left(N_{stack\_min\_v}\right) & \text{otherwise} \end{cases} \qquad v_{stack} := \begin{cases} v_{stack\_in} & \text{if } v_{stack\_in} > v_{min} \\ v_{max} & \text{if } v_{stack\_in} > v_{max} \\ v_{min} & \text{otherwise} \end{cases}$$

If desired add or subtract a few stacks to improve current density. ensure velocity is ~5.1-10.9 cm/s

$N_{stack\_adj} := 12$ $\qquad v_{stack\_adj} := \frac{Q_E\left(r_{RO}, RR_{EDM}, p_{silica}\right)}{\left(N_{stack\_adj} + N_{stack\_des}\right)\cdot Quad_{stack}\cdot t_{spacer}\cdot W_{stack}} = 7.14\cdot\frac{cm}{s}$ $\qquad A_{stack} = 0.42\,m^2$

$A_{mem\_des} := \left(N_{stack\_adj} + N_{stack\_des}\right)\cdot Quad_{stack}\cdot A_{stack}$ $\qquad A_{mem\_des} = 4578\,m^2$

Fixed current efficiency & calculate current density

$\xi_{fixed} := \xi$ $N_{stack\_adj} + N_{stack\_des} = 109$ $i_{edm\_des\_in} := \frac{Q_E(r_{RO}, RR_{EDM}, p_{silica}) \cdot (N_E - N_d) \cdot Far}{\xi_{fixed} \cdot A_{mem\_des}}$ $I_{edm} := i_{edm\_des\_in} \cdot A_{stack}$

$LCD := 74.98 \cdot \left(\frac{v_{stack\_adj}}{\frac{cm}{s}} \right)^{0.2672} \cdot \frac{A}{m^2}$ $\frac{i_{edm\_des\_in}}{LCD} = 82.7 \cdot \%$ $i_{edm\_des} := \begin{cases} i_{edm\_des\_in} & \text{if } i_{edm\_des\_in} < LCD \\ (0.95 \cdot LCD) & \text{otherwise} \end{cases}$

Conductivity is assumed for NaCl (50 S/cm) and rest are estimated using Alamogordo Cond/TDS relationship.

$mS := \frac{S}{1000}$ $\mu S := \frac{mS}{1000}$

$K_d := \left(0.86 \cdot \frac{\sum c_{EDMd}}{\frac{mg}{L}} + 1112 \right) \cdot \frac{\mu S}{cm} = 6.03 \times 10^{-3} \cdot \frac{S}{cm}$

$K_{NaCl} := 50 \cdot \frac{mS}{cm} = 0.05 \cdot \frac{S}{cm}$

$K_{c2} := \left(0.32 \cdot \frac{\sum c_{mNa}}{\frac{mg}{L}} + 62291 \right) \cdot \frac{\mu S}{cm} = 0.108 \cdot \frac{S}{cm}$

$K_{c1} := \left(0.37 \cdot \frac{\sum c_{mCl}}{\frac{mg}{L}} + 99459 \right) \cdot \frac{\mu S}{cm} = 0.156 \cdot \frac{S}{cm}$

$\Delta U_{dp} := \frac{R_{ideal} \cdot T_{EDMf}}{Far} \left(-\ln\left(\frac{K_{NaCl}}{K_{c1}} \right) + \ln\left(\frac{K_{c2}}{K_{NaCl}} \right) - \ln\left(\frac{K_d}{K_{c2}} \right) + \ln\left(\frac{K_{c1}}{K_d} \right) \right) = 0.21\,V$

$\Delta U_{IR} := \frac{i_{edm\_des}}{\beta} \cdot \left(\frac{t_{spacer}}{K_{c1}} + \frac{t_{spacer}}{K_{c2}} + \frac{t_{spacer}}{K_{NaCl}} + \frac{t_{spacer}}{K_d} + 2 \cdot \rho_{CEM} + 2 \cdot \rho_{AEM} \right) = 0.82\,V$

$$V_{elec} := 1.23V + 2\cdot\frac{R_{ideal}\cdot T_{EDMf}}{0.1074\cdot Far}\ln\left(\frac{i_{edm\_des}}{0.4599\frac{A}{m^2}}\right) + \frac{i_{edm\_des}\cdot 6mm}{25\frac{mS}{cm}} = 4.12\,V$$

Velec is based on Walker, et al (2014). Equations 14-18 describe electrode voltage. The first term assumes that the electrode rinse is well-buffered. The second term assumes the anode and cathode are equivalent and uses fitting parameters α and i0. Walker found α=0.1074, i0=0.4599 A/m^2. MEGA stacks are built with two spacers at each end; one is 1mm and the other is 2mm. Total width (combined anode & cathode) = 6mm. Alamogordo pilot was operated at 20-25 mS/cm

$$V_{quad} := \Delta U_{dp} + \Delta U_{IR} = 1.04\,V \qquad V_{stack} := V_{quad}\cdot Quad_{stack} + V_{elec} = 107.65\,V$$

$$P_{dc} := V_{stack}\cdot i_{edm\_des}\cdot\left(N_{stack\_adj} + N_{stack\_des}\right)\cdot A_{stack} = 516.8\cdot kW \qquad P_{ac} := \frac{P_{dc}}{Conv_{AC\_DC}} = 608.06\cdot kW$$

$$p_{edm} := \left[0.2403\cdot\left(\frac{v_{stack}}{\frac{cm}{s}}\right)^2 - 0.5953\cdot\frac{v_{stack}}{\frac{cm}{s}} + 6.5029\right]\cdot psi = 17.18\cdot psi$$

$$\xi_{pump} := 80\% \qquad Q_{Erinse} := 0.2\cdot Q_E\left(r_{RO}, RR_{EDM}, p_{silica}\right)$$

Assuming that all EDM pumps will have same flow & pressure

$$P_{EDMpumps} := 4\cdot Q_E\left(r_{RO}, RR_{EDM}, p_{silica}\right)\cdot\frac{p_{edm}}{\xi_{pump}} + Q_{Erinse}\cdot\frac{p_{edm}}{\xi_{pump}} = 123.84\cdot kW$$

$$Q_E\left(r_{RO}, RR_{EDM}, p_{silica}\right) = 3156.25\cdot gpm$$

$$P_{EDM} := P_{ac} + P_{EDMpumps} = 731.9\cdot kW$$

$$kgal := 1000gal \qquad E_{unit\_EDM} := \frac{P_{EDM}\cdot 24hr}{V_{prod}} = 5.86\cdot\frac{kW\cdot hr}{kgal}$$

4.4 RO/NF System Power Calculations

$$C_{ROf} := \sum \frac{c_{ROf}}{MM} = 0.06 \cdot \frac{mol}{L} \qquad p_{osmotic\_ROf} := R_{ideal} \cdot T_{ROf} \cdot C_{ROf} = 21.65 \cdot psi$$

$$C_{ROc} := \sum \frac{c_{ROc}}{MM} = 0.18 \cdot \frac{mol}{L} \qquad p_{osmotic\_ROc} := R_{ideal} \cdot T_{ROf} \cdot C_{ROc} = 63.18 \cdot psi$$

Back pressure for NF270 and XLE is 40 psi in ROSA modeling, and is 30 psi for NF90 and BW30

$$BackP := \begin{pmatrix} 0 \text{ if } r_{RO} < 70\% \\ 0 \text{ if MembraneChoice} = 5 \\ 0 \text{ if MembraneChoice} = 6 \\ \text{if } r_{RO} > 65\% \\ \quad \begin{pmatrix} 30 \text{ if MembraneChoice} = 2 \\ 0 \text{ if MembraneChoice} = 4 \\ 40 \text{ if MembraneChoice} = 1 \\ 40 \text{ if MembraneChoice} = 3 \end{pmatrix} \end{pmatrix} psi$$

$$P_{ROf\_NF270} := 0.7 \cdot BackP + \left[1 + \left(-0.023 \cdot \frac{p_{osmotic\_ROc}}{psi} + 1.7201\right)\right] \cdot p_{osmotic\_ROc} = 80.05 \cdot psi$$

$$P_{ROf\_NF90} := 0.4 \cdot BackP + \left[1 + \left(-0.0157 \cdot \frac{p_{osmotic\_ROc}}{psi} + 1.4816\right)\right] \cdot p_{osmotic\_ROc} = 94.12 \cdot psi$$

$$P_{ROf\_XLE} := 0.6 \cdot BackP + \left[1 + \left(-0.0201 \cdot \frac{p_{osmotic\_ROc}}{psi} + 2.2132\right)\right] \cdot p_{osmotic\_ROc} = 122.78 \cdot psi$$

$$P_{ROf\_BW30} := 0.5 \cdot BackP + \left[1 + \left(-0.0294 \cdot \frac{p_{osmotic\_ROc}}{psi} + 3.849\right)\right] \cdot p_{osmotic\_ROc} = 189.01 \cdot psi$$

$$P_{ROf\_NF90NF270\_55} := 70psi$$

$$P_{ROf\_NF90\_NF270} := \left[1 + \left(-0.0181 \cdot \frac{p_{osmotic\_ROc}}{psi} + 1.5003\right)\right] \cdot p_{osmotic\_ROc} = 85.72 \cdot psi$$

$$P_{ROf} := \begin{cases} P_{ROf\_NF270} & \text{if MembraneChoice} = 1 \\ P_{ROf\_NF90} & \text{if MembraneChoice} = 2 \\ P_{ROf\_XLE} & \text{if MembraneChoice} = 3 \\ P_{ROf\_BW30} & \text{if MembraneChoice} = 4 \\ P_{ROf\_NF90NF270\_55} & \text{if MembraneChoice} = 5 \\ P_{ROf\_NF90\_NF270} & \text{if MembraneChoice} = 6 \end{cases}$$

If desired, can enter pressure manually (but must disable preceeding calculation):

$$P_{ROf} := 82.5psi$$

$$P_{ROf} = 85.72 \cdot psi$$

$$P_{RO} := Q_{ROf}(r_{RO}) \cdot \frac{P_{ROf}}{\xi_{pump}} = 140.11 \cdot kW$$

$$P_{ROf} = 5.91 \times 10^5\ Pa$$

$$Q_{ROf}(r_{RO}) = 0.19 \frac{m^3}{s}$$

$$E_{unit\_RO} := \frac{P_{RO} \cdot 24hr}{V_{prod}} = 1.12 \cdot \frac{kW \cdot hr}{kgal}$$

$$E_{ZDD} := E_{unit\_EDM} + E_{unit\_RO} = 6.98 \cdot \frac{kW \cdot hr}{kgal}$$

NaCl purchases (no NaCl recovery)

$$M_{NaCl} = 4.34 \times 10^4 \cdot lb$$

5. ZDD Model Output

$$\text{InputsOutputs} := \begin{pmatrix} r_{RO} \\ RR_{EDM} \\ E_{Ca} \\ \frac{BackP}{psi} \\ \frac{Q_{mCl}(r_{RO}, RR_{EDM}, r_{EDM}, p_{silica})}{gpm} \\ \frac{Q_{mNa}(r_{RO}, RR_{EDM}, r_{EDM}, p_{silica})}{gpm} \\ \frac{Q_{Si}(r_{RO}, p_{silica})}{gpm} \\ r_{ZDD} \\ r_{ZDD2} \\ \frac{TDS_{prod}}{\frac{mg}{L}} \\ \frac{cROc_6}{\frac{mg}{L}} \\ \frac{A_{mem\_des}}{m^2} \\ N_{stack\_des} + N_{stack\_adj} \\ \frac{v_{stack\_adj}}{\frac{cm}{s}} \\ \frac{i_{edm\_des}}{\frac{A}{m^2}} \\ \frac{I_{edm}}{A} \\ \frac{V_{stack}}{V} \\ \frac{P_{dc}}{kW} \\ \frac{P_{ac}}{kW} \\ \frac{P_{EDMpumps}}{kW} \\ P_{EDM} \end{pmatrix} =$$

	0
0	0.7
1	2.5
2	0.25
3	0
4	21.8292
5	30.5667
6	0
7	0.9755
8	0.9751
9	420.3198
10	138.2996
11	4578
12	109
13	7.1362
14	104.8774
15	…

$$\begin{pmatrix} \frac{EDM}{kW} \\ \frac{P_{RO}}{kW} \\ \frac{E_{unit\_EDM}}{\frac{kW \cdot hr}{kgal}} \\ \frac{E_{unit\_RO}}{\frac{kW \cdot hr}{kgal}} \\ \frac{E_{ZDD}}{\frac{kW \cdot hr}{kgal}} \\ \frac{A_{evap}}{acre} \\ \frac{M_{NaCl}}{lb} \cdot 365 \end{pmatrix}$$

6. Salt Recovery & Evaporation Ponds

There are three methods included in this model:

1. Low Recovery: Blend Mixed Na + Mixed Cl w/o magnesium recovery or optimization of CaSO4 recovery.
2. Medium Recovery: Blend Mixed Na + Mixed Cl w/o magnesium recovery, but with optimization of CaSO4 recovery.
3. High Recovery: Blend Mixed Na + Mixed Cl w/ magnesium recovery and optimization of CaSO4 recovery.

Note: in all cases, the silica purge goes to a separate pond. In stoichiometric mix options (cases 2 and 3), the excess Mixed Na stream is sent to the same pond as the silica purge.

$$Comp_{conc} := \begin{pmatrix} "Ca" \\ "Mg" \\ "Na" \\ "Cl" \\ "HCO3" \\ "SO4" \end{pmatrix} \quad z_{conc} := \begin{pmatrix} 2 \\ 2 \\ 1 \\ -1 \\ -1 \\ -2 \end{pmatrix} \quad MM_{conc} := \begin{pmatrix} 40 \\ 24.3 \\ 23 \\ 35.45 \\ 61 \\ 96 \end{pmatrix} \cdot \frac{gm}{mol}$$

$$z_{conc} := \begin{pmatrix} 2 \\ 2 \\ 1 \\ -1 \\ -1 \\ -2 \end{pmatrix} \quad I(c_i) := 0.5 \sum \overrightarrow{\left(\frac{c_i}{MM_{conc}} \cdot z_{conc}^{\,2} \right)}$$

6.1 Low Recovery

$V_{mCl} = 1.19 \times 10^5\,L$ $V_{mNa} = 1.67 \times 10^5\,L$ $V_{NaCl\_1} := V_{mCl} + V_{mNa}$

$Q_{waste\_1} := Q_{Si}(r_{RO}, p_{silica})$

$$A_{waste\_1} := \frac{Q_{waste\_1}}{r_{evap}} = 0 \cdot acre$$

$$Q_{NaCl\_1} := Q_{mCl}(r_{RO}, RR_{EDM}, r_{EDM}, p_{silica}) + Q_{mNa}(r_{RO}, RR_{EDM}, r_{EDM}, p_{silica}) = 75450 \cdot \frac{gal}{day}$$

$$A_{NaCl\_1} := \frac{0.5 \cdot Q_{NaCl\_1}}{r_{evap}} = 7.26 \cdot acre$$

$$c_{sup\_1} := \begin{pmatrix} \frac{V_{mCl}}{V_{mNa}+V_{mCl}} \cdot c_{mCl_0} \\ \frac{V_{mCl}}{V_{mNa}+V_{mCl}} \cdot c_{mCl_1} \\ \frac{V_{mNa}}{V_{mNa}+V_{mCl}} \cdot c_{mNa_0} + \frac{V_{mCl}}{V_{mNa}+V_{mCl}} \cdot c_{mCl_2} \\ \frac{V_{mNa}}{V_{mNa}+V_{mCl}} \cdot c_{mNa_1} + \frac{V_{mCl}}{V_{mNa}+V_{mCl}} \cdot c_{mCl_3} \\ \frac{V_{mNa}}{V_{mNa}+V_{mCl}} \cdot c_{mNa_2} \\ \frac{V_{mNa}}{V_{mNa}+V_{mCl}} \cdot c_{mNa_3} \end{pmatrix} = \begin{pmatrix} 15111 \\ 3310 \\ 30593 \\ 43375 \\ 2454 \\ 52529 \end{pmatrix} \cdot \frac{mg}{L}$$

For salt recovery option 1, calculate the concentration of each ion before the precipitation occurs using a ratio of the daily volume of each of the streams. This program assumes that the Mixed Cl only contains Ca, Mg, Na, and Cl and the Mixed Na only contains Na, Cl, HCO3, and SO4. So, the Ca concentration is $(V_{mCl}/(V_{mCl} + V_{mNa}))^* C(Ca)_{mCl}$. For ions that are in both streams (i.e. Na), there are two terms: $(V_{mNa}/(V_{mCl} + V_{mNa}))^* C(Na)_{mNa} + (V_{mCl}/(V_{mCl} + V_{mNa}))^* C(Na)_{mCl}$

Calculate alkalinity as carbon for MINTEQ:

$$\frac{c_{sup\_1_4}}{MM_{conc_4}} = 40.22 \frac{mol}{m^3}$$

$$c_{sup\_1_4} \cdot \frac{12}{61} = 482.69 \cdot \frac{mg}{L}$$

$$I_{sup\_1} := \frac{I(c_{sup\_1})}{\frac{mol}{L}} = 3.42 \qquad C_{Ca\_bef\_1} := \frac{c_{sup\_1_0}}{MM_{conc_0}} = 377.78 \frac{mol}{m^3} \qquad C_{SO4\_bef\_1} := \frac{c_{sup\_1_5}}{MM_{conc_5}} = 547.18 \frac{mol}{m^3}$$

$$\Delta C_{CaSO4\_1} := 0.36517 \cdot \frac{mol}{L}$$

$$\Delta c_{Ca\_1} := \Delta C_{CaSO4\_1} \cdot MM_{conc_0} = 1 \times 10^4 \cdot \frac{mg}{L} \qquad \Delta c_{SO4\_1} := \Delta C_{CaSO4\_1} \cdot MM_{conc_5} = 35056 \cdot \frac{mg}{L}$$

$$M_{CaSO4\_1} := \left(\Delta c_{Ca\_1} + \Delta c_{SO4\_1}\right) \cdot \left(V_{mCl} + V_{mNa}\right) = 31271 \cdot lb$$

Calculate the concentration of the supernatant, which is mostly NaCl. Multiplying everything by 2 to account for evaporating half the water

$$c_{NaCl\_1} := 2 \begin{pmatrix} c_{sup\_1_0} - \Delta c_{Ca\_1} \\ c_{sup\_1_1} \\ c_{sup\_1_2} \\ c_{sup\_1_3} \\ c_{sup\_1_4} \\ c_{sup\_1_5} - \Delta c_{SO4\_1} \end{pmatrix} = \begin{pmatrix} 1009 \\ 6620 \\ 61187 \\ 86750 \\ 4907 \\ 34945 \end{pmatrix} \cdot \frac{mg}{L}$$

$$\frac{c_{NaCl\_1_4}}{MM_{conc_4}} = 80.45 \frac{mol}{m^3}$$

$$c_{NaCl\_1_4} \cdot \frac{12}{61} = 965.38 \cdot \frac{mg}{L}$$

$$I_{NaCl\_1} := \frac{I(c_{NaCl\_1})}{\frac{mol}{L}} = 3.92$$

Na in Mixed Na & Mixed Cl streams

$$C_{totNa\_1} := \frac{c_{NaCl\_1_2}}{MM_{conc_2}} = 2660 \frac{mol}{m^3}$$

Cl in Mixed Na & Mixed Cl streams $C_{totCl\_1} := \frac{c_{NaCl\_1_3}}{MM_{conc_3}} = 2447 \frac{mol}{m^3}$

$$M_{NaCl\_1} := \min\left(C_{totNa\_1}, C_{totCl\_1}\right) \cdot \left(MM_{conc_2} + MM_{conc_2}\right) \cdot \frac{\left(V_{mNa} + V_{mCl}\right)}{2}$$

$M_{NaCl\_1} = 35440 \cdot lb$ $Rec_{NaCl\_1} := \frac{M_{NaCl\_1}}{M_{NaCl}} = 81.7 \cdot \%$

6.2 Medium Recovery

ratio of SO4 (in Mixed Na) to Ca (in Mixed Cl): $SO4\_Ca2 := \frac{\frac{c_{mNa_3}}{MM_{conc_5}}}{\frac{c_{mCl_0}}{MM_{conc_0}}} = 1.03$

Volume of Mixed Na for stoichiometric blend of Ca and SO4:

$$V_{mNa2} := \begin{cases} V_{mNa} & \text{if } SO4\_Ca2 < 1 \\ \frac{V_{mNa}}{SO4\_Ca2} & \text{if } SO4\_Ca2 > 1 \end{cases}$$

Volume of Mixed Cl for stoichiometric blend of Ca and SO4:

$$V_{mCl2} := \begin{cases} V_{mCl} & \text{if } SO4\_Ca2 > 1 \\ V_{mCl} \cdot SO4\_Ca2 & \text{if } SO4\_Ca2 < 1 \end{cases}$$

$V_{NaCl\_2} := V_{mNa2} + V_{mCl2}$

$$Q_{waste\_2} := \begin{cases} Q_{Si}\left(r_{RO}, p_{silica}\right) + \frac{\left(V_{mCl} - V_{mCl2}\right)}{day} & \text{if } SO4\_Ca2 < 1 \\ Q_{Si}\left(r_{RO}, p_{silica}\right) + \frac{\left(V_{mNa} - V_{mNa2}\right)}{day} & \text{if } SO4\_Ca2 > 1 \end{cases}$$

$Q_{waste\_2} = 1463 \cdot \frac{gal}{day}$

$A_{waste\_2} := \frac{Q_{waste\_2}}{r_{evap}} = 0.28 \cdot acre$ $r_{evap} = 0.004863 \cdot \frac{m}{day}$

$Q_{NaCl\_2} := \frac{V_{mNa2} + V_{mCl2}}{day}$ $Q_{NaCl\_2} = 73987 \cdot \frac{gal}{day}$

$A_{NaCl\_2} := \frac{0.5 \cdot Q_{NaCl\_2}}{r_{evap}} = 7.12 \cdot acre$

calculate concentration in supernatant before CaSO4 precipitation:

$$c_{sup\_2} := \begin{pmatrix} \frac{V_{mCl2}}{V_{mNa2}+V_{mCl2}}\cdot c_{mCl_0} \\ \frac{V_{mCl2}}{V_{mNa2}+V_{mCl2}}\cdot c_{mCl_1} \\ \frac{V_{mNa2}}{V_{mNa2}+V_{mCl2}}\cdot c_{mNa_0}+\frac{V_{mCl2}}{V_{mNa2}+V_{mCl2}}\cdot c_{mCl_2} \\ \frac{V_{mNa2}}{V_{mNa2}+V_{mCl2}}\cdot c_{mNa_1}+\frac{V_{mCl2}}{V_{mNa2}+V_{mCl2}}\cdot c_{mCl_3} \\ \frac{V_{mNa2}}{V_{mNa2}+V_{mCl2}}\cdot c_{mNa_2} \\ \frac{V_{mNa2}}{V_{mNa2}+V_{mCl2}}\cdot c_{mNa_3} \end{pmatrix} = \begin{pmatrix} 15410 \\ 3376 \\ 30279 \\ 44179 \\ 2419 \\ 51787 \end{pmatrix}\cdot\frac{mg}{L}$$

$$\frac{c_{sup\_2_4}}{MM_{conc_4}} = 39.66\,\frac{mol}{m^3}$$

$$c_{sup\_2_4}\cdot\frac{12}{61} = 475.87\cdot\frac{mg}{L}$$

$$I_{sup\_2} := \frac{I\left(c_{sup\_2}\right)}{\frac{mol}{L}} = 3.43$$

$$C_{Ca\_bef\_2} := \frac{c_{sup\_2_0}}{MM_{conc_0}} = 385.25\,\frac{mol}{m^3} \qquad C_{SO4\_bef\_NL} := \frac{c_{sup\_2_5}}{MM_{conc_5}} = 539.45\,\frac{mol}{m^3}$$

$$\Delta C_{CaSO4\_2} := 0.37189\cdot\frac{mol}{L}$$

$$\Delta c_{Ca\_2} := \Delta C_{CaSO4\_2}\cdot MM_{conc_0} = 14876\cdot\frac{mg}{L} \qquad \Delta c_{SO4\_2} := \Delta C_{CaSO4\_2}\cdot MM_{conc_5} = 35701\cdot\frac{mg}{L}$$

$$M_{CaSO4\_2} := \left(\Delta c_{Ca\_2}+\Delta c_{SO4\_2}\right)\cdot\left(V_{mCl2}+V_{mNa2}\right) = 31229\cdot lb$$

$$c_{NaCl\_2} := 2\begin{pmatrix} c_{sup\_2_0}-\Delta c_{Ca\_2} \\ c_{sup\_2_1} \\ c_{sup\_2_2} \\ c_{sup\_2_3} \\ c_{sup\_2_4} \\ c_{sup\_2_5}-\Delta c_{SO4\_2} \end{pmatrix} = \begin{pmatrix} 1069 \\ 6751 \\ 60558 \\ 88359 \\ 4838 \\ 32171 \end{pmatrix}\cdot\frac{mg}{L}$$

$$I_{NaCl\_2} := \frac{I\left(c_{NaCl\_2}\right)}{\frac{mol}{L}} = 3.88$$

Na in Mixed Na & Mixed Cl streams $\qquad C_{totNa\_2} := \frac{c_{NaCl\_2_2}}{MM_{conc_2}} = 2633\,\frac{mol}{m^3}$

Cl in Mixed Na & Mixed Cl streams

$$C_{totCl\_2} := \frac{c_{NaCl\_2_3}}{MM_{conc_3}} = 2492\,\frac{mol}{m^3}$$

$$M_{NaCl\_2} := \min\left(C_{totNa\_2}, C_{totCl\_2}\right)\cdot\left(MM_{conc_2} + MM_{conc_2}\right)\cdot\frac{\left(V_{mNa2} + V_{mCl2}\right)}{2}$$

$$M_{NaCl\_2} = 35397\cdot lb \qquad Rec_{NaCl2} := \frac{M_{NaCl\_2}}{M_{NaCl}} = 81.6\cdot\%$$

6.3 High Recovery

Treat Mixed Cl stream with lime to precipitate Mg(OH)2, which will boost the relative concentration of calcium (assume pH=11.1) :

$$c_{mClnew} := \begin{pmatrix} c_{mCl_0} \\ c_{mCl_1} \\ c_{mCl_2} \\ c_{mCl_3} \\ 0 \\ 0 \end{pmatrix} = \begin{array}{|c|r|}\hline & 0 \\ \hline 0 & 36271 \\ 1 & 7945 \\ 2 & 8340 \\ 3 & 100326 \\ 4 & 0 \\ 5 & 0 \\ \hline \end{array} \cdot\frac{mg}{L}$$

In this case, assuming that lime will be added until the pH is 11.1 (different value could be input by user). The first part just defines the mixed Cl stream prior to lime addition.

The next part calculates how much magnesium would remain at pH 11.1. Then, I calculate how much magnesium was removed (as Mg(OH)2) and how much additional Ca is now in the mixed Cl stream.

$pH_{BL} := 7.0$ $pH_{AL} := 11.1$

$$ALK(CT, pH) := CT\cdot\left[\left(\frac{10^{-pH}}{10^{-6.3}} + 1 + \frac{10^{-10.3}}{10^{-pH}}\right)^{-1} + 2\cdot\left[\frac{\left(10^{-pH}\right)^2}{10^{-6.3}\cdot 10^{-10.3}} + \frac{10^{-pH}}{10^{-10.3}} + 1\right]^{-1}\right]\frac{mol}{L} + \frac{10^{-14}}{10^{-pH}}\cdot\frac{mol}{L} - 10^{-pH}\cdot\frac{mol}{L}$$

$\Delta C_{Mg} := 0.32662\cdot\frac{mol}{L}$ $\Delta c_{Mg} := \Delta C_{Mg}\cdot MM_{conc_1} = 7937\cdot\frac{mg}{L}$ Enter Visual Minteq output for brucite

$$C_{Lime} := \frac{\left(ALK\left(0.0\cdot\frac{mol}{L}, pH_{AL}\right) - ALK\left(0.0\cdot\frac{mol}{L}, pH_{BL}\right)\right)}{z_{conc_0}} + \Delta C_{Mg} \qquad C_{Lime} = 327.25\,\frac{mol}{m^3}$$

$$M_{Lime} := C_{Lime}\cdot\left(56\,\frac{gm}{mol}\right)\cdot V_{mCl} = 4807\cdot lb$$

$$c_{mCl\_AL} := \begin{pmatrix} c_{mClnew_0} + C_{Lime}\cdot MM_0 \\ c_{mClnew_1} - \Delta c_{Mg} \\ c_{mClnew_2} \\ c_{mClnew_3} \\ c_{mClnew_4} \\ c_{mClnew_5} \end{pmatrix} = \begin{pmatrix} 49361 \\ 8 \\ 8340 \\ 100326 \\ 0 \\ 0 \end{pmatrix}\cdot\frac{mg}{L}$$

$$M_{MgOH2} := \Delta C_{Mg}\cdot V_{mCl}\cdot\left(MM_{conc_1} + 2\cdot 17\cdot\frac{gm}{mol}\right) = 4995\cdot lb$$

ratio of SO4 (in Mixed Na) to Ca (in Mixed Cl):

$$SO4\_Ca3 := \frac{\frac{c_{mNa_3}}{MM_{conc_5}}}{\frac{c_{mCl\_AL_0}}{MM_{conc_0}}} = 0.76$$

Volume of Mixed Na for stoichiometric blend of Ca and SO4:

$$\frac{c_{mCl\_AL_0}}{MM_{conc_0}} = 1234.01\,\frac{mol}{m^3} \qquad \frac{c_{mNa_3}}{MM_{conc_5}} = 937.94\,\frac{mol}{m^3}$$

Volume of Mixed Na for stoichiometric blend of Ca and SO4:

$$V_{mNa3} := \begin{cases} V_{mNa} & \text{if } SO4\_Ca3 < 1 \\ \frac{V_{mNa}}{SO4\_Ca3} & \text{if } SO4\_Ca3 > 1 \end{cases}$$

Volume of Mixed Cl for stoichiometric blend of Ca and SO4:

$$V_{mCl3} := \begin{cases} V_{mCl} & \text{if } SO4\_Ca3 > 1 \\ V_{mCl} \cdot SO4\_Ca3 & \text{if } SO4\_Ca3 < 1 \end{cases}$$

$$V_{NaCl\_3} := V_{mNa3} + V_{mCl3}$$

$$Q_{waste\_3} := \begin{cases} Q_{Si}\left(r_{RO}, p_{silica}\right) + \frac{\left(V_{mCl} - V_{mCl3}\right)}{day} & \text{if } SO4\_Ca3 < 1 \\ Q_{Si}\left(r_{RO}, p_{silica}\right) + \frac{\left(V_{mNa} - V_{mNa3}\right)}{day} & \text{if } SO4\_Ca3 > 1 \end{cases}$$

$$A_{waste\_3} := \frac{Q_{waste\_3}}{r_{evap}} = 1.45 \cdot acre \qquad Q_{NaCl\_3} := \frac{V_{mNa3} + V_{mCl3}}{day} \qquad A_{NaCl\_3} := \frac{0.5 Q_{NaCl\_3}}{r_{evap}} = 6.53 \cdot acre$$

calculate concentration in supernatant before CaSO4 precipitation:

$$c_{sup\_3} := \begin{pmatrix} \frac{V_{mCl3}}{V_{mNa3}+V_{mCl3}}\cdot c_{mCl\_AL_0} \\ \frac{V_{mCl3}}{V_{mNa3}+V_{mCl3}}\cdot c_{mCl\_AL_1} \\ \frac{V_{mNa3}}{V_{mNa3}+V_{mCl3}}\cdot c_{mNa_0}+\frac{V_{mCl3}}{V_{mNa3}+V_{mCl3}}\cdot c_{mCl\_AL_2} \\ \frac{V_{mNa3}}{V_{mNa3}+V_{mCl3}}\cdot c_{mNa_1}+\frac{V_{mCl3}}{V_{mNa3}+V_{mCl3}}\cdot c_{mCl\_AL_3} \\ \frac{V_{mNa3}}{V_{mNa3}+V_{mCl3}}\cdot c_{mNa_2} \\ \frac{V_{mNa3}}{V_{mNa3}+V_{mCl3}}\cdot c_{mNa_3} \end{pmatrix} = \begin{pmatrix} 17366.56 \\ 2.94 \\ 33064.65 \\ 37050.14 \\ 2726.17 \\ 58362.79 \end{pmatrix}\cdot\frac{mg}{L}$$

$$\frac{c_{sup\_3_4}}{MM_{conc_4}} = 44.69\,\frac{mol}{m^3}$$

$$c_{sup\_3_4}\cdot\frac{12}{61} = 536.29\cdot\frac{mg}{L}$$

$$I_{sup\_3} := \frac{I\left(c_{sup\_3}\right)}{\frac{mol}{L}} = 3.35$$

$$C_{Ca\_bef\_3} := \frac{c_{sup\_3_0}}{EW_0} = 868.33\,\frac{mol}{m^3} \qquad C_{SO4\_bef\_3} := \frac{c_{sup\_3_5}}{EW_5} = 1215.89\,\frac{mol}{m^3}$$

$$\Delta C_{CaSO4\_3} := 0.42271\cdot\frac{mol}{L}$$

Enter Visual Minteq output here

$$\Delta c_{Ca\_3} := \Delta C_{CaSO4\_3}\cdot MM_{conc_0} = 16908\cdot\frac{mg}{L} \qquad \Delta c_{SO4\_3} := \Delta C_{CaSO4\_3}\cdot MM_{conc_5} = 40580\cdot\frac{mg}{L}$$

$$M_{CaSO4\_3} := \left(\Delta c_{Ca\_3}+\Delta c_{SO4\_3}\right)\cdot\left(V_{mCl3}+V_{mNa3}\right) = 32580\cdot lb$$

$$c_{NaCl\_3} := 2\begin{pmatrix} c_{sup\_3_0}-\Delta c_{Ca\_3} \\ c_{sup\_3_1} \\ c_{sup\_3_2} \\ c_{sup\_3_3} \\ c_{sup\_3_4} \\ c_{sup\_3_5}-\Delta c_{SO4\_3} \end{pmatrix} = \begin{pmatrix} 916 \\ 6 \\ 66129 \\ 74100 \\ 5452 \\ 35565 \end{pmatrix}\cdot\frac{mg}{L} \qquad I_{NaCl\_3} := \frac{I\left(c_{NaCl\_3}\right)}{\frac{mol}{L}} = 3.31$$

Na in Mixed Na & Mixed Cl streams

$$C_{totNa\_3} := \frac{c_{NaCl\_3_2}}{EW_2} = 2875.19\,\frac{mol}{m^3}$$

Cl in Mixed Na & Mixed Cl streams

$$C_{totCl\_3} := \frac{c_{NaCl\_3_3}}{EW_3} = 2090.28\,\frac{mol}{m^3}$$

$$M_{NaCl\_3} := \min\left(C_{totNa\_3}, C_{totCl\_3}\right)\cdot\left(MM_{conc_2} + MM_{conc_2}\right)\cdot\frac{\left(V_{mNa3} + V_{mCl3}\right)}{2}$$

$$M_{NaCl\_3} = 27246\cdot lb \qquad Rec_{NaCl3} := \frac{M_{NaCl\_3}}{M_{NaCl}} = 62.8\cdot\%$$

7. Output Data

$$RecoveryEvapOutput := \begin{pmatrix} \frac{A_{waste\_1}}{acre} \\ \frac{A_{waste\_2}}{acre} \\ \frac{A_{waste\_3}}{acre} \\ \frac{A_{NaCl\_1}}{acre} \\ \frac{A_{NaCl\_2}}{acre} \\ \frac{A_{NaCl\_3}}{acre} \\ \frac{M_{CaSO4\_1}}{lb} \\ \frac{M_{CaSO4\_2}}{lb} \\ \frac{M_{CaSO4\_3}}{lb} \\ \frac{M_{NaCl\_1}}{lb} \\ \frac{M_{NaCl\_2}}{lb} \\ \frac{M_{NaCl\_3}}{lb} \\ \frac{M_{MgOH2}}{lb} \\ \frac{M_{Lime}}{lb} \\ \frac{V_{NaCl\_1}}{gal} \\ \frac{V_{NaCl\_2}}{gal} \\ \frac{V_{NaCl\_3}}{gal} \\ \frac{V_{mCl}}{gal} \end{pmatrix} =$$

	0
0	0
1	0.28
2	1.45
3	7.26
4	7.12
5	6.53
6	$3.13\cdot10^4$
7	$3.12\cdot10^4$
8	$3.26\cdot10^4$
9	$3.54\cdot10^4$
10	$3.54\cdot10^4$
11	$2.72\cdot10^4$
12	4995.26
13	4807.44
14	$7.55\cdot10^4$
15	...

$$\text{NaCl\_quality} := \begin{pmatrix} c_{NaCl\_1_0} & c_{NaCl\_2_0} & c_{NaCl\_3_0} \\ c_{NaCl\_1_1} & c_{NaCl\_2_1} & c_{NaCl\_3_1} \\ c_{NaCl\_1_2} & c_{NaCl\_2_2} & c_{NaCl\_3_2} \\ c_{NaCl\_1_3} & c_{NaCl\_2_3} & c_{NaCl\_3_3} \\ c_{NaCl\_1_4} & c_{NaCl\_2_4} & c_{NaCl\_3_4} \\ c_{NaCl\_1_5} & c_{NaCl\_2_5} & c_{NaCl\_3_5} \end{pmatrix} = \begin{pmatrix} 1009 & 1069 & 916 \\ 6620 & 6751 & 6 \\ 61187 & 60558 & 66129 \\ 86750 & 88359 & 74100 \\ 4907 & 4838 & 5452 \\ 34945 & 32171 & 35565 \end{pmatrix} \cdot \frac{mg}{L}$$

$$\text{Ratios\_Minteqinfo} := \begin{pmatrix} \frac{\Delta C_{CaSO4\_1}}{\frac{mol}{L}} \\ \frac{\Delta C_{CaSO4\_2}}{\frac{mol}{L}} \\ \frac{\Delta C_{CaSO4\_3}}{\frac{mol}{L}} \\ \frac{\Delta C_{Mg}}{\frac{mol}{L}} \\ SO4\_Ca2 \\ SO4\_Ca3 \end{pmatrix} = \begin{pmatrix} 0.36517 \\ 0.37189 \\ 0.42271 \\ 0.32662 \\ 1.034384 \\ 0.760074 \end{pmatrix}$$

Appendix C: Sample ZDD Model Output and Cost Calculations

	A	B	C	D
1			**Output or formula**	**Result**
2	Water		Alamogordo blend	Alamogordo blend
3	Membrane		NF90-NF270	NF90-NF270
4	Qprod	gpm	2083.33333333333	2083.33333333333
5		mgd	3	3
6	QROp	gpm	2104.17	2104.17
7		mgd	=C6*1440/1000000	3.0300048
8	$r_{RO/NF}$		0.7	0.7
9	RR		2.5	2.5
10	E_{ca}		0.25	0.25
11	BackP	psi	0	0
12	QmCl	gpm	21.8292	21.8292
13	QmNa	gpm	30.5667	30.5667
14	Qsi	gpm	0	0
15	rZDD		0.9755	0.9755
16			=C15*100	97.55
17	rZDD2		0.9751	0.9751
18	Permeate TDS	mg/L	420.3198	420.3198
19	Reject SiO2	mg/L	138.2996	138.2996
20	Amem	m2	4578	4578
21	Nstacks		109	109
22	vstack	cm/s	7.1362	7.1362
23	iedm	A/m2	104.8774	104.8774
24	Iedm	A	44.0485	44.0485
25	Vstack	V	107.6478	107.6478
26	Pdc	kWDC	516.848	516.848
27	Pac	kWAC	608.0564	608.0564
28	PEDMpumps	kWAC	123.8441	123.8441
29	PEDM	kWAC	731.9006	731.9006
30	PRO/NF	kW	140.1051	140.1051
31	EEDM	kWh/kgal	5.8552	5.8552
32	ERO/NF	kWh/kgal	1.1208	1.1208
33	EZDD	kWh/kgal	6.976	6.976
34	EEDM	kWh/m3	=C31*264.172/1000	1.5467798944
35	ERO/NF	kWh/m3	=C32*264.172/1000	0.2960839776
36	EZDD	kWh/m3	=C33*264.172/1000	1.842863872
37	Evap pond size	acre	14.5142	14.5142
38	NaCl Needed	lb/yr	15839000	15839000
39				

	A	B	C	D
1			**Output or formula**	**Result**
40	Awaste1	acre	0	0
41	Awaste2	acre	0.28	0.28
42	Awaste3	acre	1.45	1.45
43	ANaCl1	acre	7.26	7.26
44	ANaCl2	acre	7.12	7.12
45	ANaCl3	acre	6.53	6.53
46	MCaSO4_1	lb/day	31300	31300
47	MCaSO4_2	lb/day	31200	31200
48	MCaSO4_3	lb/day	32600	32600
49	MNaCl_1	lb/day	35400	35400
50	MNaCl_2	lb/day	35400	35400
51	MNaCl_3	lb/day	27200	27200
52	MMgOH (case 3)	lb/day	4995.26	4995.26
53	MLime (case 3)	lb/day	4807.44	4807.44
54	VNaCl - salt recovery 1	gal/day	75500	75500
55	VNaCl - salt recovery 2	gal/day	74000	74000
56	VNaCl - salt recovery 3	gal/day	67900	67900
57	VmCl - salt recovery 3	gal/day	31400	31400
58	***Coefficients & ratios***			
59	ΔCaSO4_1	mol/L	0.36517	0.36517
60	ΔCaSO4_2	mol/L	0.37189	0.37189
61	ΔCaSO4_3	mol/L	0.42271	0.42271
62	ΔMg	mol/L	0.32662	0.32662
63	SO4_Ca2	(ratio)	1.034384	1.034384
64	SO4_Ca3	(ratio)	0.760074	0.760074
65	MNaCl1/MNaCl		=C49*365/C$38	0.815771197676621
66	MNaCl2/MNaCl		=C50*365/C$38	0.815771197676621
67	MNaCl3/MNaCl		=C51*365/C$38	0.626807247932319
68				
69	**Capital Costs**	assumptions		
70	EDM	$1300/m2	=1300*C20	5951400
71	RO/NF	$1.50/gpd ROp	=1.5*C7*1000000	4545007.2
72	Concentrate Management & Salt Recovery			
73	Evaporation pond - no salt recovery	$200K/acre	=200000*C37	2902840
74	Evaporation ponds - salt recovery 1	$200K/acre	=200000*(C40+C43)	1452000
75	Evaporation ponds - salt recovery 2	$200K/acre	=200000*(C41+C44)	1480000
76	Evaporation ponds - salt recovery 3	$200K/acre	=200000*(C42+C45)	1596000
77	Gypsum reactor - salt recovery 1	$0.79/gpd feed	=0.79*C54	59645

	A	B	C	D
1			**Output or formula**	**Result**
78	Gypsum reactor - salt recovery 2	$0.79/gpd feed	=0.79*C55	58460
79	Gypsum reactor - salt recovery 3	$0.79/gpd feed	=0.79*C56	53641
80	Lime softening system - salt recovery 3	$0.96/gpd feed	=0.96*C56	65184
81				
82	Annual Production	gal,90% capacity factor	=0.9*365*C5*1000000	985500000
83	Total Capital Cost	$		
84	Installation factor	1.5		
85	No Salt Recovery		=$B$84*(C$70+C$71+C73)	20098870.8
86	Salt Recovery - 1		=$B$84*(C$70+C$71+C74+C77)	18012078.3
87	Salt Recovery - 2		=$B$84*(C$70+C$71+C75+C78)	18052300.8
88	Salt Recovery - 3		=$B$84*(C$70+C$71+C76+C79+C80)	18316848.3
89	Total Annual CapEx	6%, 20 yr		
90	No Salt Recovery		=-PMT(0.06,20,C85)	1752311.14643298
91	Salt Recovery - 1		=-PMT(0.06,20,C86)	1570375.06681786
92	Salt Recovery - 2		=-PMT(0.06,20,C87)	1573881.84766086
93	Salt Recovery - 3		=-PMT(0.06,20,C88)	1596946.30424769
94				
95	**Annual Operations & Maintenance Costs**		=C33/1000*C82	6874848
96	Power	$/year, $.10/kWh	=C33/1000*C82*0.1	687484.8
97	NaCl Purchased	='mineral prices'!G75	/lb (USGS)	/lb (USGS)
98	No salt recovery		=0.9*C38*$B$97	821571.520715588
99	Salt recovery - 1		=C$98-0.9*365*C49*$B$97	151357.13728443
100	Salt recovery - 2		=C$98-0.9*365*C50*$B$97	151357.13728443
101	Salt recovery - 3		=C$98-0.9*365*C51*$B$97	306604.53683628
102	Lime Purchased ($/lb, USGS)	='mineral prices'!J9	=$B$102*0.9*365*C53	87095.308806
103	RO Chemicals	0.07/kgal feed	=0.07*C7/C8*1000*365	110595.1752
104	RO membrane replacement	0.16/kgal feed	=0.16*C7/C8*1000*365	252788.971885714
105	EDM membrane & electrode replacement	0.32/kgal perm	=0.32*C5*1000*365	350400
106	Evap pond Annual Costs	$/year, 0.5% of installed evap pond cost (Mickley 2006-See La Junta final report)		
107	No salt recovery		=0.9*(0.005*C73)	13062.78
108	Salt recovery - 1		=0.9*(0.005*C74)	6534
109	Salt recovery - 2		=0.9*(0.005*C75)	6660
110	Salt recovery - 3		=0.9*(0.005*C76)	7182
111	Total O&M Costs	$/year		
112	No salt recovery		=C$96+C98+C103+C104+C105+C107	2235903.2478013
113	Salt recovery - 1		=C$96+C99+C103+C104+C105+C108	1559160.08437014
114	Salt recovery - 2		=C$96+C100+C103+C104+C105+C109	1559286.08437014
115	Salt recovery - 3		=C$96+C101+C102+C103+C104+C105+C110	1802150.79272799

Vita

Malynda Aragon Cappelle earned her Bachelor of Science in Chemical Engineering from the University of New Mexico in 2000. In 2002, she received her Master of Science degree in Chemical Engineering from the University of California at Davis. Malynda joined the doctoral program in Civil Engineering at The University of Texas at El Paso in 2010, but switched to the College of Business in 2011. Ms. Cappelle received a Master of Business Administration in 2013, then returned to doctoral work in 2014.

Malynda was a recipient of the El Paso Water Utilities Desalination Concentrate Fellowship in 2014 and received the Ed Archuleta Desalter Scholarship in 2016. The following year, Ms. Cappelle was on the review team for the Scholarship candidates. In 2014, Ms. Cappelle was part of a student team that won the Paso del Norte Venture Competition + Expo and competed at the Global Venture Labs Investment Competition in Austin, Texas.

While pursuing her degree, Malynda served as the Associate Director at UTEP's Center for Inland Desalination Systems. In this capacity, she led research projects that were sponsored by government programs and private companies. Ms. Cappelle still serves in this capacity as well as starting a company that is developing a hardness sensor that was developed at UTEP. Ms. Cappelle has interest in continuing research related to regional water and wastewater, water conservation, and sustainability.

Permanent address: malynda7@gmail.com

This dissertation was typed by the author.